Experimental Investigation on Machining Process Performance for Carbon Fiber Reinforced Polymer Composites: Part Quality, Tool Wear and Dust Emission

by

Tarek ELGNEMI

MANUSCRIPT-BASED THESIS PRESENTED TO ÉCOLE DE TECHNOLOGIE SUPÉRIEURE IN PARTIAL FULFILLMENT FOR THE DEGREE OF DOCTOR OF PHILOSOPHY
Ph.D.

MONTREAL, DECEMBER 30, 2021

ÉCOLE DE TECHNOLOGIE SUPÉRIEURE
UNIVERSITÉ DU QUÉBEC

BOARD OF EXAMINERS

THIS THESIS HAS BEEN EVALUATED

BY THE FOLLOWING BOARD OF EXAMINERS

Mr. Victor Songmene, Thesis supervisor
Department of Mechanical Engineering, École de Technologie Supérieure

Mr. Michel Rioux, Chair, Board of Examiners
Department of Systems Engineering, École de Technologie Supérieure

Mr. Emad Elgallad, External Independent Examiner
Département des sciences appliquées, Université du Québec à Chicoutimi

Mr. Fawzy-Hosny Samuel, External Examiner
Département des sciences appliquées, Université du Québec à Chicoutimi

THIS THESIS WAS PRESENTED AND DEFENDED

IN THE PRESENCE OF A BOARD OF EXAMINERS AND THE PUBLIC

ON DEFENSE DATE

AT ÉCOLE DE TECHNOLOGIE SUPÉRIEURE

ACKNOWLEDGEMENTS

I want to express my feelings and gratitude to my great supervisors Prof. Victor Songmene for his support and guidance and thank him for offering me the opportunity to work under his supervision. I truly appreciate the time he gave whenever I needed his assistance. Being your student has been the most remarkable experience that I obtained in my academic life. I would like to extend my feelings and gratitude to all the members of the jury for agreeing to read the manuscript and to participate in the defense of this thesis.

I am truly grateful to Advanced Center of Technology (ACT-Tripoli) and Ministry of Higher Education and Scientific Research of Libya for giving me the opportunity to study abroad.

Additionally, a special thanks go to Prof. Martin B.G. Jun, Dr. Jules Kouam, and Dr. Agnes Samuel and all my friends and colleagues in mechanical engineering department at Ecole Technologies Superrior for their kind friendship and continues support.

Lastly, and most importantly, I would like to thank my dad, mom, brothers and sisters for their emotional care and unconditioned support. Furthermore, I desire to thank my wife for her continuous support and encouragement over the years that we spent here. Your kindness and patience during hard times we went through together is priceless support that I will appreciate for the rest of my life. Also, my sweethearts Noor, Niroz and Robine; and my beloved one Mohab; I could never express how grateful I am for the sacrifices you made during this long journey.

Étude expérimentale sur les performances des processus d'usinage pour les composites polymères renforcés de fibres de carbone : qualité des pièces, usure des outils et émission de poussière

Tarek ELGNEMI

RÉSUMÉ

L'utilisation du polymère renforcé de fibres de carbone (CFRP) dans les industries ne cesse de croître en raison de ses propriétés exceptionnelles telles que sa haute résistance, son faible poids et sa résistance à la corrosion. Bien que les pièces en CFRP puissent être moulées à une géométrie proche de la forme nette, des processus d'usinage (fraisage, perçage) sont souvent nécessaires pour obtenir la forme finale. Cependant, le CFRP ne se comporte pas comme le plastique pur ou les métaux pendant l'usinage. La formation de copeaux pour le CFRP est en grande partie constituée de factures fragiles causées par le cisaillement des fibres et de la matrice. De plus, le CFRP produit des copeaux poudreux ou de la poussière pendant l'usinage à sec, qui sont actuellement considérés comme polluantes et un danger pour la santé des travailleurs. De plus, son inhomogénéité et la nature abrasive des fibres apportent des défis supplémentaires lors de l'usinage : délamination, température de coupe, émission de poussières et durée de vie limitée des outils.

En conséquence, ce travail vise à étudier le fraisage des CFRP et les facteurs clés qui affectent son usinabilité. L'application d'un fluide de coupe conventionnel est une solution courante pour augmenter la durée de vie de l'outil, réduire les forces de coupe ou diminuer l'émission et la dispersion des poussières. Cependant, cette solution ne peut pas être appliquée à l'usinage du CFRP, car l'humidité peut endommager l'intégrité structurelle de la pièce en composite.

Dans cette thèse basée sur des manuscrits, une étude expérimentale est d'abord menée pour examiner la faisabilité et l'efficacité de l'application d'un fluide de coupe atomisé dans le fraisage du CFRP (article 1, chapitre 3). Le fluide de coupe est décomposé en gouttelettes de taille micrométrique qui sont pulvérisées directement dans la zone de coupe pour lubrifier l'interface entre le copeau et l'outil, et aussi pour dissiper la chaleur générée par évaporation rapide. En raison du taux d'évaporation nettement plus élevé du fluide de coupe atomisé, le liquide de refroidissement appliqué n'est pas absorbé par le matériau de la pièce à usiner. Dans l'étude, les opérations de fraisage de CFRP sont menées dans une gamme de vitesse de coupe élevée, jusqu'à 40,000 rpm, et des vitesses d'avance jusqu'à 6 μm par dent sous différentes conditions de coupe : en coupe à sec et en semi-lubrifiés sous deux types de fluides de coupe, un liquide de refroidissement semi-synthétique d'usage général et un liquide de refroidissement à base d'huile végétale. Les résultats montrent que l'utilisation d'huile végétale atomisée permet de réduire de manière significative la force de coupe, l'usure de l'outil et la délamination des fibres par rapport au fraisage à sec.

La performance d'usinage des CFRP pourrait également être influencée par l'orientation des fibres et ses interactions avec les paramètres et les conditions d'usinage. Dans l'article 2 (chapitre 4), les effets de l'orientation des fibres (0°, 30° 45°, 60° and 90°) sur la formation de copeaux, la

délamination, l'usure de l'outil et les forces de coupe lors du fraisage à sec et avec un fluide à base d'huile végétale sont étudiés. Il a été constaté que la direction de coupe, en relation avec l'orientation des fibres, influence fortement la formation de copeaux, la force de coupe, la rupture des fibres, l'usure de l'outil, la qualité de la surface usinée de la pièce et la délamination, selon les paramètres et conditions d'usinage utilisés. Le pourcentage de délamination lors de la coupe à des angles d'orientation outil-fibre de 0°, 30° 45°, 60° and 90° a été amélioré de 65%, 91%, 54%, 66% et 75%, respectivement, dans des conditions ACF (huile végétale) à 3μm. L'ampleur de la force de coupe résultante s'est avérée être plus importante dans la condition sèche par rapport à la condition ACF de plus de 23% selon les angles d'orientation des fibres et la vitesse d'avance utilisés.

Certains fabricants pourraient hésiter à utiliser un fluide quelconque pour l'usinage du CFRP, car l'humidité pourrait endommager l'intégrité structurelle du composite. L'usinage à sec pourrait apporter des défis supplémentaires en matière de performance des outils, de qualité des pièces et de sécurité au travail. Dans l'article 3, chapitre 5, le fraisage à sec du CFRP est étudié en mettant l'accent sur les forces de coupe, les énergies spécifiques de coupe, la température de coupe, l'usure de l'outil et l'émission de poussières fines. La température de coupe a été examinée à l'aide de modèles analytiques et empiriques, et des expériences de coupe (plan factoriel complet) ont été menées pour évaluer la fiabilité des prédictions théoriques. Enfin, les résultats de l'optimisation expérimentale sont présentés, et le modèle est validé. Il a été constaté, entre autres conclusions, que lors du fraisage du CFRP testé, des particules fines (diamètres allant de 0,5 à 10 μm) sont émises et que leur concentration peut atteindre 2776 particules par centimètre cube. L'ensemble des résultats obtenus aident à mieux comprendre les phénomènes spécifiques associés au fraisage des CFRP et fournissent les moyens de sélectionner des paramètres de fraisage efficaces pour améliorer la technologie et l'économie du processus.

Mots-clés: CFRP, fraisage, force de coupe, l'usure de l'outil, température, l'émission de poussières fines

Experimental Investigation on Machining Process Performance for Carbon Fiber Reinforced Polymer Composites: Part Quality, Tool Wear and Dust Emission

Tarek ELGNEMI

ABSTRACT

The use of carbon fibre reinforced polymer (CFRP) in industries is continuously increasing because of its exceptional properties such as high strength, low weight, and corrosion resistance. Although CFRP parts can be moulded to a near-net-form geometry, machining processes (milling, drilling) are frequently required to achieve the final shape. However, CFRP does not behave like pure plastic or metals during machining. The chip formation for CFRP is largely brittle factures caused by shearing of the fibres and matrix. Also, CFRP produces powdery chips or dust during dry machining, which are currently categorised as a nuisance pollutant and cause of health hazard. Moreover, its inhomogeneity and the abrasive nature of the fibres bring additional challenges during machining: delamination, cutting temperature, dust emission, and limited tool life.

Accordingly, this work aims to investigate the milling of CFRP and key factors that affect its machinability. The application of conventional cutting fluid is a common solution for increasing the tool life, reducing cutting forces or lowering the dust emission and dispersion. However, this solution cannot be applied to the machining of CFRP, because moisture may damage the structural integrity of the composite workpiece.

In this manuscript-based thesis, an experimental study was first conducted to examine the feasibility and effectiveness of applying atomized cutting fluid in milling of CFRP (article 1, chapter 3). The cutting fluid is broken down into micrometer size droplets that are sprayed directly into the cutting zone to lubricate the chip and tool interface, and also to dissipate the heat generated by fast evaporation. Because of the significantly higher evaporation rate of the atomized cutting fluid, the applied coolant not get absorbed into the workpiece material. In the study, CFRP milling operations were conducted in a range of high cutting speed, up to 40,000 rpm, and feed rate values up to 6 μm under different machining conditions: dry condition, and using two types of cutting fluids, a general purpose semisynthetic coolant and a vegetable-oil-based coolant. The result showed that using atomized vegetable oil helps significantly in reducing the cutting force, tool wear, and fibre delamination as compared to the dry milling condition.

The machining performance of CFRP could also be influenced by fibre orientation and its interactions with the machining parameters and conditions. In article 2 (chapter 4) the effects fibres orientation (0°, 30° 45°, 60° and 90°) on chip formation, delamination, tool wear and cutting forces when milling dry and with vegetable oil-based fluid was investigated. It is found that the cutting direction, in relation to the fiber orientation, strongly influences chip formation, the cutting force, fiber breakage, tool wear, surface quality of the part machined and the delamination, according to the machining parameters and conditions used. The delamination percentage when cutting at tool-fiber orientation angles of 0°, 30° 45°, 60° and 90° were

improved by 65%, 91%, 54%, 66%, and 75%, respectively, under ACF (vegetable oil) conditions at 3μm feed rate. The magnitude of the resultant cutting force was found to be greater in the dry condition relative to the ACF condition by more than 23% depending on fibre orientation angles and feed rate used.

Some manufacturers might be very hesitant in using any fluid when machining CRFP because moisture may damage the structural integrity of the composite. Machining dry could bring additional challenges to tool performance, part quality and occupational safety. In article 3, (chapter 5), the dry milling of CFRP machining is investigated with special focus on cutting force, specific cutting energy, cutting temperature, tool wear, and fine dust emission. The cutting temperature was examined using analytical and empirical models, and cutting experiments (full factorial design) were conducted to assess the reliability of the theoretical predictions. Finally, results of the experimental optimization are presented, and the model is validated. It was found in, among other conclusions, that during milling of the tested CRPF, fine particles were emitted (diameters ranging from 0.5–10 μm) and that their concentration can reach 2776 particles per cubic centimeters. All the obtained results help to better understand specific phenomena associated with milling of CFRPs and provide the means to select effective milling parameters to improve the technology and economics of the process.

Keywords: CFRP, milling, cutting force, tool wear, temperature, fine dust emission

TABLE OF CONTENTS

LIST OF TABLES

LIST OF FIGURES

LIST OF ABBREVIATIONS

ACF	Atomization Cutting Fluid
APS	Aerodynamic Particles Sizer
ANOVA	Analysis of Variance
CFRP	Polymère renforcé de fibres de carbone
CFRP	Carbon Fiber Reinforced Polymer
CNC	Computer Numerical Control
DF	Degree of Freedom
DP	Delamination Percentage
DOE	Design of Experiments
DAQ	Data Acquisition
FOA	Fiber Orientation Angle
MWF	Metal Working Fluid
MQL	Minimum Quantity of Lubrication
MS	Mean Squares
RSM	Response Surface Methodology
SEM	Scanning Electron Microscopy
SS	Sum of Squares
Tg	Glass Transition

LIST OF SYMBOLS AND UNITS OF MEASUREMENTS

ap	Depth of cut (mm)
C	Heat capacity (J/g-C)
$C\rho$	Specific heat ($j/mm^3 - C$)
α	Thermal conductivity (j/s-mm $C°$)
Dp	Delamination percentage (%)
f	feed rate (μm/tooth)
Fc	Cutting force (N)
Ft	Thrust force (N)
Fx, Fy, Fz	Cutting force components in x, y and z directions (N)
K	Thermal diffusivity of work material (mm^2/s)
μm	Micrometer
R	Resultant cutting force (N)
s	Spindle speed (rpm)
T	Temperature rises at tool-chip interface (C°)
TFOA	Tool Displacement Fiber Orientation Angles: θ (°)
W	Original slot width (mm)
W_{max}	Maximum damage width (mm)
α	Rake angle (°)
β	Friction angle (°)

ϕ	Shear angle (°)
ρ	Density (g/cm^3)
U	Specific cutting energy (Nm/mm^3)
Vc	Cutting speed (m/min)

INTRODUCTION

The application of fiber reinforced polymer composite materials is being used in increasing quantities in advanced structures due to their superior specific strength and stiffness compared to other material systems including metals. Major structural application areas include aircraft, space, automotive, sporting goods, civil engineering, and energy production. Figure 0.1 depicts some of the application. Other application areas include electronics with fiber reinforced polymer composites being used for circuit boards. In the medical industry, composites are being used for sockets, implants, and prosthetic limbs (Eneyew & Ramulu, 2012). Many industrial products utilize composites including ladders, tanks, and power transmission shafts. The power industry is utilizing fiber reinforced composites for wind generation and transformer housings. Additional fields that would benefit from the performance advantages of composites include, but are not limited to, the capability to produce near net shape parts, design flexibility, increased specific strength, corrosion resistance, dimensional stability, and fatigue damage tolerance.

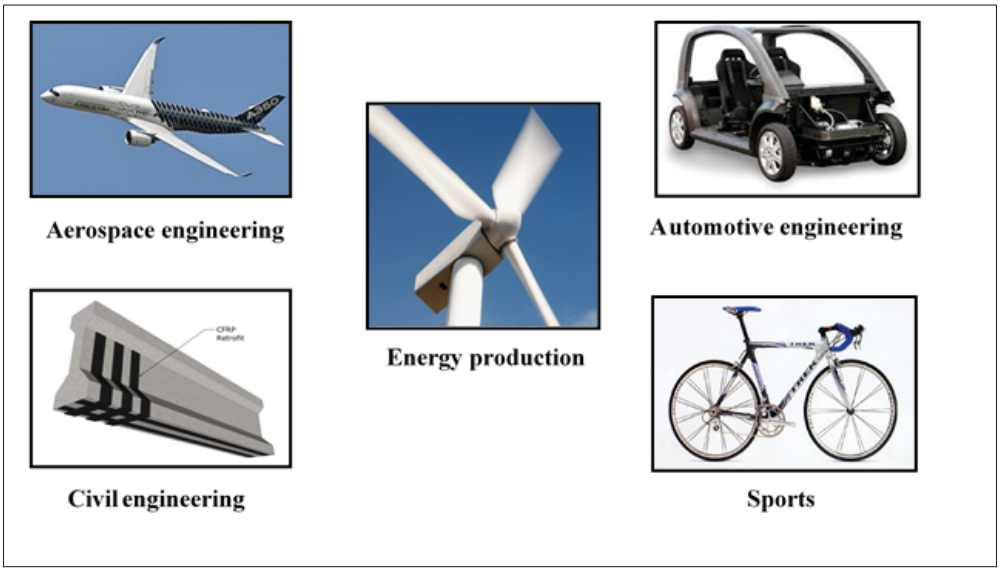

Figure 0.1 Examples of some carbon fiber application (Das *et al.*, 2019)

Fiber reinforced polymer composites are being utilized in increasing percentages of the total structural weight for both military and commercial aircraft where weight reduction is essential for higher speeds, increased payloads, and improved fuel economy. Starting with the use of boron fiber-reinforced epoxy skins for the F-14 stabilizers in 1969, the use of fiber reinforced composites in aircraft structure has seen steady growth. With composites first being used in selective secondary aircraft structural components, carbon fiber reinforced epoxy has become the primary material in many wings, fuselage, and empennage components. Typical percentage of composite usage is shown in B-2 and V-22 military aircraft in Figure 0.2. In 1988, Airbus introduced the A320 with an all-composite tail including tail cone, horizontal, and vertical stabilizers. In 1995, Boeing introduced the 777, which utilizes composites for approximately 10% of its total structural weight. The structural weight of the Airbus A380, introduced in 2007, is approximately 20% composites utilizing carbon, glass, and quartz fibers. The Boeing 787 and Airbus A350 XWB are both advertising 50% and 52%, respectively of the total structural aircraft weight being made primarily from carbon epoxy composites as illustrated in Figure 0.3.

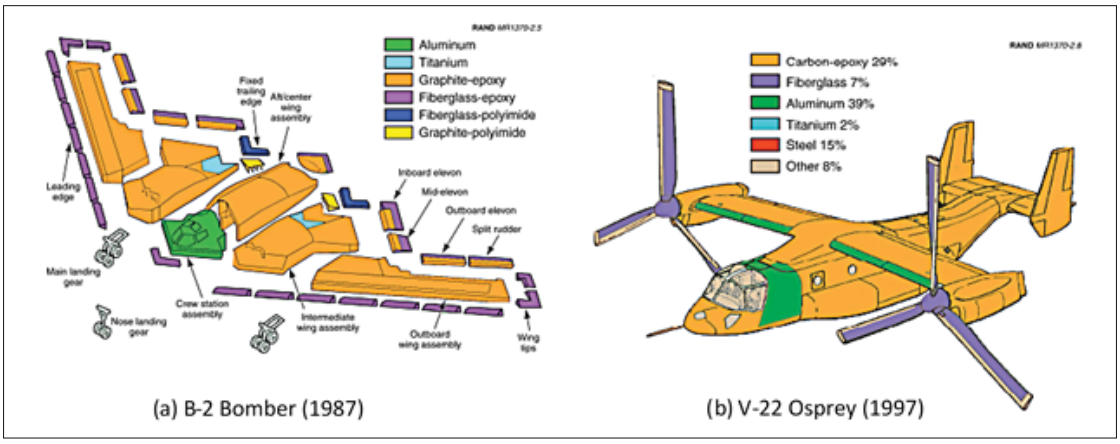

Figure 0.2 Use of composites in US military aircraft (B-2, V-22) – adapted from (Miller, 2014)

The use of these materials, particularly carbon fibre reinforced plastic (CFRP) systems for aerospace constructions, has resulted in the development of products that are stronger, lighter,

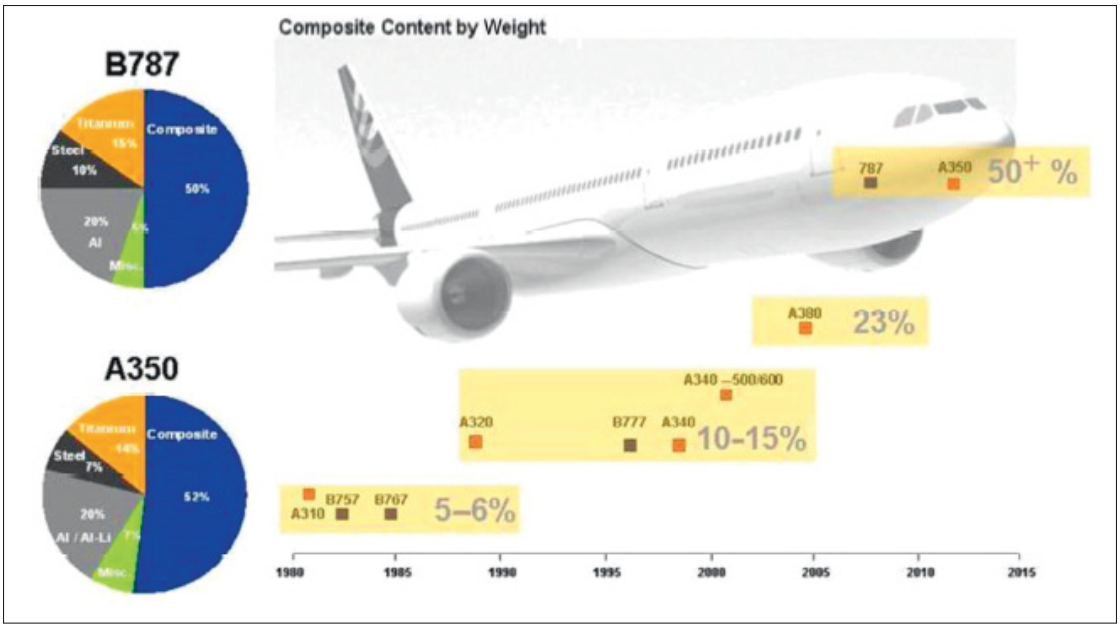

Figure 0.3 Increase of the weight content of composites in aircraft structures over a 30-year – adapted from (Giurgiutiu, 2015)

and more corrosion resistant, as well as having a longer fatigue life. Although carbon/epoxy material can be moulded to near-net-shape geometry, machining is frequently required to permit assembly due to tolerance and surface finish requirements. Milling of Composite is difficult because of the anisotropic and abrasive character of the material. Delamination, fuzzing, fiber withdrawal, and short tool life are just a few of the issues. Electrically conductive chips or dust created during carbon fiber milling can cause shorting in electrical equipment. Furthermore, airborne carbon fibers, which are now classed as a nuisance particulate, can sensitise and irritate the nasal and respiratory systems, as well as cause skin irritation in some individuals. These problems are quite distinct from those found when milling homogeneous materials like metals, and thus merit study to understand the mechanics of the milling processes in CFRP composite materials.

CHAPTER 1

PROBLEM STATEMENT, RESEARCH OBJECTIVES, AND THESIS OUTLINE

1.1 Problem statement

Carbon Fiber Reinforced Polymers (CFRP) offer higher strength to weight ratio and superior corrosion and fatigue resistance compared to traditional metals. Mechanical machining processes such as milling and drilling are usually a critical part of the assembly and finishing stage of producing CFRP parts in a wide range of applications such as aerospace, automotive, and biomedical devices. The machinability of CFRP materials is limited by the excessive tool wear due to the abrasiveness of carbon fibers, and by the machining-induced damages such as delamination that is produced by the low interlaminar strength of composite layers (Bhatnagar, Ramakrishnan, Naik & Komanduri, 1995) (Santhanakrishnan, Krishnamurthy & Malhotra, 1988) (Teti, 2002). As a result, it will reduce of the mechanical properties in the assembly of many components, and thus decreases the reliability and performance of the final product.

When machining, the majority of cutting power is converted to heat (Sato, Tamura & Tanaka, 2011). Due to the lower thermal conductivity of CFRP, 50% of the cutting temperature is absorbed by the tool, compared to 18% when machining metallic materials (König & Grass, 1989). Owing to the brittle nature of chips and the intermittent cutting action of processes such as end milling/routing, heat absorption by the chip is low (Yashiro, Ogawa & Sasahara, 2011). A key measure in assessing damage threshold is the rise in temperature beyond Tg, which is defined as the transition between the rubbery and glassy state of the binder phase which normally ranges from 180 - 270 C° for epoxy based composites (Wang, Sun, Li, Lu & Li, 2016). Controlling the heat generated at the zone is the key requirement to produce “first-time right” parts in order to avoid the high cost of part rejection (Karaguzel, Bakkal & Budak, 2016). Cutting temperature not only plays a role in tool life and workpiece quality, but it can also affect dust particle size and concentration in the air, which can have adverse effects on health as reported by (Haddad,

Zitoune, Eyma & Castanie, 2014) and consequently, there is a need to measure and understand the factors affecting temperature.

Moreover, carbon fibers are the major source of respirable dust because they may splinter lengthwise during machining producing fibrils of diameters less than 6 μm. Machining processes of CFRP produces dust-like chips (visible and invisible) that may become airborne. Some of this dust might be small enough to make its way to the lower respiratory tract and hence poses a health hazard which is directly related to the dust generated during machining cannot be overlooked. This dust can be inhaled and can even penetrate the skin or the eye, causing multiple irritations. These problems, resulting from the harmful dust produced by CFRPs entail a risk for both employees and machines (Haddad, Zitoune, Eyma, Castanié & Bougherara, 2012). In fact, it is the small size of these particles that poses the hazard. These particles reach the lowest part of the respiratory system and tend to stay there, reducing the exchange surface between the blood and the respiratory system during oxygen-carbon dioxide exchange. Since the toxicity of these particles has not been studied and determined, its impact has not been seriously felt as well.

In addition, dust generated from machining CFRPs are harmful to the machine tool as well. Carbon fibers are also electrically conductive. Due to the small size of the dust particles and the fibers, and their ability to become airborne, it is very likely that these particles will penetrate into tight spaces between machine components and into the machine control box. The prolonged contact of the abrasive dust with the moving machine elements such as slideways, ball screws, and bearings may lead to wear. Deposition of the carbon fibers on printed circuit boards on the machine control will cause short circuits and very expensive damage to the machine tool.

1.2 Research objectives

The present study aims to achieve the following goals:

1) To study the effects of atomization-based cutting fluid sprays in high speed milling of CFRP.
2) To investigate the influence of machining parameters and cutting conditions on surface defects, delamination, tool wear that would be generated during machining CFRP.

3) To develop cutting conditions that will help in reducing the cutting temperature and amount of dust that would be generated by using an experimental study.
4) To develop predictive models for predicting cutting temperature during the milling of CFRP.

1.3 Thesis outline

This PhD thesis comprises six chapters which are briefly described below:

Chapter 1 explains the research objectives of the present thesis and outlines the thesis scope.

Chapter 2 provides a critical review of the current research on the machinability of CFRP. It also presents a short overview of milling process for composites and the previous experimental and modeling researches made on the milling of CFRP materials.

Chapter 3 describes the experimental setup and procedure (devices and equipment, workpiece materials and cutting tools) used to accomplish the declared objectives. Furthermore, explains the analytical methodology adopted to conduct the desired simulations required to perform the study.

Chapter 4 studies the feasibility and effectiveness of applying atomization based cutting fluid application in improving the machinability of CFRP. High speed milling operations are conducted in a range of cutting speed and feed rate values under dry milling conditions, and using two types of cutting fluids, a general-purpose semisynthetic coolant and vegetable-oil-based coolant as a sustainable alternative to conventional coolants.

Chapter 5 focuses on the interactions between the fiber orientation, the machining parameters and the tested vegetable oil-based fluid. Based on the findings of Chapter 4, the application of vegetable oil was found to be more effective in improving the machinability of CFRP comparing to milling in dry condition and atomized general-purpose semisynthetic coolant. Accordingly, Chapter 5 is devoted to investigating the milling performance of CFRP composite and atomized vegetable oil as a function of fiber orientation. The tool displacement-fiber orientation angles (TFOA) tested are 0°, 30° 45°, 60°, and 90°. The output responses analyzed were cutting force,

delamination, tool wear, chip formation, and impact of fiber orientation on CFRP surface finish. The results could help in selecting appropriate cutting parameters and thus improve the machined part quality and productivity of the machined part.

Chapter 6 focuses on the interaction effect of cutting parameters (cutting speed, and feed rate) on the machining process performance indicators: cutting force, specific cutting energy, cutting temperature, tool wear, and fine dust emission (in term of number of particles) during dry milling of CFRP. Additionally, an analytical model was proposed to predict the temperature and then experimental tests were used to verify the results obtained by the model. In this study, the relationships between milling temperature, milling force, fine dust emission, and cutting parameters are analyzed using response surface methodology (RSM), and the corresponding mathematical models are established to optimize the cutting parameters.

Finally, the conclusions from obtained results, main contributions, and recommendations for future work are presented in additional sections at the end of the thesis.

CHAPTER 2

STATE OF THE ART IN MACHINING OF CFRP

2.1 Carbon fiber reinforced polymer

Composite materials are consist of two materials; one material is called the reinforcement or discrete phase. The other is called a matrix or continuous phase. The fiber and the matrix have their own properties but when combined together they form a material with notably different properties that are not established in either of the individual materials, such as high strength per weight ratio, high corrosion and thermal resistance and high stiffness, which are markedly superior to those of comparable metallic alloys. The typical structure of CFRP can be illustrated as Figure 2.1. The purpose of the matrix phase is to hold the reinforcement in order to create

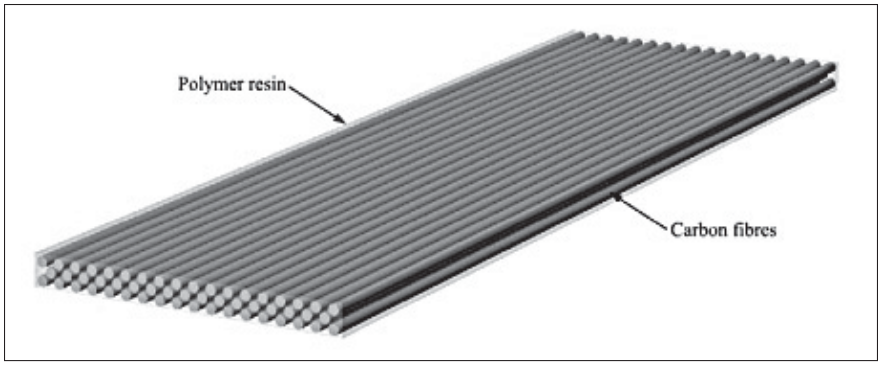

Figure 2.1 Typical structure of Carbon Fiber Reinforced Polymer (CFRP)

the desired shape; while the function of the reinforcement is to support the major exterior load, and thus improves the overall mechanical properties of the matrix. When the two phases are mixed completely, the new combined material present best strength than would each individual material (Mazumdar, 2001).

Composites are generally categorized using two distinct standards. The first standard is made with respect to the matrix constituent. Classes of composite matrix constituents include organic matrix composites (OMC), metal matrix composites (MMC), ceramic matrix composites (CMC), and

polymer matrix composites (PMC). The second standard includes the reinforcement constituents. Different classes of reinforcements include particle reinforcements, whisker reinforcements, continuous and discontinuous fiber reinforcements, and woven reinforcements. A reinforcement is considered to be a particle if all its dimensions are approximately equal. Continuous fiber reinforcements have lengths much greater than their cross-sectional dimensions. The architecture of a woven reinforcement includes weaving, braiding, or knitting the fiber or fiber bundle tows to create interlocking fibers that have an orientation slightly or fully orthogonal to the primary structural plane. The essential purpose of the reinforcement is to give excellent levels of strength and stiffness to the composite, where fibers are the principal load carrying members. The purpose of the matrix is to bind the reinforcements together through its adhesive characteristics, to transfer load between the reinforcements, keep the fibers in the desired orientation, and to protect the reinforcements from environmental and handling damage (Miracle, Donaldson *et al.*, 2001).

2.1.1 Types of composites

2.1.1.1 Polymer matrix composites

Polymer matrix composites (PMC) (See Figure 2.2) and fiber reinforced plastics (FRP) are referred to as Reinforced Plastics. Common fibers used are glass (GFRP), graphite (CFRP), boron, and aramids (Kevlar). These fibers have high specific strength (strengthto-to-weight ratio) and specific stiffness (stiffness-to-weight ratio).

2.1.1.2 Fiber reinforced composites

FRP (fiber reinforced polymer) is an acronym usually used in the composite industry and it refers to plastic and polymer materials that are reinforced with structural fiber such as fiber glass, carbon fiber, or aramid fiber. FRP can be further used as a replacement for the term "composite". Most often, FRP products are structured using thermoset resins such as polyester, vinyl ester or epoxy, but they can also use thermoplastic resins. The fiber can be intermittent such as fiber that

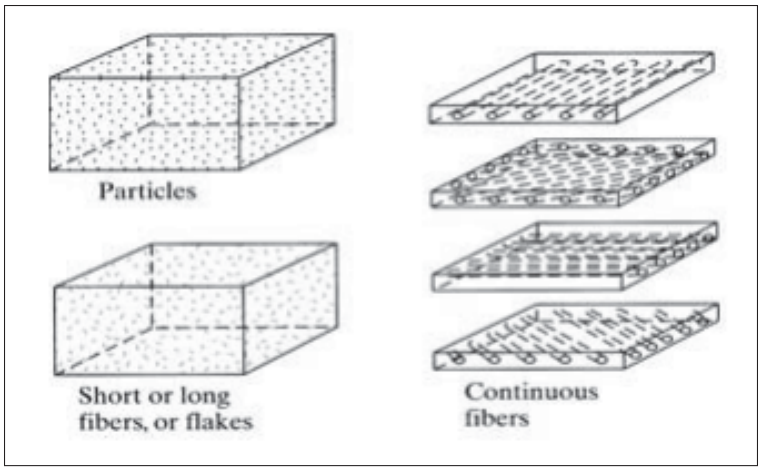

Figure 2.2 Polymer matrix composites – adapted from (Campbell, 2010)

is found in chopped strand mat, or glass fiber used in gun roving (See Figure 2.3). The fiber could also be continuous direct-end roving, which is generally used in filament winding and pultrusion. Other constructions of fiber include woven roving and stitched fabrics. Woven is identical to other structural fibers (Sheikh-Ahmad, 2009).

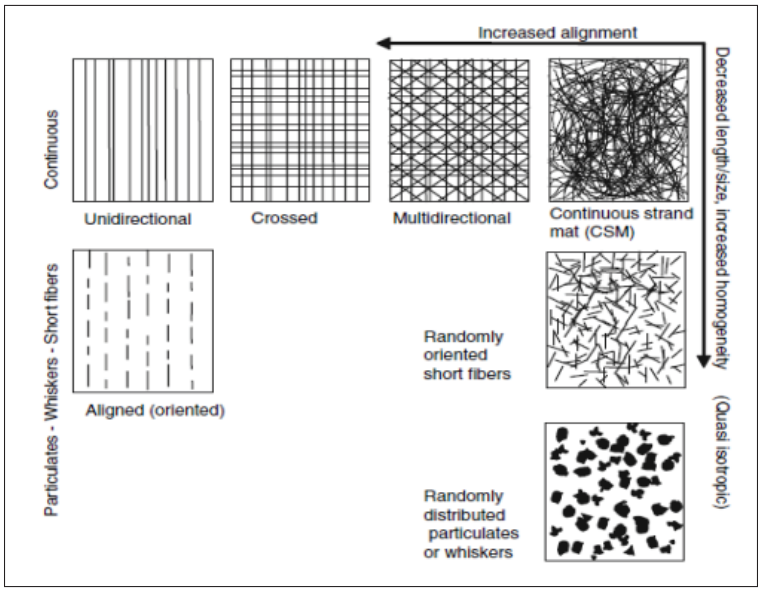

Figure 2.3 Different reinforcement arrangements in composites – adapted from (Sheikh-Ahmad, 2009)

2.1.1.3 Metal matrix composites

Metal matrix composites (MMC) offer higher modulus of elasticity, ductility, and resistance to elevated temperature than polymer matrix composites. However, they are heavier and more difficult to process.

2.1.1.4 Ceramic matrix composites

Ceramic matrix composites (CMC) are used in applications where resistance to high temperature and corrosive environment is desired. CMCs are strong and stiff but they lack toughness (ductility). Matrix materials are usually silicon carbide, silicon nitride and aluminum oxide, and Mullite (compound of aluminum, silicon and oxygen). They retain their strength up to 3000 F°. Fiber materials used commonly are carbon and aluminum oxide. CMCs are used in jet and automobile engines, deep-see mining, cutting tools, dies and pressure vessels (Iyer, 2015).

2.2 Milling of CFRPs

Machinability is the facility with which a material can be machined under a specified set of cutting conditions. it is rather a relative concept and depends on the end-user, which is assessed with reference to various key performance indicators such as the tool life, cutting force, power consumption, surface quality, cutting temperature, chip formation, etc. Machining of composites is widely performed in order to do the final processing of the near-net shape material in order to meet tolerance requirements in assembly. Drilling and milling are the most commonly used machining processes. Milling is used, as a rule, as a reformative end-machining process or to manufacture defined high-quality surfaces. The material is removed from the workpiece by a rotary cutterhead that might have more than one active cutting edge. High cutting-edge sharpness and a small cutting-edge radius are additional requirements. However, milling process is complex due to the variation of fiber orientation, chip size and cutting forces with tool rotation. As shown in Figure 2.4, face milling machining is performed by a tooth on both the end and the

periphery of the face milling cutter. A high production rate is known as an important feature of face milling due to the large cutter diameter used in this process.

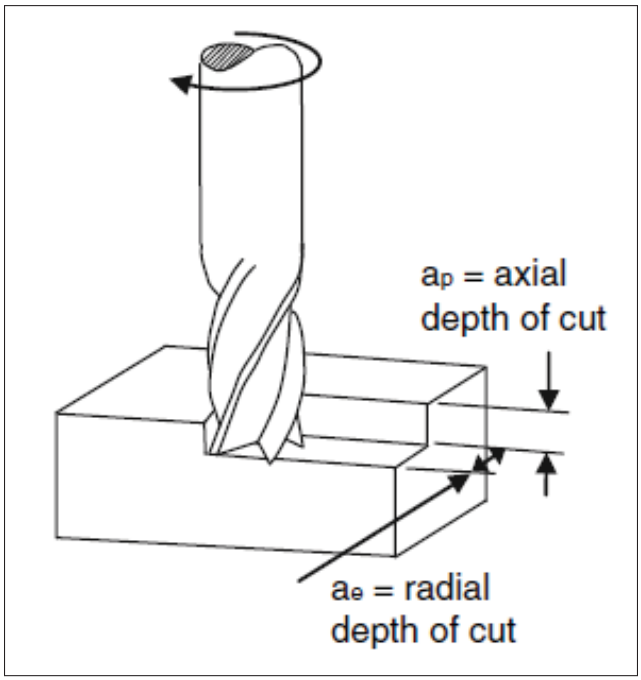

Figure 2.4 Face end milling process

There are three types of milling operations used in practice:

(i) Face milling operations, in which entry and exit angles of the milling cutter relative to the workpiece are nonzero;

(ii) Up-milling operations, in which the entry angle is zero and the exit angle is nonzero; and

(iii) Down-milling operations, in which the entry angle is not zero and the exit angle is zero.

Both up- and down-milling operations are called peripheral or end milling operations. The geometry of chip formation in milling is shown in Figure 2.5.

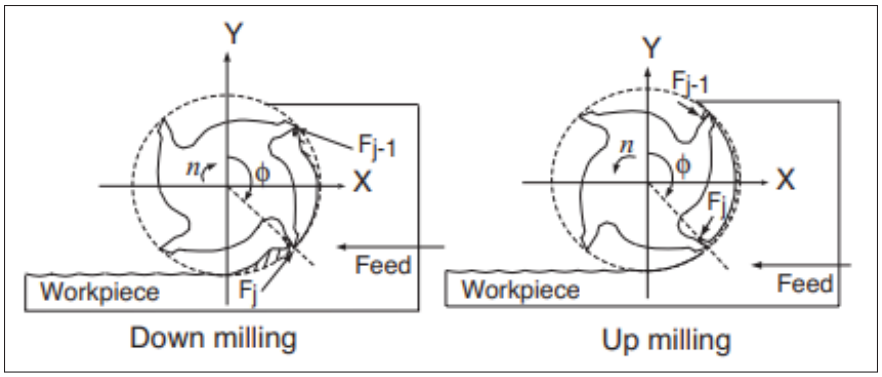

Figure 2.5 Geometry of milling process – adapted from (Altintas & Ber, 2001)

2.3 Milling process parameters and cutting conditions

Cutting speed (Vc) is an important parameter indicating the speed at which the cutting edge machines the workpiece and is defined by the following equation:

$$Vc = \frac{\pi \times D \times N}{1000}(m/min) \tag{2.1}$$

where D and N represent the tool diameter and spindle speed respectively.

Feed speed (Vf) is the feed of the tool against the workpiece in units of distance per time and feed per revolution (f) is a value used to determine finishing capacity. These two parameters are related by the following equation:

$$f = \frac{Vf}{N}(mm/rev) \tag{2.2}$$

Milling tools are multi-edge cutters, and the feed per tooth (af), as a value for ensuring that each edge machines under satisfactory condition, is defined by the following equation:

$$af = \frac{Vf}{N \times z}(mm/tooth) \tag{2.3}$$

where, z is number of edges of the tool.

2.4 Cutting force

Cutting force is considered as the signal which best describes the cutting process in terms of accuracy and fast responses to changes in cutting conditions. In addition, it has been widely used for monitoring purposes in all machining processes (Turning, Milling, Drilling, etc.). This signal/parameter can be used to monitor a wide range of machining variables such as tool wear, tool breakage/chipping, chatter vibration, and the quality and geometric profile of the cutting surface which makes it a perfect candidate to be used in a comprehensive machining monitoring system (Freyer, Heyns & Theron, 2014), (Zhang, Li & Wang, 2012). However, this method has its limitations, with respect to the size of the part that can be clamped onto the dynamometer. Also, the recorded cutting forces could vary during the machining experiments, since the dynamometer will be affected by the changing of the workpieces.

As shown in Figure 2.6, there are four forces in total in a typical machining process. The friction force (F) is the frictional force which resists the flow of the chip along the rake face of the tool. The normal force to friction (N) is perpendicular to the friction force. The shear force (F_s) is the force that causes shear deformation to occur in the shear plane, and the normal force to shear (F_n) is perpendicular to the shear force. However, when a cutting tool is forced into a working material, two forces are needed, and these are measurable. The cutting force is in the direction of cutting, the same direction as the cutting speed. The thrust force is perpendicular to the cutting force and is associated with the chip thickness before the cut.

The following equations can be derived to relate the forces that cannot be measured to the forces that can be measured (Shaw & Cookson, 2005):

$$F = -F_c \sin\alpha + F_t \cos\alpha \tag{2.4}$$

$$N = F_c \cos\alpha - F_t \sin\alpha \tag{2.5}$$

$$F_s = F_c \cos\phi - F_t \sin\phi \tag{2.6}$$

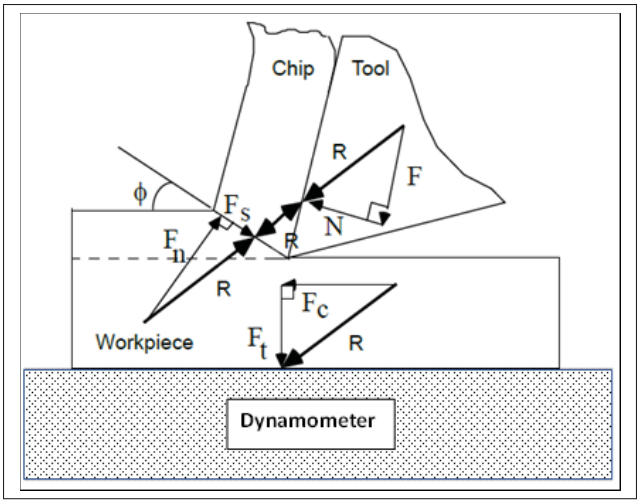

Figure 2.6 Force diagram showing geometric relationships between F, N, Fs, Fn, Fc, and Ft)

$$F_n = F_c \sin\phi + F_t \cos\phi \tag{2.7}$$

$$\mu = \frac{F}{N} \Rightarrow \mu = \tan\beta \tag{2.8}$$

where μ is the coefficient of friction between tool and chip and β is the friction angle.

From these force components and the area of the shear plane, it is possible to calculate the shear stress. Using the geometric relation shown in Figure 2.7 and the calculated force components, the shear stress τ and the normal stress σ can be derived as shown by Equations (2.9) and (2.10).

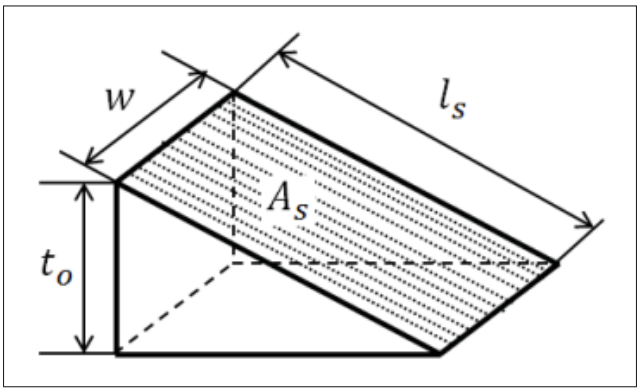

Figure 2.7 Geometric relation of the shear plane

$$\tau = \frac{F_s}{A_s} \tag{2.9}$$

$$A_s = \frac{t_0 W}{\sin \phi} \tag{2.10}$$

By substituting Equation (2.6) and Equation (2.10) into Equation (2.9), the expression for the shear stress can be defined in terms of the measured quantities by Equation (2.11).

$$\tau = \frac{(F_c \cos \phi - F_t \sin \phi) \sin \phi}{t_0 W} \tag{2.11}$$

The normal stress in the shear plane can be determined in the same fashion and given by equation (1.12).

$$\sigma = \frac{F_n}{A_s} = \frac{(F_c \sin \phi + F_t \cos \phi) \sin \phi}{t_0 W} \tag{2.12}$$

2.5 Tool wear

Tool wear is considered as undesired removal of tool material from the cutting edge or the permanent deformation of the cutting edge leading to undesirable changes in the cutting edge geometry. Once the initial cutting geometry is changed, the cutting tool becomes least efficient in performing its major functions, which are material removal and generating good quality machined surface. The wear mode while cutting CFRP is now known to be very different from the conventional wear modes observed in cutting metallic alloys, i.e., flank and crater wear (Nguyen, Abdullah, Khawarizmi, Kim & Kwon (2020)). Tool wear is generally a gradual process and depends on:

1) Cutting Temperatures
2) Tool geometry
3) Process parameters (e.g. speed, feed, and depth of cut)
4) Machine tool characteristics
5) Tool and workpiece materials
6) Cutting Fluids

2.5.1 Wear mechanisms

Several wear mechanisms may occur simultaneously, or one of them may dominate the process. They can be listed as *abrasion, adhesion, diffusion, and oxidation wear*.

1) Abrasion wear is occurs when a harder material (i.e., the tool) shears away small particles from the softer work material.
2) Adhesion wear When there is a relative motion between the two bodies that are under the normal load, fragments of softer work material adhere to the harder tool.
3) Diffusion wear When the temperatures of the tool and work materials increase at the contact zones, the atoms in the two materials become restive and migrate to the opposite material where the concentration of the same atom is lower.
4) Oxidation wear The atoms in the cutting tool and/or work material form new molecules at the contact boundary where the area is exposed to the air (i.e., oxygen) (Altintas & Ber, 2001) Sheikh-Ahmad (2009).

It should be mentioned that wear mechanisms do not proceed in a similar way under a given set of cutting conditions, and interactions between them may occur. The relative effects of these wear mechanisms are functions of cutting temperatures, cutting forces, and workpiece machining properties.

2.5.2 Types of tool wear

1) Flank wear is caused by friction between the flank face (primary clearance face) of the tool and the machined workpiece surface (Figure 2.4 (a)). At the tool flank–workpiece surface contact area, tool particles adhere to the workpiece surface and are periodically sheared off. This type of wear can be used in tool life expectancy equation.
2) Rack wear or Crater wear occurs at the tool–chip contact area where the tool is subject to a friction force of the moving chip under heavy loads and high temperatures (Figure 2.4 (a)). At higher speeds, the temperature rises on the rake face of the tool. As a result, the atoms in the tool continuously diffuse to the moving chip. The temperature is greatest near the

midpoint of the tool–chip contact length, where the greatest amount of crater wear occurs because of intensive diffusion.

3) Edge chipping: this type of wear is more popular when the cutting tool does not have enough toughness to withstand the extremely fluctuating cutting forces, when the depth of cut is too large and under discontinuous cutting conditions.

Figure 2.4 (a) shown different forms or types of cutting tool wear. Figure 2.4 (b) shown a cross section of a worn cutting edge in which edge rounding is clearly apparent.

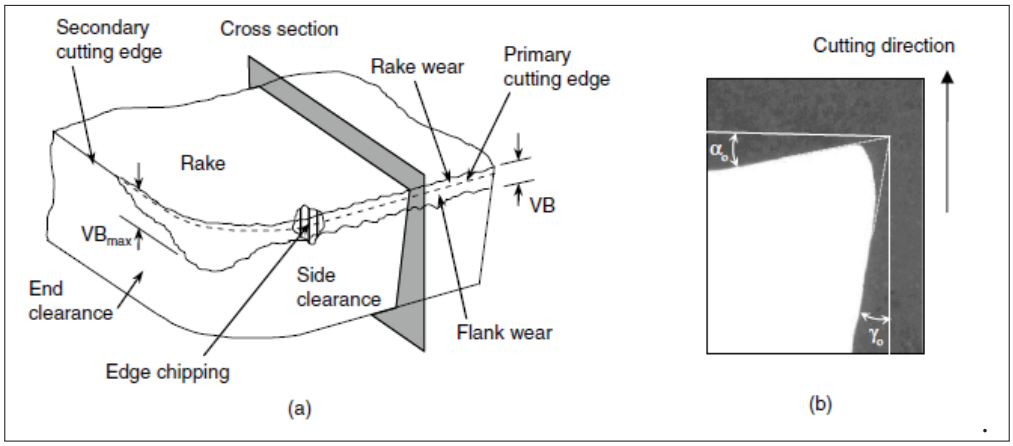

Figure 2.8 Types of tool wear in machining CFRP (a), and cross section of a replica of the cutting edge (b) – adapted from (Sheikh-Ahmad, 2009)

2.5.3 Tool failure

Tool failure generally refers to the sudden loss of tool material and shape (e.g. chipping) and is caused by:

1) Mechanical shock - impact by interrupted cutting (e.g. spline, hex. bar, sudden feed/speed change).

2) Thermal fatigue - cyclic variations in temperature in interrupted cutting, often in the form of thermal cracks, perhaps where a defect already exists.

2.6 Chip formation mechanism

The orientation of the fibres controls the chip formation mechanism in CFRP milling. During the milling process, the fibres' orientation changes continuously as the tool rotates. As a result, different cutting mechanisms are responsible for chip formation during mill rotation. Several researchers carried out orthogonal cutting tests on unidirectional CFRP in order to investigate the mechanisms of chip formation. They found that the cutting mechanism is affected by the fiber orientation, the tool geometry, and the cutting condition Li *et al.* (2016). The fiber orientation, the cutting edge radius, and the feed were assessed as the most important parameters for chip formation Bhatnagar *et al.* (1995). Figure 2.8 schematically shows the numerous mechanisms of chip formation when machining CFRPs with a sharp cutting edge, depending on fiber orientation and cutting edge rake angle Sheikh-Ahmad (2009).

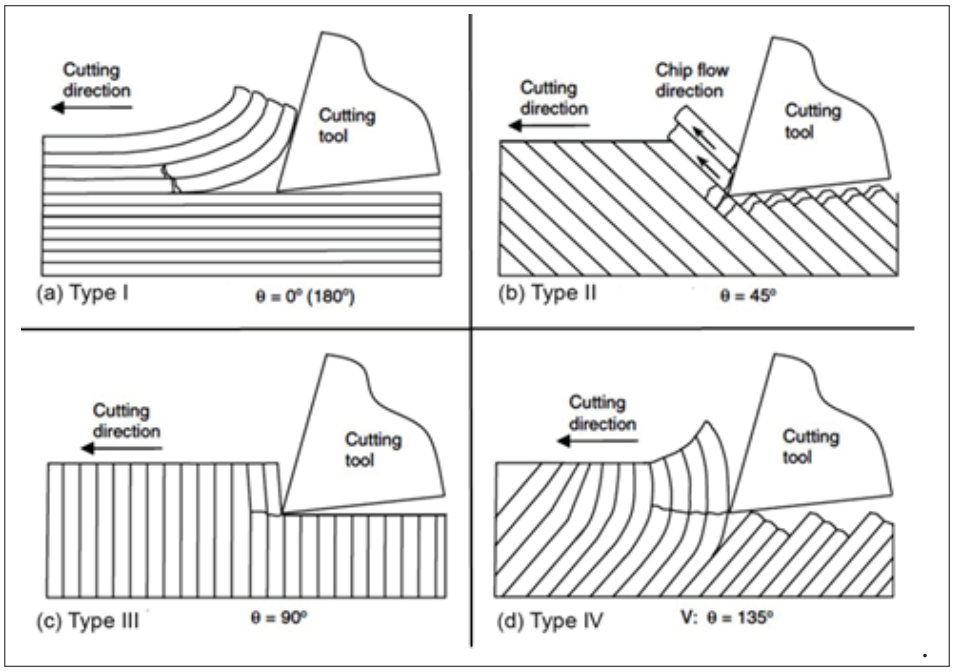

Figure 2.9 Cutting mechanisms in different fiber orientations – adapted from (Sheikh-Ahmad, 2009)

Delamination type chip formation (Type I) occurs for the 0° fiber orientation and positive rake angles (Figure 2.8 a), a crack starts at the contact point of the workpiece and tool; and it

grows along with the fiber-matrix interface. When the tool advances into the workpiece, the peeled layers bend and compress in the opposite direction to fibers. The fiber-matrix debonding continues until the bending stress in the fibers increases up to failure stress, and fiber failure happens ahead of the cutting tool.

The second type of chip formation (Type II) is fiber cutting with continuous chip that occurs for fiber orientations between 0° and 90° (Figure 2.8 b). The chip formation mechanism consists of fracture from compression-induced shear perpendicular to the fiber axis followed by shear fracture along the fiber–matrix interface occurring with the cutting edge movement. The cracks generated in the fibers above and below the cutting plane during the compression stage of the chip formation remain after machining and cause low quality machined surfaces.

For fibers at 90° orientation (Figure 2.8 c), fibers crush and fail at the contact point of the tool and the workpiece and each fiber is cut separately. The chip formation mechanism in this case is called fiber cutting type (with discontinuous chip).

For large fiber orientation angles (105°–150°) where the tool enters the workpiece and grabs onto a peeled fiber, the fiber-matrix interfacial failure occurs below the cutting plane (Figure 2.8 d). Fiber failure below the cutting plane occurs when the bending stresses that develop in the fibers below the surface of the cut are large enough for fracture. In this type of chip formation (type IV- macrofracture) discontinuous chips are formed. A poor surface quality consequences from this orientation because of comprehensive fiber pull-out and delamination cracking (Sheikh-Ahmad (2009), Teti (2002)).

2.7 Effect of milling parameters on tool wear and surface roughness

Another series of studies utilized experimental design to evaluate the effect of cutting tool material with respect to tool life. (Chao & Hwang, 1997) conducted experiments in milling CFRP composites to validate a Taguchi model with factors including feed rate, cutting speed, depth of cut, grade of carbide tool, and tool relief angle. In this work, the authors assumed the best operating condition was the combination of factors and levels that produced the minimum cutting

force which was measured by a 3 channel milling dynamometer. (Rahman, Ramakrishna & Thoo, 1999) performed a machining study of a 450AC carbon/PEEK thermoplastic with a 30% fiber volume fraction to investigate the effects of machining parameters on tool wear and surface quality of the workpiece. The design of experiments used factors including cutting speed, feed rate, depth of cut, and use of coolant. The tools employed in the study were uncoated cemented carbides. The authors found that depth of cut, feed rate, and cutting speed were the most significant factors affecting the amount of tool wear, while use of coolant had the least significant effect. Surface finish was found to improve until a critical cutting speed was reached and then became independent of the machining parameters above this speed. The cutting temperature at this critical cutting speed was found to exceed the glass transition temperature of the material, at which point the polymer becomes rubbery, thus cutting marks became indistinguishable. Also lower cutting force was encountered above the critical cutting speed.

In another study, (Davim & Reis, 2005) evaluated the effect of cutting parameters including cutting speed and feed rate on surface roughness and damage of a CFRP material with 55% fiber volume. The cutting tools were two-flute and six-flute cemented carbide K10 end mills each 6mm in diameter. Three levels of both cutting speed and feed rate were used in a L9 orthogonal array experiment for both types of end mills. Delamination factor was measured in addition to surface roughness. Multiple regression analysis (MRA) was used to correlate factors of cutting speed and feed rate to surface roughness and delamination factor. The R value, for the two-flute end mill was R=.93 for surface finish and R=.89 for the delamination factor. For the six-flute end mill, R=.94 for surface finish and R=.67 for the delamination factor. From the cutting tests, the two flute end mill was found to produce less damage on the CFRP composite than the six-flute end mill and had a smaller delamination factor. Feed rate was found to have a more significant influence than cutting speed on surface roughness and delamination factor for both end mill sizes. Surface roughness was found to increase with feed rate and decrease with cutting velocity. Delamination factor increased slightly with increasing feed rate for both size end mills.

(Ucar & Wang, 2005) performed experiments to characterize the wear behavior of chemical vapor deposition (CVD) diamond coated carbide tools during edge trimming of CFRP using

a low and high feed rate. The material used in the study was a CFRP laminate consisting of 12 plies of interwoven fiber fabric with a 50% fiber volume fraction. A four flute helical end mill was used in the study with (three) coating configurations. The first cutter configuration was an uncoated C2 grade tungsten carbide with medium grain size and 6% cobalt content. The second cutter used had a thin 10 μm diamond coating applied to the substrate by the hot filament CVD process and third cutter consisted of a thicker 20 μm diamond coating applied to the substrate. Measurements included cutting force, tool flank wear, and workpiece surface roughness. The diamond coated tools demonstrated much better performance in wear resistance than the uncoated tool at low and high feedrates. Wear of the diamond coated tools is dependent on the feed rate, where at low feed rates the tool wore by uniform abrasion of the diamond film and substrate, and at high feed rates the diamond film chipped with apparent delamination.

2.8 Dust generation during machining of CFRP

The cutting process is used to produce the final product from metallic materials. Despite the several advantages of cutting machines, the dust generated during the process is considered risky for workers and for the surrounding environment. In fact, all cutting processes produce aerosols in a liquid or solid form in different sizes that are harmful to both worker health and the environment. Carbon fibers are the major source of respirable dust because they may splinter lengthwise during machining producing fibrils of diameters less than 6 μm. Machining processes of CFRP produce both visible and invisible dust-like chips that may become airborne. Some of this dust might be small enough to make its way to the lower respiratory tract and hence poses a health hazard that is directly related to the dust generated during machining cannot be over looked. This dust can be inhaled and can even penetrate the skin or the eye, causing multiple irritations.

To date, only a few studies have focused on dust generated during machining of composites. Ramulu, Young & Kao (1999) reported that dust generated during the machining process can affect the torque during a drilling of graphite composite material. They found that tool geometry must be designed and chosen to minimize the amount of holes damaged in the

form of delamination. They reported a PCD four-face drill produced the highest-quality holes and suffered the least amount of wear. During the machining of metal matrix composites, Kremer & El Mansori (2009) found that a smooth coating tool produced more dust than a rough one. A later study conducted Kremer & El Mansori (2011) showed that the dust created during cutting of metal matrix composites is affected differently depending on the tool type.

In addition, studies were conducted by Haddad *et al.* (2012), Haddad *et al.* (2014) studied the effect of machining parameters on dust generation and particle counts. They used a GRIMM 1.209 dust monitor which measures the percentages of dust sizes from 0.25 μm to above 30 μm to estimate average particle size. The material was T700/M21 with a fiber volume of 59 %. Spindle speed was varied between 18570 and 74270 rpm with linear feed rate between 125 to 500 mm/min. Depth of cut was 2 mm and cutting direction was down milling. Highest particles were between 0.25 to 1 μm. Chip size measurements showed that 87 % – 95 % of the inhaled dust could reach the pulmonary alveoli. The number of particles were also found to increase with increasing cutting speed. The feed-rate appeared to have less of an effect at a constant cutting speed on the number of particles generated.

With respect to the metal matrix composite milling, Marani, Songmene, Kouam & Zedan (2018) found that the cutting conditions and the microstructure of the workpiece material have a direct impact on the dust generated. Recently, Songmene, Kouam & Balhoul (2018) found that fine particles generation is remarkably reduced by using Minimum Quantity Lubrication (MQL) in the polishing of granite, while ultrafine particle generation is insensitive to the use of water.

Despite the fact that various approaches for reducing particle emissions while machining composites have been suggested in the literature, there is not enough knowledge to reduce dust emissions when milling CFRPs in particular. As a result, the behaviour of particle emissions during the machining of CFRP composite was investigated in this study. Based on experimental results, the optimal cutting condition was then selected to reduce dust emissions throughout the machining process.

2.9 Cutting temperatures during machining of CFRP

The measurement of cutting temperature is important when dealing with carbon fiber-reinforced plastics (CFRPs). Temperatures higher than the glass-transition (Tg), temperature of the matrix resin are not favorable as it possibly causes the delamination and reduces its strength. In addition, the cutting temperature has long been recognized as an important factor influencing the surface quality of milled materials and the tool life. In order to decide the appropriate cutting condition which guarantees the soundness of CFRP after cutting, it is necessary to evaluate the highest temperature at the cutting point, and the temperature distribution of a machined surface layer. However, there is little research reported on the cutting temperature with respect to CFRP machining. If the cutting temperature exceeds the glass transition temperature of the thermosetting matrix resin, degradation of resin will occur within the machined surface or surface layer. For a typical epoxy-based CFRP material, this critical temperature is approximately 180°. The degradation of the resin causes delamination and reduces the strength, leading to serious defects Chatterjee (2009). In regard to CFRP cutting temperature measurement Yashiro, Ogawa & Sasahara (2013) measured the cutting temperature during machining of a CFRP composite laminate and the temperature distribution through the laminate thickness during machining. They used three measurement methods: one using an infrared camera, a second one using a tool–workpiece thermocouple, and a third one using embedded thermocouples between the layers of the composite. Their observations showed that the temperature at the tool–workpiece contact point reached 180° (the glass transition temperature) at 25 m/min of cutting speed and then increased to 300° at 50 m/min. The cutting temperature tended to stabilize and remain constant when the cutting speed was increased further. The cutting temperature in the workpiece material was relatively low (104°) compared to the tool–workpiece contact point, even at high cutting speeds (300 m/min). In a recent research, Liu *et al.* (2014) investigated the workpiece temperature variation in helical milling of CFRP. They concluded that the workpiece temperature increases with increasing spindle speed and axial cutting depth. They also showed that the axial cutting depth has more influence on the temperature variation of the workpiece than spindle speed, while the influence of the tangential feed per tooth is less than the other

factors. thus, cutting temperature not only plays a role in tool life and workpiece quality, but it can also affect dust particle size and concentration in the air, which can have adverse effects on health as described earlier in section 2.6.

2.10 Summary on the state of the art

Some issues of concern in the machining of CFRPs are brought to light from the above discussions on the state of the art as follows.

1) Machining of composite materials differs significantly in many aspects from machining of conventional metals and their alloys. In the machining of composites, the material behavior is not only non-homogeneous, but it also depends on diverse reinforcement and matrix properties, reinforcement architecture and orientation, and relative content of matrix and reinforcement.
2) Fiber orientation plays a major role in milling of composite materials. Fiber orientation is not constant and varies continuously with the cutting edge position. Further, chip formation is controlled by fiber orientation and is effectively a series of uncontrolled fractures where the chips exhibit very little plastic deformation as is observed in the case of metals. The matrix material also influences chip formation.
3) Tool wear changes the cutting edge geometry which also affects the cutting forces. Tool wear is in turn influenced by machining process parameters including cutting speed, feed rate, and depth of cut. Cutting edge sharpness is important to ensure the fibers are cut cleanly. Among the possible wear mechanisms, only abrasion, surface damage and sometimes adhesion are of significance for the machining of CFRP materials.
4) The cutting parameters have an influence on the surface finish and dust particle size and concentration. It is advisable to operate at high cutting speed and low feed rate to obtain lower roughness and delamination rate. These settings are also recommended to limit tool wear and thermal damage to the die.
5) Fine dust emitted during the machining of materials directly affects the machine operators' health. Several studies have focused only on factors affecting fine dust generated from the

machining of metal and metal matrix composites. However, few investigations have focused on the interaction effect of cutting force, cutting temperature, and dust emission in CFRP milling simultaneously.

CHAPTER 3

RESEARCH METHODOLOGY

This chapter provides information about the experimental methods and techniques utilized during this research work. Detailed description is provided in Papers I, II, and III. The chapter also provides detailed information about the workpiece and tool materials used, design of experiments, actual test setups and equipment utilized to measure input and output machining variables.

3.1 Design of experiments (DOE)

Any metal cutting operation is governed by different variables. These process variables have a controlling influence on the operation. Therefore it is essential to explore the opportunity of controlling these variables to make the operation as efficient as possible. Design of experiments (DOE) is a systematic approach to determine the influence of controlling factors on the output of the process (Montgomery, 2017). It is a method to understand the cause and effect relationship of a certain process. DOE approach mainly consists on the following phases as mentioned below;

Planning phase, This phase mainly deals with the activities based on problem statement, aims and objectives of experiments, development of experimental matrix with different levels of parameters and experimental setups to conduct experiments.

Execution phase, This phase consists of execution of experiments and collection of all output variables required to judge the process.

Results and analysis, in this phase results and conclusions have been drawn by analysing the experimental data sets. To validate the conclusions more experiments are required for confirmation.

3.2 Planning of experiments

CFRP milling operations are conducted under dry, and coolant conditions. In all of the appended publication, experiments were conducted using full factorial model. In this thesis, the phases of DOE were employed as per the following steps;

3.3 Tested hypothesis:

1) **The effectiveness of atomization based cutting fluid application.** (**Article I)**
   Purpose: to investigate the effects of atomization-based cutting fluid sprays system using two types of cutting fluids, a general purpose semi-synthetic coolant and vegetable-oil-based coolant as a sustainable alternative to conventional coolants in milling of CFRP.
2) **The impact of fiber orientation and its corresponding on cutting force, tool wear, and delamination during milling CFRP.** (**Article II)**
   Purpose: to investigate the impact of fiber orientation on tool wear when milling CFRP with particular fiber orientation angles of 0°, 30°, 45°, 60°, and 90° using vegetable oil-in-water emulsion obtained through ultrasonic atomization as an effective and environmentally friendly lubricant for improving the machining of CFRP.
3) **Effects of cutting temperature and its corresponding dust emission during milling CFRP.** (**Article III)**
   Purpose: to investigate interaction effect of cutting parameters (cutting speed, and feed rate) on the machining process performance indicators: Cutting force, specific cutting energy, cutting temperature, tool wear, and fine dust emission (in term of number of particles) during dry milling of CFRP.

3.4 Experimental work

1) **Identification of influencing processing parameters:** machining parameters (cutting speed, feed, depth of cut and cutting environment), cutting forces, tool wear, surface roughness, delamination, cutting temperature and Dust emission. For the atomization-based

cutting fluid sprays system additional parameters such as flow-rate, type of lubricant and nozzle orientation are also important.

2) **Selection of cutting conditions:** All cutting conditions were selected based on the tool factory's recommendations for the composite. These conditions should be chosen in a way that it does not exceed the maximum power and torque of the machine and also does not cause the tool to be damaged.

3) **Output parameters:** Outputs are the variables that are going to be measured during the experimental testing. Table 3.1 listed the outputs of the experiments and their measuring system. Aerodynamic particle sizer (APS).

Table 3.1 Sensors and equipment used for measurements

No.	Outputs	Measuring device/sensor
1	Cutting force	MiniDyn 9256C1 dynamometer
2	Tool wear	Optical microscope (Olympus BXFM)
3	Surface quality	3D Optical profiler (Zeta microscope)
4	Delamination	3D Optical profiler (Zeta microscope)
5	Chip morphology	Hitachi S-4800 FESEM
6	Cutting temperature	Type K thermocouple
7	Dust emission	(APS)

4) **Development of analytical model:** An analytical method for predicting the cutting temperature and its impact on cutting speed and dust emissions during routing machining (**Paper III**).

5) **Execution of experiments:** execution of experimental setups and collection of the experimental data.

6) **Results and analysis:** Analyze the data using the appropriate analysis techniques and interpret the results. At the same time some sets of experimental data will be used to validate analytical models.

3.4.1 Workpiece material

The workpiece material used in milling test was Multi-layer CFRP sheets of 1.56 mm (1/16 in) thickness were milled in each experiment. Each CFRP sheet consists of four unidirectional tapes of equal thickness that are laid up in (0F/90/0F/90/0F/90/0F/90).

3.4.2 Cutting tool material

The experimentation on milling setup was conducted using two types of cutting tools, uncoated tungsten carbide (WC-Co) 2-flutes end-mills and chip breaker router 6-flutes end-mills. Table 3.2 and 3.3 presents general specifications of the tools. These cutting tools were selected on recommendation of experts in the field of machining.

Table 3.2 Tool specification of uncoated tungsten carbide (WC-Co) 2-flutes end-mill

Cutting diameter	Flute length	Overall length	Rake angle	Clearance angle
3.175 mm	6.35mm	38.1mm	7°	30°

Table 3.3 Tool specification of chip breaker router 6-flutes end-mill

Cutting diameter	End cut	No of flutes	Flute length	Overall length	Helix
3.175 mm	Fish Tail	6	6.477 mm	38.1 mm	25°

3.5 Experimental setups

CNC milling center was used to perform all of the cutting experiments mainly for semi-finishing operation. Each test was repeated twice to reduce experimental errors. Kistler multi-channel dynamometer was utilized for measuring the cutting forces generated, more details in Section (3.6.1). In this research, the effectiveness of atomization based cutting fluid application in improving the machinability of CFRP is studied experimentally. A description of the atomization-based cutting fluid application system is provided in Section 3.5.

Figures 3.1, 3.2, and 3.3 show the experimental setups used to investigate different aspects of machining performance with respect to the papers numbers assigned in section I.

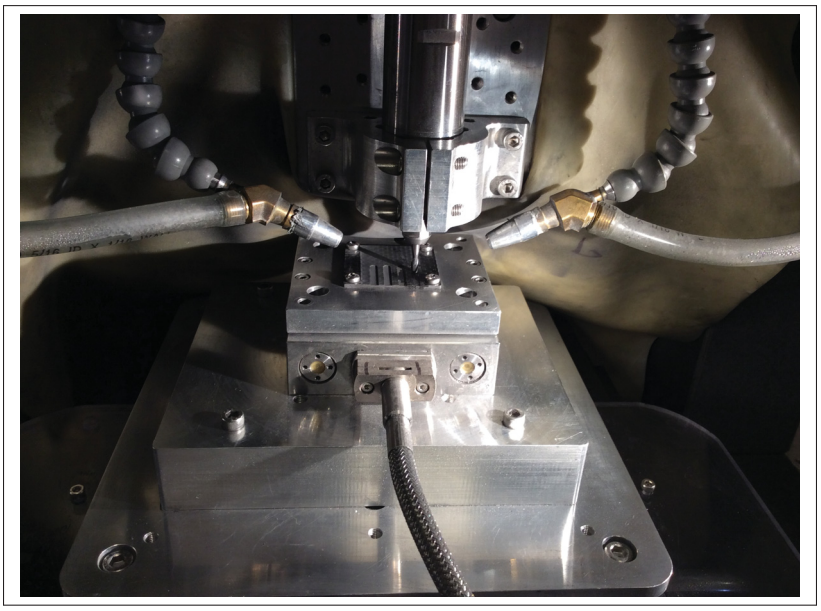

Figure 3.1 Experimental setups for Article I

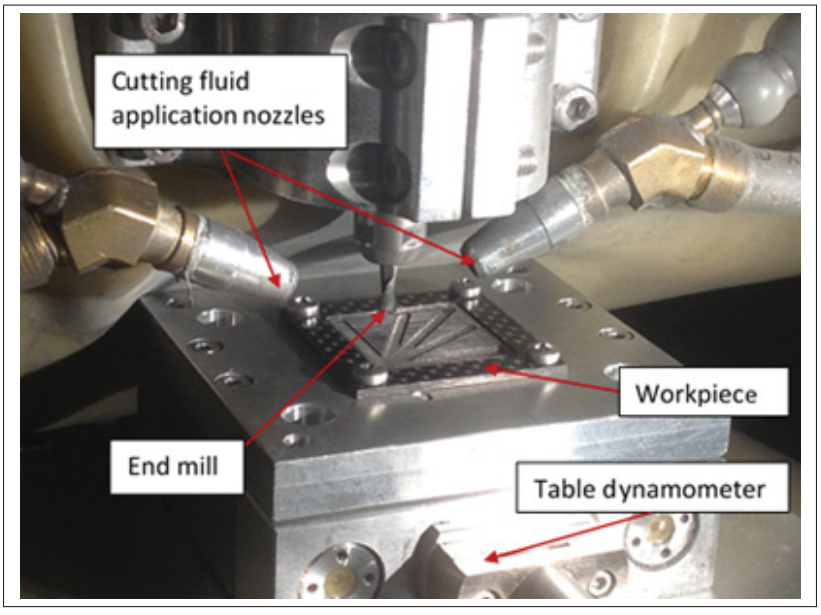

Figure 3.2 Experimental setups for Article II

Figure 3.3 Experimental setups for Article III

3.6 Description of atomization-based cutting fluid spray system

To study the effectiveness of applying atomized coolant, the experiments were carried out in dry condition and using two types of cutting fluid: (a) general-purpose multi-metal (TRIM®) SC520cutting fluids and (b) Canola vegetable oil. In both cases, the cut-ting fluid was diluted to 5% in volume by adding distilled water in the atomizer's reservoir. The atomized droplets are carried through the tube of 25.4 mm diameter and the air jet pipe has an inner diameter of 1.6 mm. The ultrasonic atomizer is a 22.0 mm diameter piezo transducer at 1 MHz For droplets generated by ultrasonic atomization, the droplet size generally depends on the frequency of ultrasonic vibration and fluid properties. The average droplet size of Canola vegetable oil around 2.1 μm. For comparison, conventional(TRIM®) SC520 mixed at 5% with water is also observed under an optical microscope and the size of oil droplets seems to be similar to that of canola oil droplets emulsified in water (Jun, Joshi, DeVor & Kapoor, 2008). The nozzles were aimed at the cutting zone with 45° so that the spray jet effectively wets and cools the cutting zone and simultaneously flushes away chips.

3.7 Measurements of machining variables

The equipment used to measure machining variables is discussed in detail in the below section.

3.7.1 Measurement of cutting force

Cutting forces were measured using a Kistler MiniDyn9256C1 dynamometer. The measured cutting force signals were digitized and transferred to the computer using a NI PCI-6133 data acquisition board. In order to obtain signal charge amplifiers (Kistler Type 5814B1) was used. A sampling rate of 100 kHz was used to process the measured force data, and the tool position coordinates were acquired at 100 Hz, which is the maximum capacity of the controller. Figure 3.4 shows cutting force data evaluation system. CutPro software program (developed by Prof Y. Altintas' team, University of British Colombia, Vancouver, Canada) was used to receive data from the DAQ board during the machining operation. The dynamometer is capable of measuring feed force (Fx), thrust force (Fy) and main cutting force (Fz) which occurs during milling operations. The resultant force is used as the measured cutting force, which can be found from Equation 3.1:

$$R = \sqrt{Fx^2 + Fy^2 + Fz^2} \tag{3.1}$$

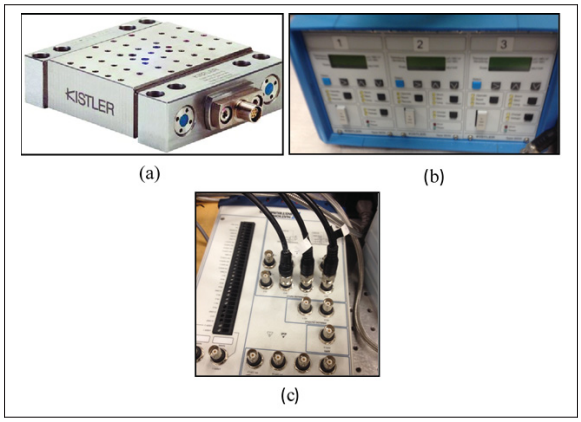

Figure 3.4 Cutting force data evaluation system, (a) Kistler MiniDyn 9256C1 Dynamometer, (b) Kistler 5814B1 charge amplifie,r and (c) NI PCI-6133 data acquisition board

Table 3.4 Specifications of kistler dynamometer

Model	**9256C1 (Dynamometer)**
Calibration Range (100%)	
Fx direction	0 - 250 (N)
Fy direction	0 - 250 (N)
Fz direction	0 - 250 (N)
Sensitivity (pC/N)	
Fx	-26
Fy	-13
Fz	-26
Overload (N)	
Fx, Fy, Fz	-300/300

3.7.2 Measurement of tool wear

In this study, changes in cutting edge evolution was taken into consideration. 3D Optical microscope was performed in order to determine the edge radius of the tool, the tools were cleaned by ultrasonicating in acetone at a frequency of 1000 kHz, temperature of 60 °C, and power of 60W for 30 min.

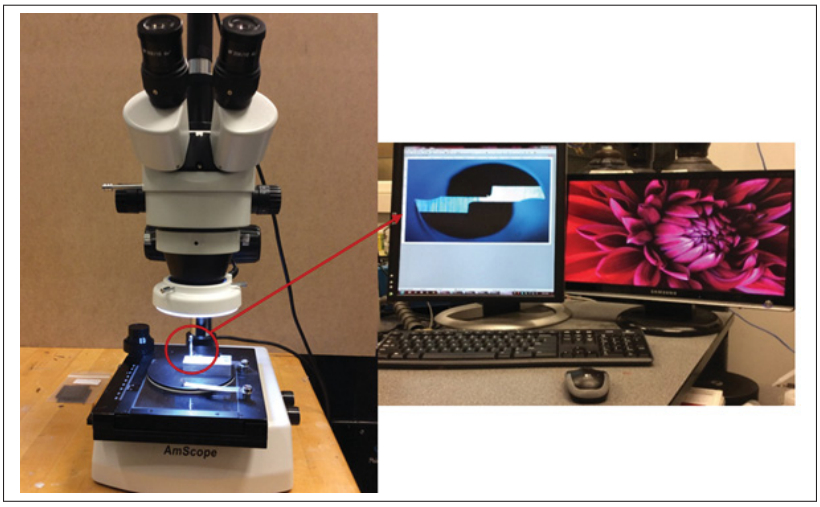

Figure 3.5 Tool wear under microscope

3.7.3 Measurement of surface roughness

The surface roughness (Ra) was measured with a 3D Optical profiler (Zeta microscope) as shown in Figure 3.6. The Z range selected to be 30 µm. The apparatus collects multiple images and the step size determines the number of images collected to calculate the surface roughness. The selected field of view is 474 µm × 356 µm. Figure 3.7 shows the data sheet generated to measure the surface roughness of the samples, for which a horizontal line has been drawn to calculate the mean Ra value (i.e. 1.602 µm). The 2D and 3D images of the same sample are shown in Figure 3.7. The measurements were carried out at the feed direction of slots. Finally, each measurement was replicated three times and the average value was utilized for the study.

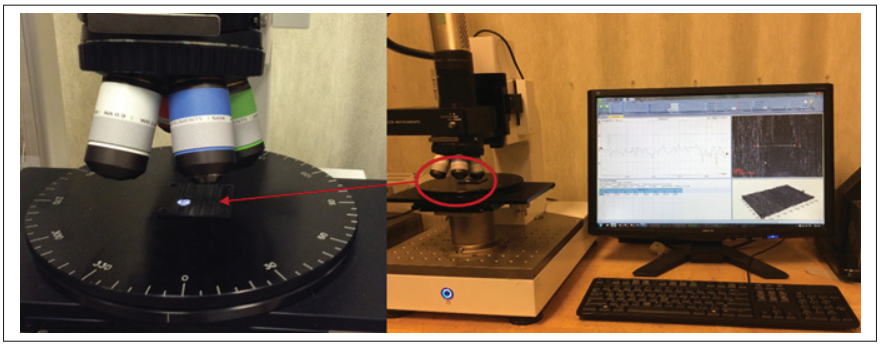

Figure 3.6 Surface roughness evaluated with a ZETA instrument

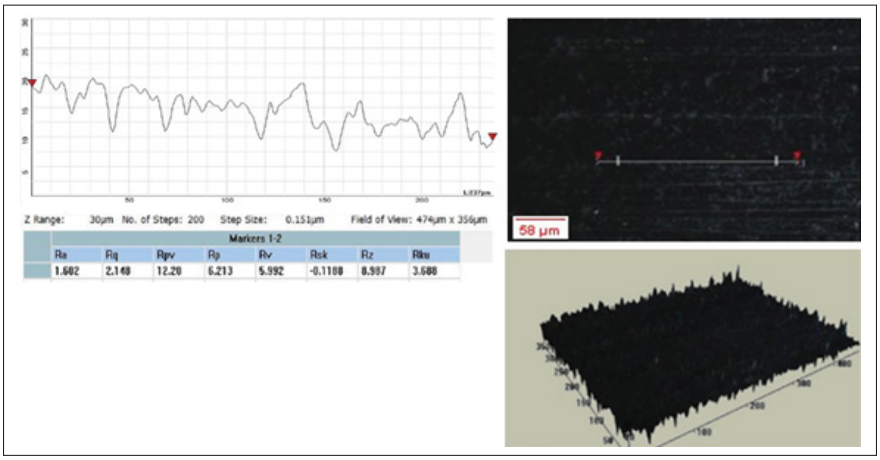

Figure 3.7 Surface roughness measurement

3.7.4 Measurement of chip formation

A scanning electron microscope (SEM, Hitachi S4800) was performed in order to evaluate the chip formation as shown in Figure 3.8. The lengths of exposed long fibers were estimated using Image J software.

Figure 3.8 Scanning Electron Microscope (SEM, Hitachi S4800)

Table 3.5 Specifications of Scanning Electron Microscope (SEM, Hitachi S4800)

Specifications
• 0.5 kV to 30 kV accelerating voltage
• 1 nm resolution at 15 kV, 1.4 nm at 1 kV
• Magnification from 30x to 800,000 x
• Maximum specimen size = 100 mm
• Super ExB filter technology
• Dry vacuum system
• X+Y motorized eucentric stage with trackball interface (tilt and Z by manual control)
• Ring-type YAG backscatter detector

3.7.5 Measurement of cutting temperature

Cutting temperature was measured on the rake face of the tool using a standard K type thermocouple. The chip breaker was carefully clamped on the tool rake face under the optical microscope so that the hot junction was mechanically fixed at a specified distance from the cutting edge.

3.7.6 Measurement of dust emission

Dust emission from milling operations was collected through the Aerodynamic Particle Sizer (APS, model 3321, TSI Inc., Shoreview, MN, USA) capable of measuring the aerodynamic size of particles from 0.5 to 20 microns. The dust samples were sucked by a pump (1.5 L/min) through a 10 mm suction tube, with the end of a tube placed near the machining area. The suction tube was connected to the dust measurement system, which consisted of aerodynamic particle sizer (APS) spectrometer. The collected data was then analyzed using the TSI's Aerosol Instrument Manager software as shown in Figure 3.9.

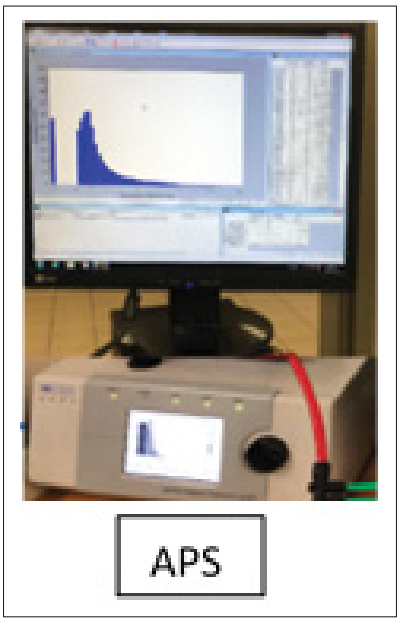

Figure 3.9 Aerosol Particle Sizer (APS)

CHAPTER 4

EFFECTS OF ATOMIZATION-BASED CUTTING FLUID SPRAYS IN MILLING OF CARBON FIBER REINFORCED POLYMER COMPOSITE

Tarek Elgnemi[a] , Keivan Ahmadi[a] Victor Songmene[b] , Jungsoo Nam[c]Martin B.G. Jun[c,*]

[a] Department of Mechanical Engineering, University of Victoria, 3800 Finnerty Road, Victoria, BC, Canada V8P 5C2
[b] Department of Mechanical Engineering, École de Technologie Supérieure (ÉTS), 1100 Notre-Dame West, Montreal, Quebec, Canada H3C 1K3
[c] Department of Mechanical Engineering, Purdue University, 610 Purdue Mall, West Lafayette, IN 47907, USA

Published in Journal of Manufacturing Processes 30 (2017) 133–140

Abstract

Carbon Fiber Reinforced Polymers (CFRP) are considered hard to cut materials, because of the abrasiveness of carbon fibers and the low transverse strength of the composite layers that leads to delimitation under machining forces. The application of cutting fluid is a common way of reducing tool wear and machining forces in machining of metallic materials, yet this solution cannot be applied in machining of CFRP, because moisture damages the structural integrity of the composite workpiece. In this paper, an experimental study is conducted to examine the feasibility and effectiveness of applying atomized cutting fluid in milling of CFRP. In the studied atomization-based method, the cutting fluid is broken down into micrometer size droplets that are sprayed directly into the cutting zone. In the presented study, two types of cutting fluids, general purpose semisynthetic coolant and vegetable oil, are applied by atomization, and their performances in reducing cutting forces, tool wear, surface roughness, and delamination are studied over a range of cutting speeds and feed rate values.

Keywords: Cutting fluid, CFRP composite, Milling, Atomization

4.1 Introduction

Carbon Fiber Reinforced Polymers (CFRP) offer a higher strength to weight ratio and superior corrosion and fatigue resistance com-pared to traditional metals. Mechanical machining processes such as milling and drilling are usually a critical part of the assembly and finishing stage of producing CFRP parts in a wide range of applications such as aerospace, automotive, and biomedical devices. The machinability of CFRP materials is limited by the excessive tool wear due to the abrasiveness of carbon fibers, and by the machining induced damages such as delamination that is caused by the low interlaminar strength of composite layers (Teti, 2002), (Rahman *et al.*, 1999), (Santhanakrishnan *et al.*, 1988), (Bhatnagar *et al.*, 1995). The application of cutting fluid is a common solution for increasing the tool life and reducing cutting forces in the machining of metallic materials. Cutting fluid dissipates the generated heat and reduces the friction between the chip and the cutting edge, and consequently lowers the tool wear, reduces cutting forces, and improves the extent of machining induced damages (Brinksmeier, Walter, Janssen & Diersen, 1999), (Shaw, Pigott & Richardson, 1951). Nevertheless, the application of cutting fluid in the machining of CFRP is not common, because moisture damages the structural integrity of CFRP (Turner, Scaife & El-Dessouky, 2015). Devising a cutting fluid application method that provides the lubricating and cooling effects of the cutting fluid without it being absorbed into the material could significantly improve the tool life and reduce cutting forces in the machining of CFRP. In addition, the application of cutting fluid could reduce the level of the dust and airborne contaminations that are dispersed into the shop environment and cause hazard to the health of the operator, and damage the machine tools.

Atomization-based cutting fluid application has been studied as an effective method of cooling and lubricating the cutting zone in several applications such as micromachining (Han, Liu & Sun, 2005), (Mathews, Lee & Peters, 2003), (Jun *et al.*, 2008). In this method, the atomized cutting fluid is sprayed directly into the cutting zone to lubricate the chip and tool interface, and also to dissipate the generate heat by fast evaporation. Because of the significantly higher evaporation rate of the atomized cutting fluid, the applied coolant does not absorb into the workpiece material.

Therefore, atomization of the cutting fluid may provide a viable method for applying cutting fluid in CFRP cutting.

In this paper, the effectiveness of atomization based cutting fluid application in improving the machinability of CFRP is studied experimentally. CFRP milling operations are conducted in a range of cutting speed and feed rate values in dry condition, and using two types of cutting fluids, a general purpose semisynthetic coolant and vegetable-oil-based coolant as a sustainable alternative to conventional coolants. The resulting cutting forces, tool wear, surface roughness, and delamination are measured to study the machinability of CFRP in each test.
In the next section, a brief description of the atomization-based cutting fluid application system is provided. In Section 4.3, the experimental setup and the design of experiments are described. The measured cutting forces, tool wear, surface roughness, and delamination are discussed in Section 4.4.

4.2 Atomization-based cutting fluid spray system

A schematic of the cutting fluid application system that is used in this study is shown in Figure 4.1. This system is similar to the atomization setup that was used in (Jun *et al.*, 2008). An experimental evaluation of an atomization-based cutting fluid application system for micromachining. A brief description of the atomization-based cutting fluid application system is presented in this section; more details are available in. An experimental evaluation of an atomization-based cutting fluid application system for micromachining. As shown in Figure 4.1, the ultrasonic vibrations of the piezoelectric actuator breaks down the cutting fluid that is stored in the reservoir into micrometer diameter droplets. The atomized cutting fluid is carried through the fluid application pipe with the aid of a low velocity air. A small diameter pipe that lies inside the coolant pipe delivers the highpressure air to the tip of the coolant pipe to spray the atomized fluid into the cutting zone.

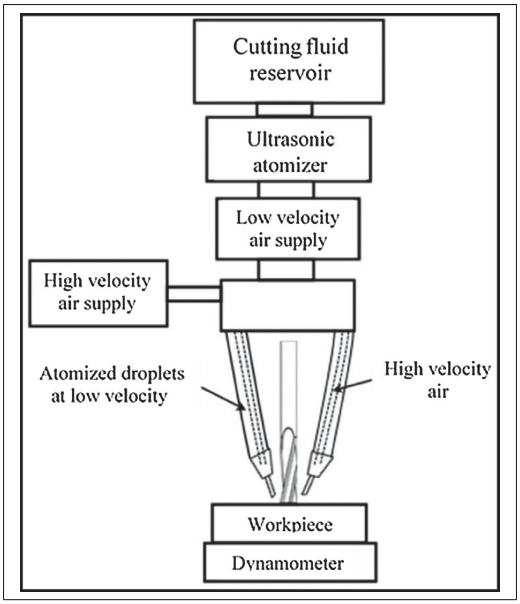

Figure 4.1 A schematic design of the atomization-based cutting fluid application system

4.3 CFRP milling experiments

4.3.1 Experimental setup and conditions

The experimental setup is shown in Figure 4.2 (a). The nozzle is directed to the cutting zone, so that the spray jet effectively wets and cools the cutting zone and simultaneously flushes away chips. Milling experiments were performed using a custom built machine tool (Alio Industries). The machine tool is equipped with a NSK E800Z spindle with maximum applicable speed of 80,000 rev/min. Two-fluted flat end mills of 3.175 mm in diameter are used for milling operations. The dimensions of the end mill are shown in Table 4.1. Cutting forces are measured using a Kistler MiniDyn 9256C1 dynamometer. The measured cutting force signals were digitized and transferred to the computer using a NI PCI-6133 data acquisition board. The shape of the generated chips, quality of machined surface, and delamination formations are evaluated using an optical microscope (Olympus BXFM) and a Scanning Electron Microscopy (SEM, Hitachi S4700).

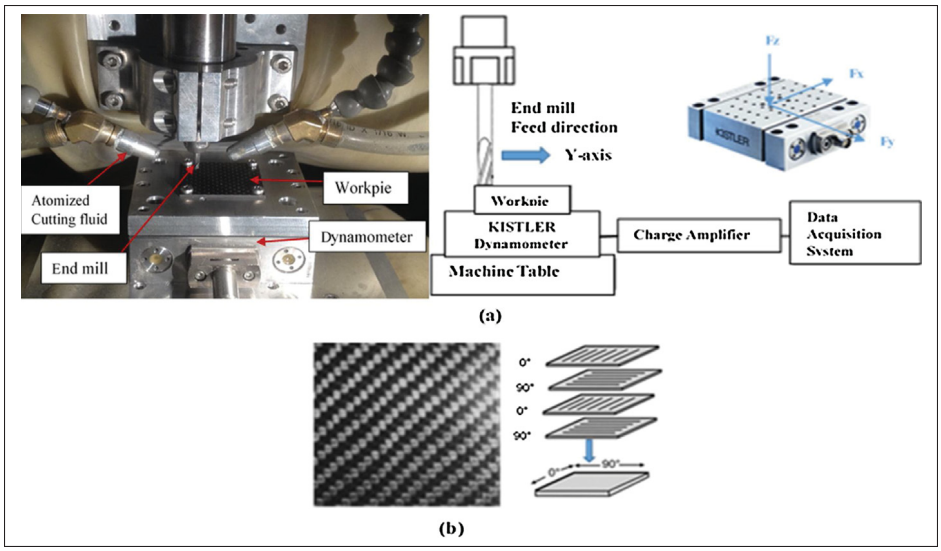

Figure 4.2 (a) Experimental setup, (b) Composite lay-up

Table 4.1 Tool specifications

Cutting Diameter	Flute Length	Overall Length	Rake Angle	clearance Angle
3.175 mm	6.35mm	38.1mm	7°	30°

To study the effectiveness of applying atomized coolant, the experiments were carried out in dry condition and using two types of cutting fluid: (a) general-purpose multi-metal (TRIM®) SC520 cutting fluids and (b) Canola vegetable oil. In both cases, the cutting fluid was diluted to 5% in volume by adding distilled water in the atomizer's reservoir. The atomized droplets are carried through the tube of 25.4 mm diameter and the air jet pipe has an inner diameter of 1.6 mm. The ultrasonic atomizer is a 22.0 mm diameter piezo transducer at 1 MHz For droplets generated by ultrasonic atomization, the droplet size generally depends on the frequency of ultrasonic vibration and fluid properties. The average droplet size of Canola vegetable oil around 2.1 μm. For comparison, conventional (TRIM®) SC520 mixed at 5% with water is also observed under an optical microscope and the size of oil droplets seems to be similar to that of canola oil droplets emulsified in water (Jun *et al.*, 2008). Multi-layer CFRP sheets of 1.56 mm (1/16 in) thickness were milled in each experiment. Each CFRP sheet consists of four unidirectional tapes of equal thickness that are laid up in (0F/90/0F/90/0F/90/0F/90) configuration as shown in

Figure 4.2 (b). The approximate fiber volume in each tape is 54%. The Young's modulus of the fibers was estimated at 225 GPa and the Young' modulus of the sheets was estimated at 65 GPa.

4.3.2 Design of experiments

The effect of various machining parameters and cooling methods on the machinability of CFRP is studied by conducting a full factorial experimental design. The three machining parameters that are studied include a) feed rate, b) cutting speed, and c) cooling method. Three feed rate levels (2, 4, and 6 micrometers/tooth), two cutting speed levels (20,000 and 40,000 rev/min), and three cooling methods (dry, conventional coolant, and vegetable oil) were examined in the experiments. A full factorial design of experiments across the three factors of feed, speed, and cooling type, and their corresponding levels require 3 × 2 x 3 = 18 experiments. The cutting conditions in each of the 18 experiments are listed in Table 4.2.

Table 4.2 Design of experimental layout using an L18 orthogonal array (Atomization based cutting fluid, ACF)

NO	Cutting Fluids	Feed [μm/tooth]	Speed [rpm]
1	Dry	2	20,000
2	Dry	4	20,000
3	Dry	6	20,000
4	Dry	2	40,000
5	Dry	4	40,000
6	Dry	6	40,000
7	ACF (conventional coolant)	2	20,000
8	ACF (conventional coolant)	4	20,000
9	ACF (conventional coolant)	6	20,000
10	ACF (conventional coolant)	2	40,000
11	ACF (conventional coolant)	4	40,000
12	ACF (conventional coolant)	6	40,000
13	ACF (vegetable oil)	2	20,000
14	ACF (vegetable oil)	4	20,000
15	ACF (vegetable oil)	6	20,000
16	ACF (vegetable oil)	2	40,000
17	ACF (vegetable oil)	4	40,000
18	ACF (vegetable oil)	6	40,000

In each of the experiments, a new tool was used and eight slots of 18 mm length were cut with full-immersion milling. The axial depth of cut was 0.3 mm in all of the experiments.

4.4 Experimental results

4.4.1 Cutting forces

The peak-to-peak values of the measured cutting forces in the conducted experiments are shown in Figure 4.3. Each diagram in Figure 4.3 shows the peak-to-peak magnitudes of the resultant forces during the machining of eight slots using a specific feed rate, spindle speed, and coolant type. Regardless of the feed rate or spindle speed, two important observations are consistently made in all of the experiments. The first observation is that the cutting forces are higher in dry cutting, and reduce when the atomized coolant is used. This observation may be attributed to the reduction in the friction between the chip and the rake face of the tool, or the alteration of the chip formation mechanism when atomized coolant is used. The second observation is that under identical cutting conditions, cutting forces increase as we move from the first slot to the eighth slot. The rate at which the forces increase is the fastest in dry cutting and the slowest when atomized vegetable oil is used.

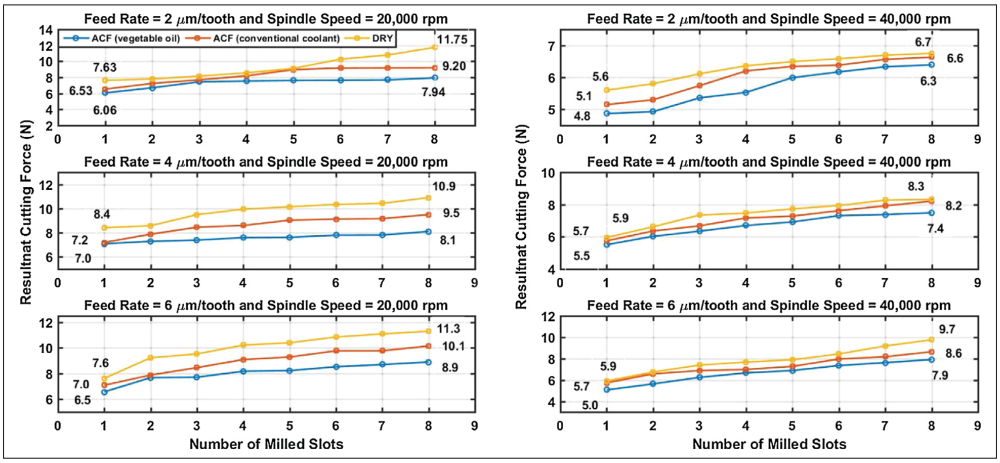

Figure 4.3 Resultant cutting forces with different cutting fluid conditions at the feed rates

This observation can be explained due to the higher rate of the tool wear in dry cutting and slower tool wear when atomized vegetable oil is used. Our observation of the tool wear progression is described in Section 4.4.2 which confirms the correlation between the increase in the tool wear and the cutting forces.

The bar diagram in Figure 4.4, shows the average of the measured resultant cutting forces across all of the eight slots. Expectedly, the cutting forces increase proportionally as the feed rate (i.e. chip thickness) increases. Also observed in the presented diagram is the consistently lower cutting forces in the tests that were conducted at 40,000 rev/min spindle speed compared to the ones that were performed at 20,000 rev/min. Cutting speed may affect the mechanics of chip formation in two competing ways (Sheikh-Ahmad, 2009), (Dandekar & Shin, 2012), (Wang, Ramulu & Arola, 1995). A higher cutting speed increases the strain rate at which the chip is formed, which may result in increasing cutting forces. At the same time, more heat is generated in high speed cutting, which softens the material and reduces the forces. Depending on the workpiece material and cutting condition, either of these effects may dominate the process and increase or decrease the resulting forces. In the experiments conducted in this work, we consistently observe higher forces at lower (20,000 rev/min) speed than in higher (40,000 rev/min) speed.

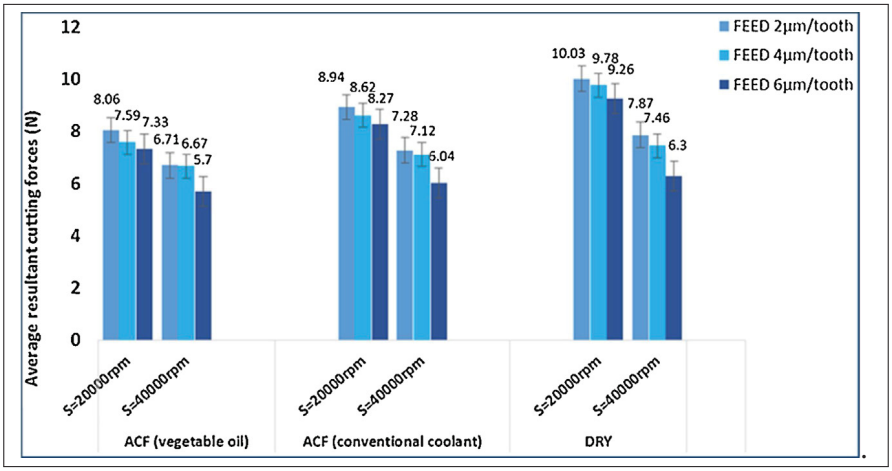

Figure 4.4 Average resultant cutting forces over the number of slots with different cutting fluid conditions

4.4.2 Tool wear

The cutting edge photographs were taken using a 3D Optical microscope (Zeta microscope). Figure 4.5 shows tool wear after the eighth slots milled using the cutting conditions and coolant types that are indicated on the figure. Also a photograph of the sharp cutting edge is shown in Figure 4.6. Comparing the images of the cutting edges in Figure 4.5 with the image of the sharp edge in Fig. 4.6, it is evident that regardless of the type of the coolant, cutting edges develop a larger edge radius due to abrasive tool wear. Considering the increase in the edge radius as a measure of the tool wear, one can see that the tool wear is significantly higher in dry cutting, compared to the experiments where atomized coolant was used. To present a quantitative comparison of the tool wear progression, tool wear is characterized by the reduction in the surface area of the cutting edge as it is observed under the microscope.

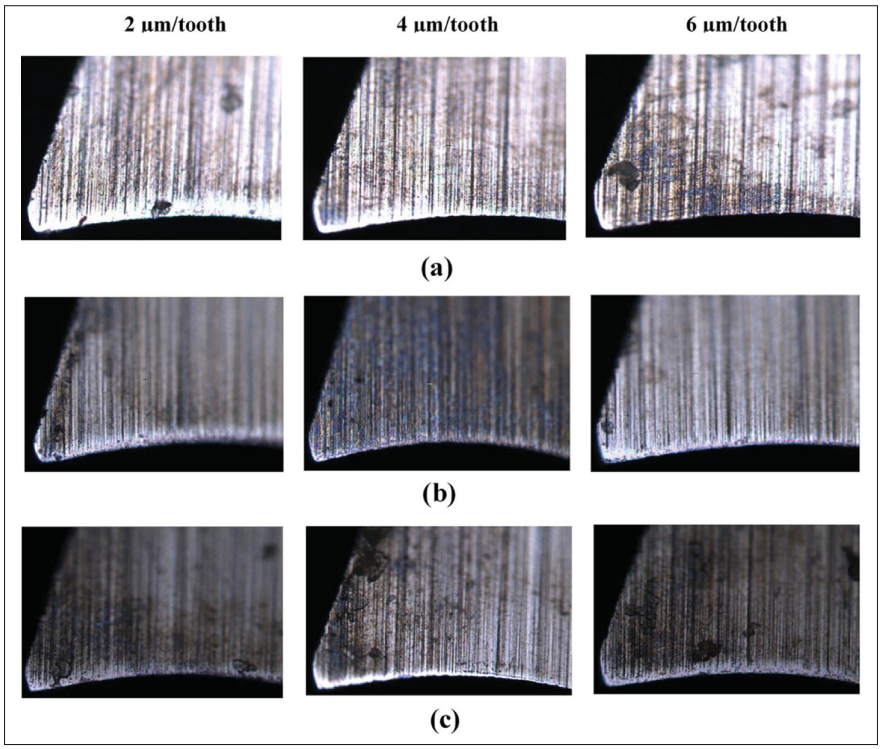

Figure 4.5 Progression of wear after milling 8 slots of (a) Dry, (b) Atomization-based spray with conventional cutting fluids and (c) Atomization-based spray with vegetable oil

Figure 4.6 shows the microscope images of a sharp cutting edge and the microscope image of the same cutting edge after milling eight slots in test number two. The hone radius of the sharp cutting edge is assumed to be negligible and two lines (l_{s1} and l_{s2}) are fitted tangential to the rake and clearance faces of the cutting edge, as shown in Figure 4.6, the angle between l_{s1} and l_{s2} was measured at 60°. Similarly,two lines (l_{w1} and l_{w2}) are fitted tangential to the rake and clearance faces of the worn tool while maintaining 60° angle between the fitted lines. Circle C is also plotted on the image of the worn edge such that C is tangential to l_{w1} and l_{w2} and passes through the tip of the worn cutting edge. The area that is confined between the fitted circle (C) and the two lines (l_{w1} and l_{w2}) is computed numerically and is considered as the resulting tool wear area.

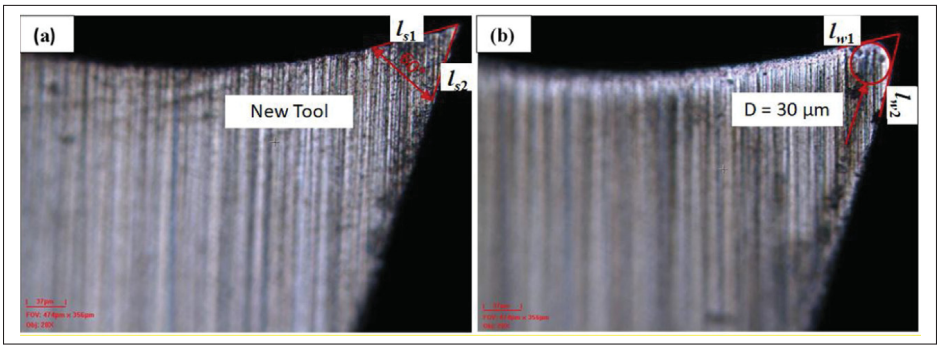

Figure 4.6 Images of cutting tool, (a) fresh end-mill, (b) corner diameter End-mill

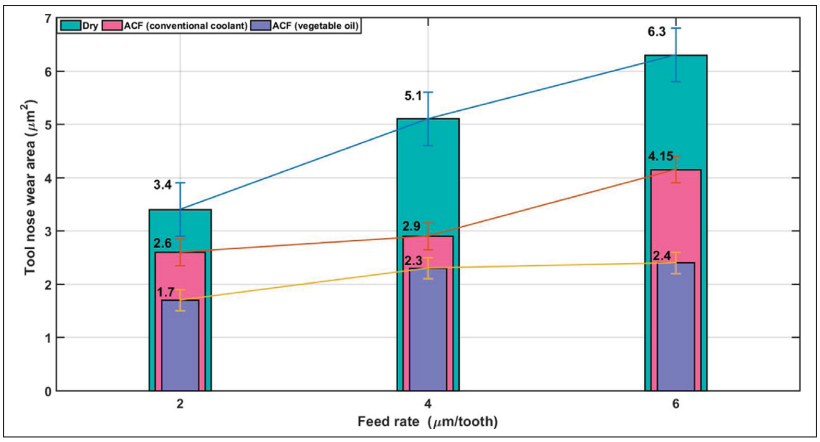

Figure 4.7 Variation of wear on cutting edge with feed rate at 20,000 rpm

The estimated tool wear area in the tests that were conducted at 20,000 rev/min spindle speed is shown in Figure 4.7. Regardless of the type of the coolant that is used, the tool wear area increases by increasing the feed rate. Also, in all of tested feed rate values, dry cutting leads to a significantly higher wear and applying atomized vegetable oil results in the smallest wear.

4.4.3 Surface quality

A 3D Optical profiler (Zeta microscope) was used to measure the surface roughness in the feed direction of the slots. Figure 4.8 shows the Ra values of the measured surface roughness curves in all the 18 tests. As shown in this figure, surface roughness is consistently lower in higher cutting speed, 40,000 rev/min, compared to the tests at 20,000 rev/min. Improvement in the surface finish by increasing the cutting speed has also been reported in the literature and may be attributed to the change in the mechanics of chip formation in higher speed.

The effect of using atomized coolant on improving the roughness of the machined surface is evident from Figure 4.8. A significantly higher surface roughness is observed in dry cutting, compared to the tests conducted using atomized coolant. Slight improvement in surface roughness is also observed when vegetable oil was used, compared to the conventional coolant.

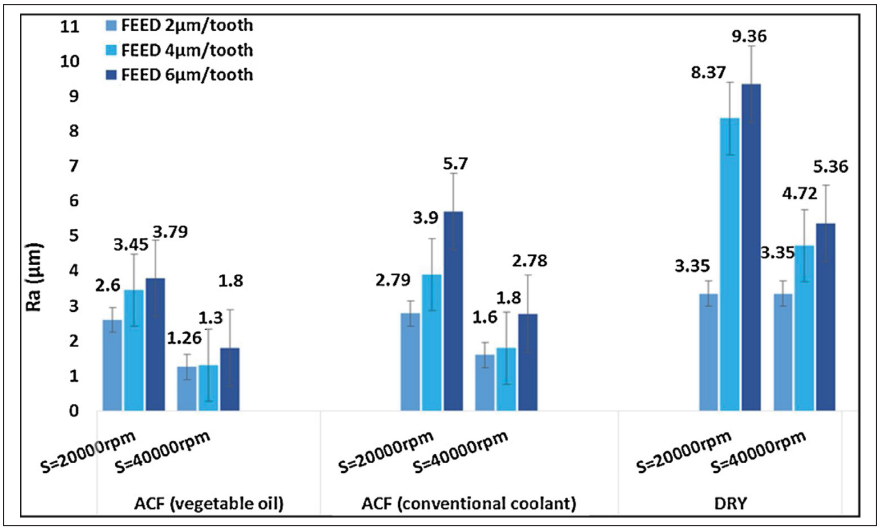

Figure 4.8 Surface roughness of CFRP with different cutting fluids and feed rates at speed 20,000 and 40,000 rpm

4.4.4 Data analysis

Analysis of variance (ANOVA) is a statistical technique used todetermine the main effects of the process parameters and to estab-lish the optimal conditions. Table 4.3 lists the ANOVA and F-testresults for Ra as an example. Critical F value at 0.05 (F_{crit}(0.05))is quoted from Statistical Tables. If the calculated F values exceed F_{crit}(0.05) (Table 4.3), then the contribution of the input parameters,such as spindle speed, is defined as significant. Thus, the significantparameters can be categorized into two levels which are signif-icant and sub-significant. All of them are based on the fact thatthe F values are much larger than F_{crit}(0.05) and denoted as **and * respectively. For instance, to evaluate the Ra, the significantparameter is spindle speed. The remaining parameters only slightlycontribute to the evaluation of the Ra. Similar calculations are alsoapplied in evaluating the cutting force as shown in Table 4.4. For cut-ting forces, feed rate and cutting fluids were found to be significantand sub-significant parameters, respectively.

Table 4.3 ANOVA table for Ra

Parameter	DOF	SS	MS	F	F_{crit}(0.05)	Contribution%
Spindle speed	1	20.866	20.866	19.14 **	4.45	23.66
Feed rate	2	16.372	8.186	7.51	3.59	9.26
Cutting fluids	2	37.879	18.940	17.38 *	3.59	21.47
Error	12	13.080	1.090			45.61
Total	17	88.179				

Table 4.4 ANOVA table for cutting force

Parameter	DOF	SS	MS	F	F_{crit}(0.05)	Contribution%
Spindle speed	1	3.191	3.191	12.281	4.45	7.68
Feed rate	2	30.549	15.274	119.67 **	3.59	36.78
Cutting fluids	2	6.222	3.111	23.94 *	3.59	7.49
Error	12	1.559	0.1299			48.05
Total	17	41.521				100

** Significant parameter

* Sub significant parameter

4.4.5 Delamination and chip formation

Delamination of composite layers appears in various forms such as fiber pull-out, broken fibers, and irregular edges. Figure 4.9 shows the images of the eighth slots that are machined using various feed rate values and cooling types at 20,000 rev/min. As shown in this figure, delamination appears in dry cutting in the form of fiber pullout. When atomized coolant is applied, delamination in the form of irregular and broken edges at the top of the slots is more evident. In addition, the application of coolant leads to accumulation of the generated dust and debris in the corners of the slots due to surface tension, whereas in dry cutting the generated dust tends to disperse in the air as shown in Figure 4.10.

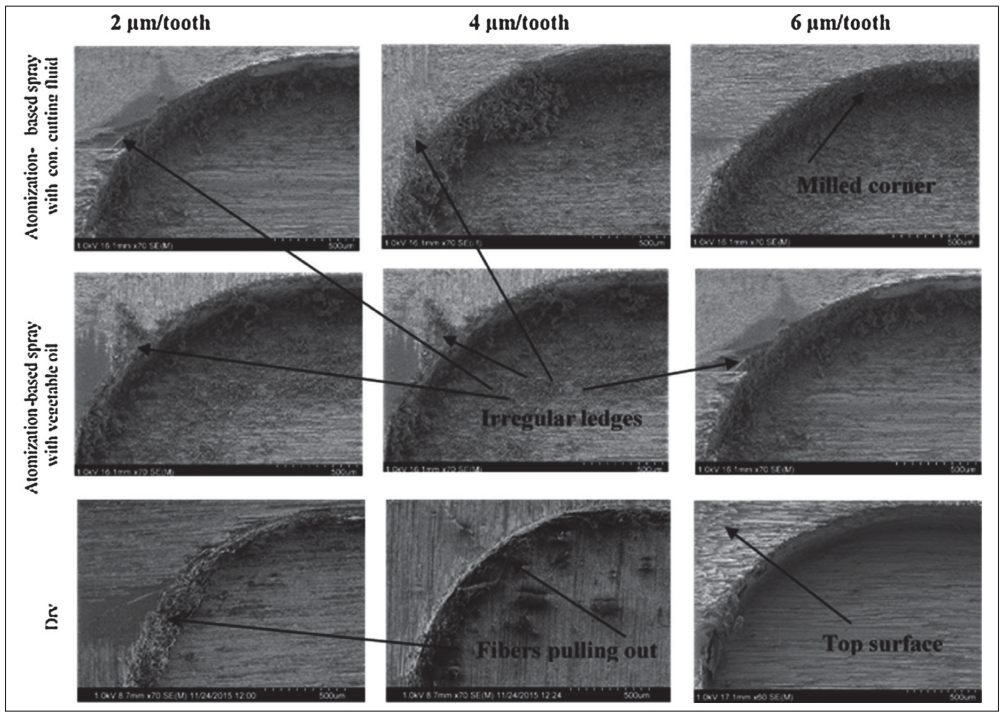

Figure 4.9 Photographs of burrs formed on the corner slot after machining eight slots

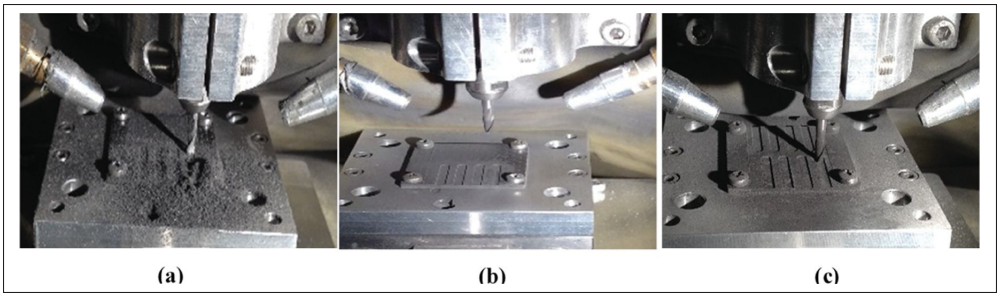

Figure 4.10 Dust sticking in machined slots for different cutting fluid conditions. (a) Dry, (b) ACF vegetable oil, (c) ACF conventional coolant

4.4.6 Chip morphology

CFRP chip are broken into smaller dust particles because of high abrasive characteristic. To evaluate the chip morphology, chips were collected during the machining of CFRP, and then imaged and examined using the SEM. Figure 3.11(a)–(c) show the SEM pictures of machined CFRP at different machining conditions. It is observed from the figure that with lower feed rate 2 μm/tooth the chips collected showed small fragmented chips indicating crushing failure, while the chips collected at higher feed rate 6 μm/tooth were significantly longer.

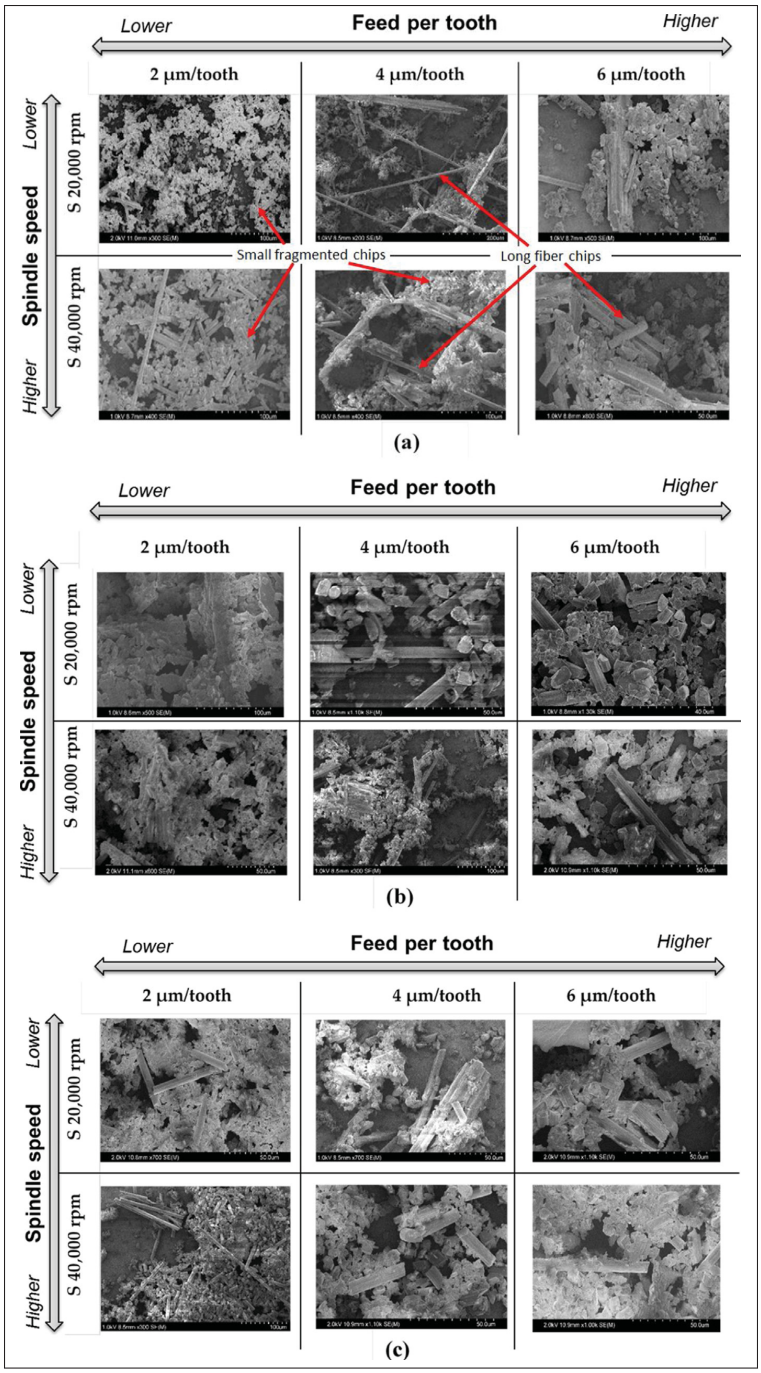

Figure 4.11 SEM photographs of generated CFRP chips with (a) Dry, (b) ACF with vegetable oil, (c) ACF with conventional cutting fluids

4.5 Conclusions

The feasibility and effectiveness of applying atomized cut-ting fluid in improving the machinability of CFRP was studied experimentally. Compared to milling in dry condition, after the application of atomized cutting fluid to the cutting zone, cut-ting forces and tool wear improve significantly. Also, significant improvement in surface roughness was observed. In addition, the application of cutting fluid reduces the level of dust and air-borne contamination that are generated in machining. Analysis of variance (ANOVA) results show that the process parameters significantly affect the performance characteristics. Spindle speed mainly affects the Ra and the feed rate largely affects the cutting force. Delamination and chip shape were compared qualitatively, but further studies are needed to determine the effect of applying cutting fluid on the extent and type of delamination and chip formation process. Atomized general purpose semisynthetic coolant and vegetable oil coolants were examined in this study. The application of vegetable oil was more effective in reducing cutting forces and improving the tool wear.

CHAPTER 5

MILLING PERFORMANCE OF CFRP COMPOSITE AND ATOMISED VEGETABLE OIL AS A FUNCTION OF FIBER ORIENTATION

Tarek Elgnemi[1] , Martin B.G. Jun[2] Victor Songmene[1,*] , Agnès Marie Samue[1]

[1,3] Department of Mechanical Engineering, École de Technologie Supérieure (ÉTS), 1100 Notre-Dame West, Montreal, Quebec, Canada H3C 1K3
[2] Department of Mechanical Engineering, 610 Purdue Mall, West Lafayette, IN 47907, USA

Published in journal of Materials 2021, 14, 2062

Abstract

Carbon fiber reinforced polymers (CFRPs) have found diverse applications in the automotive, space engineering, sporting goods, medical and military sectors. CFRP parts require limited machining such as detouring, milling and drilling to produce the shapes used, or for assembly purposes. Problems encountered while machining CFRP include poor tool performance, dust emission, poor part edge quality and delamination. The use of oil-based metalworking fluid could help improve the machining performance for this composite, but the resulting humidity would deteriorate the structural integrity of the parts. In this work the performance of an oil-in-water emulsion, obtained using ultrasonic atomization but no surfactant, is examined during the milling of CFRP in terms of fiber orientation and milling feed rate. The performance of wet milling is compared with that of a dry milling process. The tool displacement-fiber orientation angles (TFOA) tested are 0∘, 30∘, 45∘, 60∘, and 90∘. The output responses analyzed were cutting force, delamination, and tool wear. Using atomized vegetable oil helps in significantly reducing the cutting force, tool wear, and fiber delamination as compared to the dry milling condition. The machining performance was also strongly influenced by fiber orientation. The interactions between the fiber orientation, the machining parameters and the tested vegetable oil-based fluid could help in selecting appropriate cutting parameters and thus improve the machined part quality and productivity

Keywords: CFRP, dry/vegetable oil, Cutting force, Delamination, Tool edge rounding

5.1 Introduction

Carbon fiber reinforced polymers (CFRP) find many industrial applications (automotive, aerospace, sporting goods, medical and military) because of their very attractive specific strength, specific modulus, damage tolerance characteristics (Wang, Liu, An & Chen, 2017), (Hu & Zhang, 2004), and resistance to fatigue and corrosion (Dandekar & Shin, 2012), (Che, Saxena, Han, Guo & Ehmann, 2014). Despite their many promising outlooks, the machinability of CFRPs has often been poor because of excessive tool wear, machining-induced delamination, fiber fragmentation, pull-out and spalling (Bhatnagar *et al.*, 1995), (Rahman *et al.*, 1999), (Santhanakrishnan *et al.*, 1988), (Teti, 2002), (Ho-Cheng & Dharan, 1990), (Chen, 1997), (Che *et al.*, 2014). In particular, abrasive carbon fibers rapidly wear out the tool, changing its geometry and damaging the subsurface of the work piece (Shen *et al.*, 2015). Alternative machining strategies must be found to shape CFRPs parts with acceptable tool life and good part quality: accuracy and less surface and subsurface damages.

Structural CFRP parts are shaped using milling process and then drilled in order to assemble them (riveting, bolting) with other components (Calzada, Kapoor, DeVor, Samuel & Srivastava, 2012), (Geng *et al.*, 2019). Most researchers recognize the difficulties in applying knowledge obtained during machining of metals or other type of materials to CFRPs because of inhomogeneity, anisotropy and damages occurring during cutting (Koenig, Wulf, Grass & Willerscheid, 1985), (Xu & Zhang, 2015), (Ramulu, Faridnia, Garbini & Jorgensen, 1991). In fact, during machining of CFRPs, plowing, cutting, and cracking occur (Wang *et al.*, 1995), (Pwu & Hocheng, 1998), (Turner *et al.*, 2015) whereas the machining of metals takes place by shearing and plastic deformation. The machining of CFRPs is also influenced by the machining parameters and conditions which affect the cutting force/temperature and therefore the tool wear and the part quality (Ghafarizadeh, Lebrun & Chatelain, 2016), (Liu *et al.*, 2014). It is thus understandable that several studies investigated the machining of CFRPs in order to propose optimal machining parameters and conditions (KOPLEV *et al.*, 1980), (Sakuma & Seto, 1983), (Takeyama & Iijima, 1988), (Hocheng, Puw & Huang, 1993), (Zhang, Zhang & Wang, 2001), (Wang & Zhang, 2003), (Sheikh-Ahmad & Yadav, 2008), (Lopez de Lacalle, Lamikiz, Campa, Valdivielso & Etxeberria,

2009), (López de Lacalle & Lamikiz, 2010), (Karpat, Bahtiyar & Değer, 2012), (Shahrajabian, Hadi & Farahnakian, 2012). These works demonstrate, among other things, the influence of cutting direction relative to fiber orientation on the machinability of CFRPs, particularly on tool wear and part quality. Part subsurface damage and high surface roughness are unacceptable for use of these composites (Wang & Zhang, 2003).

Cutting fluids are usually used for improving tool life, surface finish and lowering cutting forces when machining metallic materials. They also flush chips away from the cutting zone and reduce dust generated in the working environment, thus improving occupational safety. In the case of CFRPs, this is inadvisable because of the negative impact on the structural integrity of the composite (Turner *et al.*, 2015).

An innovative method (fully wet or semi-wet) that can cool down the tool or lubricate the cutting process without being absorbed by the workpiece material would be feasible for the machining of CFRPs. This is the case for cryogenic machining which was found to improve the tool life and the part surface integrity during drilling of CFRPs (Xia, Kaynak, Arvin & Jawahir, 2016), (Basmaci, Yoruk, Koklu & Morkavuk, 2017), (Impero *et al.*, 2018), (Giasin, Ayvar-Soberanis & Hodzic, 2016), (Joshi, Rawat & Balan, 2018), or the application of chilled air (Khairusshima, Hassan, Jaharah, Amin & Idriss, 2013), (Khairusshima & Sharifah, 2017). In recent years, some authors (Khairusshima *et al.*, 2013), (Khairusshima & Sharifah, 2017), (Khairussaleh, Haron & Ghani, 2016) have studied tool wear in the milling and edge-trimming of CFRPs using chilled air and dry cutting conditions. They observed that using chilled air improved the tool life of uncoated carbide cutting tools compared to dry machining, provided the feed rate was selected with care, being an influential process parameter.

Moreover, vegetable-based oils are also proposed as a viable alternative (Filipovic & Stephenson, 2006), (Siniawski, Saniei, Adhikari & Doezema, 2007) as they are environmentally friendly and highly suitable lubricity and other characteristics. These vegetable oils include canola, soybean, and rapeseed oil. Research works on the development and formulation of vegetable oil-based metal working fluids (MWFs) can be found in (Zimmerman, Clarens, Hayes & Skerlos, 2003),

(Raynor, Kim & Bhattacharya, 2005), while their performance is reported in (Shashidhara & Jayaram, 2010), (Abdalla, Baines, McIntyre & Slade, 2007), (Gryglewicz, Piechocki & Gryglewicz, 2003), (Alves & de Oliveira, 2006). These vegetable-based oils appear definitively as a good alternative to minerals-based cutting oils. Ultrasonic vibration can be used to emulsify vegetable oil in water (Sakai, 2008), (Kamogawa *et al.*, 2001), (Kamogawa *et al.*, 1999), (Kamogawa *et al.*, 2004). However, the feasibility of using such fluid as an MWF for machining has not been investigated, with the exception of the authors' previous works (Elgnemi, Ahmadi, Songmene, Nam & Jun, 2017), (Jun *et al.*, 2008), (Burton, Goo, Zhang & Jun, 2014), (Rukosuyev, Goo & Jun, 2010). The performance of such a cutting fluid on CFRPs was studied in Elgnemi *et al.* (2017) and it was reported that this fluid effectively reduced tool wear, cutting forces, surface roughness, burr occurrence, dust and airborne concentrations in the machining environment. However, they did not address the effect of fiber orientation.

Therefore, this work is mainly motivated by two objectives: (i) the need to study the performance of ultrasonic atomized vegetable oil in water as a sustainable alternative to conventional cutting oils and coolants; and (ii) to study the impact of fiber orientation on the tool degradation mode (edge rounding); the quality of the machined surface, the delamination percentage and fiber length are also considered in regard to the latter.

5.2 Methodology

5.2.1 Machining process setup

The system of atomization-based cutting fluid spray is similar to the one given by (Elgnemi *et al.*, 2017). The atomized canola vegetable oil and water is directly applied to the cutting zone to lubricate the chip and tool interface. The average droplet size of the canola oil is around 2.1 µm (Jun *et al.*, 2008). More details are available in (Burton *et al.*, 2014), (Rukosuyev *et al.*, 2010).Slot milling tests are carried out under cutting conditions as shown in Figure 5.1.

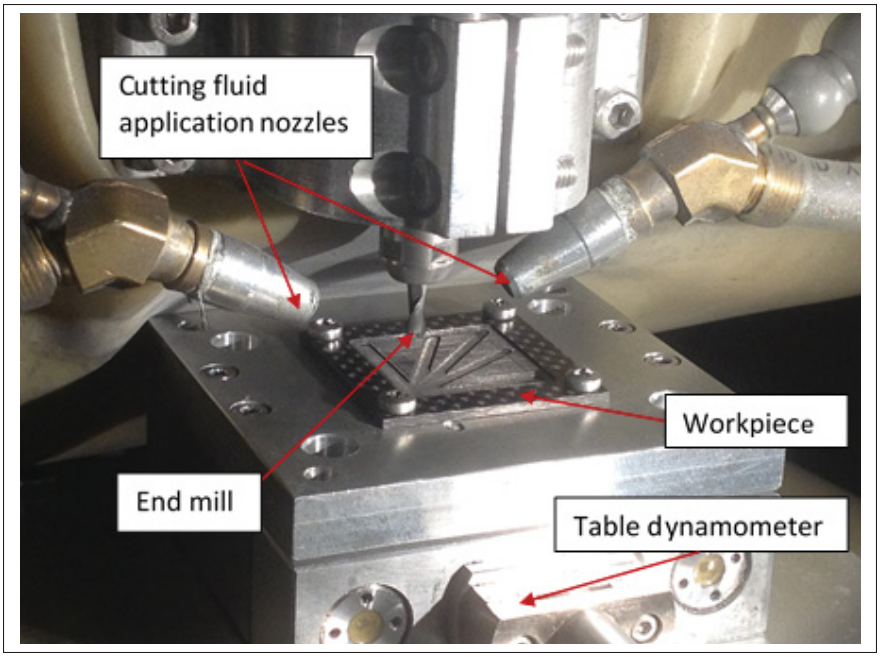

Figure 5.1 Experimental set-up consisting of a workpiece mounted on table dynamometer, end mill cutting tool and cutting fluid application nozzles

The machine-tool used in this work was ALIO vertical milling machine (supplied by Alio Industries) which has a spindle speed range of 10,000 to 80,000 rpm. The workpiece was clamped on the table dynamometer fixed on the machining center. Cutting forces were measured using a Kistler MiniDyn 9256C1 dynamometer as shown in Figure 5.1. A data acquisition (DAQ) board from National Instruments (NI-P/N-USB-6251 BNC) was used to acquire the measured forces from the dynamometer. The CutPro software program (developed by Prof Y. Altintas' team, University of British Colombia, Vancouver, Canada) was used to receive data from the DAQ board during the machining operation. A sampling rate of 100 kHz was used to process the measured force data. For comparison purposes, the experiments were carried out in both dry conditions and wet conditions using canola vegetable oil. In the latter case, distilled water was added into the atomizer to dilute the fluid at 5 vol%.

5.2.2 Workpiece materials and cutting tool

Multi-layer CFRP sheets 1.56 mm thick were used as the workpiece materials in this study.Each cut was done at a unidirectional fibers orientation with a depth of cut of 0.3 mm. Each composite sheet consisted of four unidirectional tapes (54 vol% fibers per tape) laid up in 0° and 90° orientations. The combined Young's modulus of 104 fibers (in the sheets) was 225 GPa (65 GPa per tape). The workpiece materials were cut into small sheets of 38 mm length × 38 mm width. The tests were performed on unidirectional laminates and the cutting directions were set so that the fiber orientation angle with respect to the cutting direction was 0°, 30° 45°, 60° and 90°. The tool geometry information for the uncoated tungsten carbide (WC-Co) 2-flutes end-mills (MSC Industrial Supply, Elkhart, IL, USA) used in the experiment are summarized in Table 5. 1.

Table 5.1 Description of the geometry of end mill used

Cutting Dia.	Flute Length	Shank Dia.	Overall Length	Rake Angle	Helix angle
0.125 in	0.250 in	1/8 in	1.50 in	7°	30°
3.175 mm	6.35 mm	3.175 mm	38.1 mm	7°	30°

5.2.3 Measurement of cutting forces and friction angle

The forces Fc, Ft and R are the main cutting force, thrust force and resultant cutting force, respectively. They are calculated from the measured normal force Fx and the feed force Fy in the x and y directions. The magnitude of Fz was negligible compared to Fx and Fy. The relationships between these forces are: (Maegawa, Morikawa, Hayakawa, Itoigawa & Nakamura, 2016).

$$Fc = -Fx \sin \varnothing + Fy \cos \varnothing \tag{5.1}$$

$$Ft = Fx \cos \varnothing + Fy \sin \varnothing \tag{5.2}$$

$$R = \sqrt{Fc^2 + Ft^2} \tag{5.3}$$

Since the un-deformed thickness of the chip t is almost the same as the depth of cut used, (given the brittle nature of the CFRP (Sheikh-Ahmad, 2009), (Liu *et al.*, 2017b), the shear angle ($\varnothing$)

can be estimated through the tool rake angle (α) by:

$$\varnothing \approx \tan^{-1}\left(\frac{cos\alpha}{1 - sin\alpha}\right) \tag{5.4}$$

and the friction angle (β) by (Maegawa *et al.*, 2016):

$$\tan(\beta) = \frac{Ft + Fc\tan\alpha}{Fc - Ft\tan\alpha} \tag{5.5}$$

5.2.4 Edge rounding measurement

The effective cutting-edge radius affects the machining performance (forces, power requirements) and the part surface finish. In this study, changes in cutting edge evolution were taken into consideration. A 3D optical microscope (Olympus BXFM) was employed for monitoring the change in the tool point or nose radius. Microscope images of a sharp cutting-edge are shown in Figure 5.2 (a) and microscope image of the same cutting edge after milling three slots (total cutting distance of 66 mm) is shown in Figure 5.2 (b). The tools were cleaned in acetone in an ultrasonic bath at 60° C for 30 min (frequency: 1000 kHz, power: 60 W) (Liu *et al.*, 2017b), (Zhao & Li, 2010),and (Nguyen *et al.*, 2020). The radius was estimated using the best-fit radius (highlighted circle) between the flank and the rake face of the worn tool. The tangential intersection with the flank face and the tangential intersection with rake face represent a series of radiuses measured from the worn cutting-edge profile between flank and rake face, as shown in Figure 5.2 (b). The radius of the circle that is confined between the two lines is considered as the resulting tool wear.

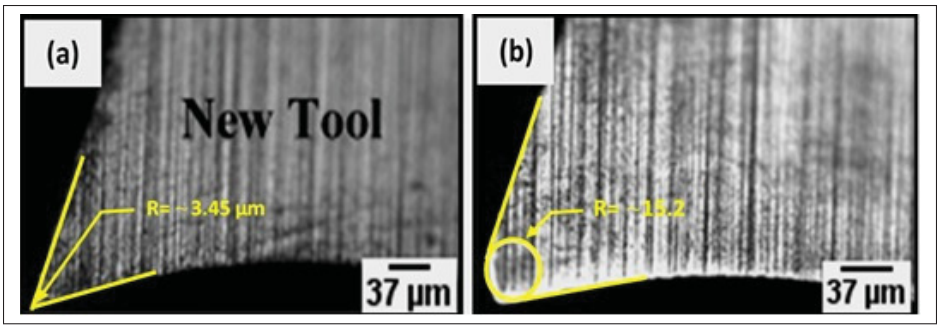

Figure 5.2 Procedure for measuring the tool nose radius. (a) New tool, (b) worn tool for a cutting distance of 66 mm with 0° TFOA at a feed rate of 3 µm/tooth and 20,000 rpm, in the dry condition

5.2.5 Delamination measurement

Delamination is a common occurrence when milling CFRPs. This machining-induced damage can be estimated using the delamination percentage *Dp*, measured using the maximum damage width (W_{max}) and the programmed slot width *(W)*, corresponding to endmill diameter in Equation (5.6) (Shirazinia, Moya & Muñoz, 2011). W_{max} was estimated using optical microscope observations. Figure 5.3 shows a schematic representation of these terms.

$$Dp = 100\frac{Wmax - W}{W} \tag{5.6}$$

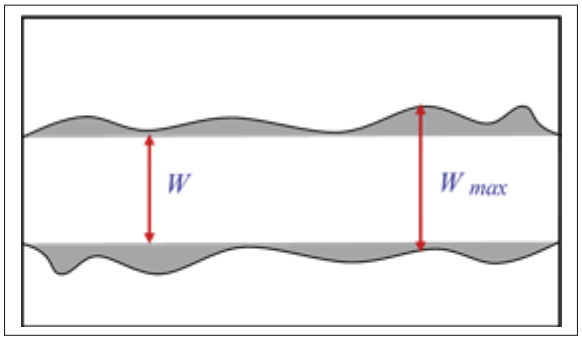

Figure 5.3 Schematic representation of CFRP damage measurement technique

5.2.6 Chip formation characterization processes

After machining, chips were collected for each of the cutting directions (0°, 30° 45°, 60° and 90°) relative to fiber orientations (TFOA) of CFRP. These chips were then measured and imaged employing a Hitachi S-4800 FESEM. Figure 5.4 shows the technique for measuring the fiber length as well as examples of chip morphologies observed. In this image, we can distinguish fibers separated from the matrix. Broken short fibers may have been wiped out during the cleaning procedure. The lengths of exposed long fibers were estimated using Image J software.

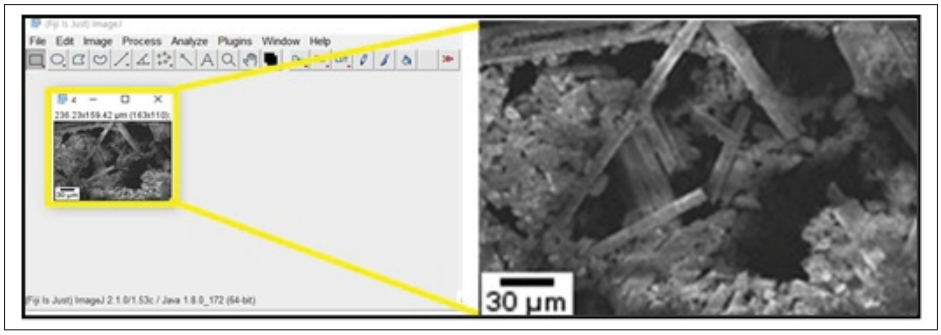

Figure 5.4 Fiber length measurement technique

5.2.7 Experimental design

A factorial design approach was implemented to look into the milling parameters and cooling method effects on the machining of CFRP. The tested factors included: (a) the fiber orientation angle with respect to the cutting direction as shown in Figure 5.5; (b) the feed rate; and (c) the cooling method. Five fiber orientation angles (TFOA: 0°, 30° 45°, 60° and 90°), two feed rates and two cooling methods (dry versus atomized vegetable oil) were selected. In all, twenty experiments were necessary for the full factorial design. Each test was repeated three times. A new tool was used for each test. Table 5.2 summarizes the con-trolled factors, their level and the output responses analyzed. The others milling parameters were set as follows:

(i) Spindle speed: 20,000 rpm

(ii) Tool immersion: 100%

(iii) Axial depth of cut: 0.3 mm

(iv) Length of each slot: 22 mm

The depth of cut was chosen so as to be able to make three passes on the same fiber orientation.

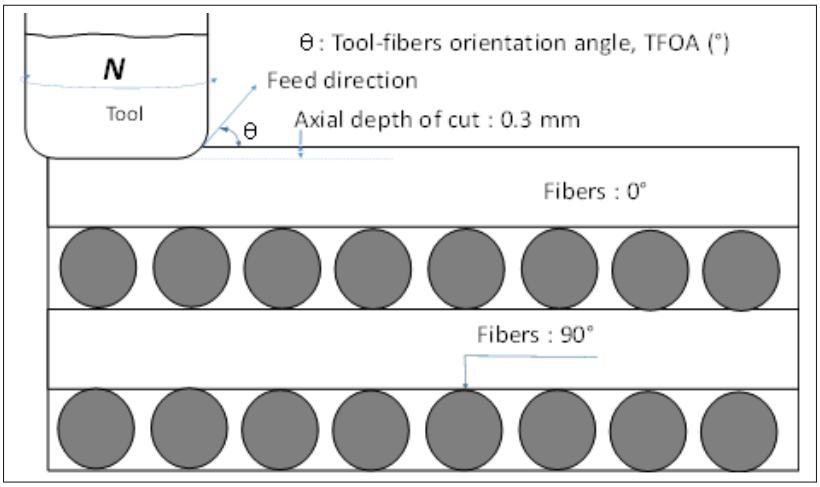

Figure 5.5 Schematic representation of tool displacement-fibers orientation angle

Table 5.2 Details of milling experiments with and without atomization-based cutting fluid (ACF)

Ident.	Control Variables	Levels	Response Variables
A	Fiber orientation ($\theta°$)	0, 30, 45, 60, 90	1. Cutting forces
B	Feed rate (μ**m**/tooth)	3, 6	2. Tool wear
C	Cutting fluids	Dry-ACF (vegetable oil)	3. Delamination
			4. Surface damage
			5. Chip formation

5.3 Results and discussion

5.3.1 Cutting forces

The influence of feed rate and fiber orientation on the resultant cutting force *(R)* obtained when using dry and ACF (atomized cutting fluid i.e., vegetable oil) milling conditions are shown in Figure 5.6. For all tested parameters, a slight increase in *R* was observed with dry milling

of uni-directional or UD-CFRP laminates compared to atomization-based spray machining regardless of TFOA and feed rate. This can be attributed to the lubricating effect due to the ACF resulting in reduced friction at the tool/chip and tool/work piece interfaces when atomized cutting fluid is used. Moreover, in Figure 5.7 the highest magnitude of R is noted at 90° fiber orientation, where-as the R value is lowest for 0° orientation, namely when the cutting direction and fibers are parallel. In such a setting, the main mechanism for chip formation is delamination, and therefore the interaction of fibers with the cutting edge is limited. In the opposite case, when the fibers are perpendicular to the cutting direction (i.e., at 90° TFOA), the tool must cut the fibers that have a higher Young's modulus than the matrix. For the 45° fiber orientation, the fibers undergo both pulling and shearing (Nguyen *et al.*, 2020). It appears in Figure 5.6 that the resultant force increases proportionally to the feed rate, as usually expected when machining metals, polymers and composites since the chip thick-ness and cross section, and therefore the metal removal rates, are increased at a high feed rate (Kumar & Gururaja, 2020). The results presented in Figures 5.6 and 5.7 demonstrate that the machining of CFRP is improved with the use of the atomization-based vegetable oil spray as the lubricant.

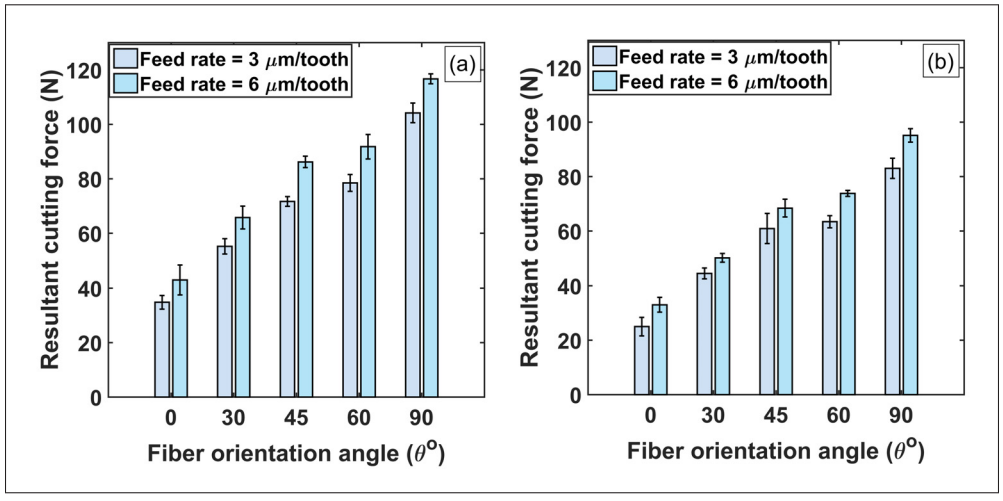

Figure 5.6 Influence of feed rate and fiber orientation on resultant cutting forces. (a) dry, and (b) ACF vegetable oil conditions (at 20,000 rpm speed)

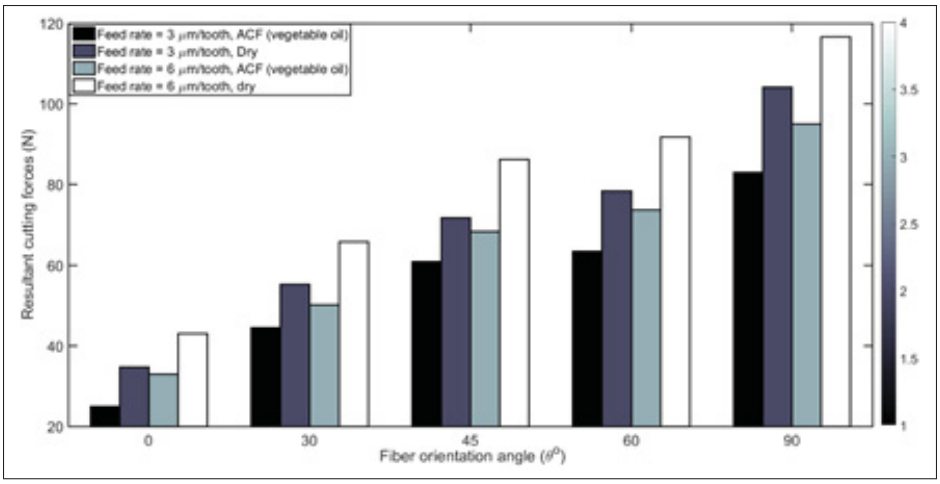

Figure 5.7 Resultant cutting forces for all fiber orientations using 3 and 6 μm/tooth feed rates and different cutting conditions. (Speed: 20,000 rpm)

5.3.2 Friction angle

The bar diagram in Figure 5.8 illustrates the friction angle by feed rate and fiber orientation. The friction angle β is plotted according to Equation (5.5). Regardless of the dry or lubricated conditions, it appears that the friction angle decreases as the cutting direction changes from 0° to 90° orientation. The reduction in β is limited from 0° to 45° and high when cutting in fiber orientation be-tween 60° to 90°. This can be explained by the fact that, for high fiber angles (more than 45°), the double fiber removal actions of pulling and shearing lead to reduction in chip-tool contact length and thus reduce the friction. The rupture of fibers strongly depends also on the TFOA as well as the effective rake angle α, Equation (5.5) (Xiao, Gao & Ke, 2018). Figure 5.8 also shows that β decreases proportionally with an increase in the feed rate (i.e., chip thickness) for each unidirectional CFRP laminate when the cutting conditions are the same. This observation may be ascribed to the reduction in the undeformed chip thickness which depends on the amount of feed per tooth; as a result the friction angle β at the tool face will decrease as the feed per tooth is increased (Niknam & Songmene, 2014). The other differences in friction angles observed, especially as a function of TFOA, could be attributed to the chip formation process (Sheikh-Ahmad, 2009). Finally, the use of ACF lubricant will also reduce the friction angle. Moreover, referring to Equation (5.5), the theoretical friction angle would decrease with a

higher cutting force. The parameters affecting the machining force, as described in the previous sub-section, further corroborates the correlation between the increase in cutting force and the decrease in friction angle.

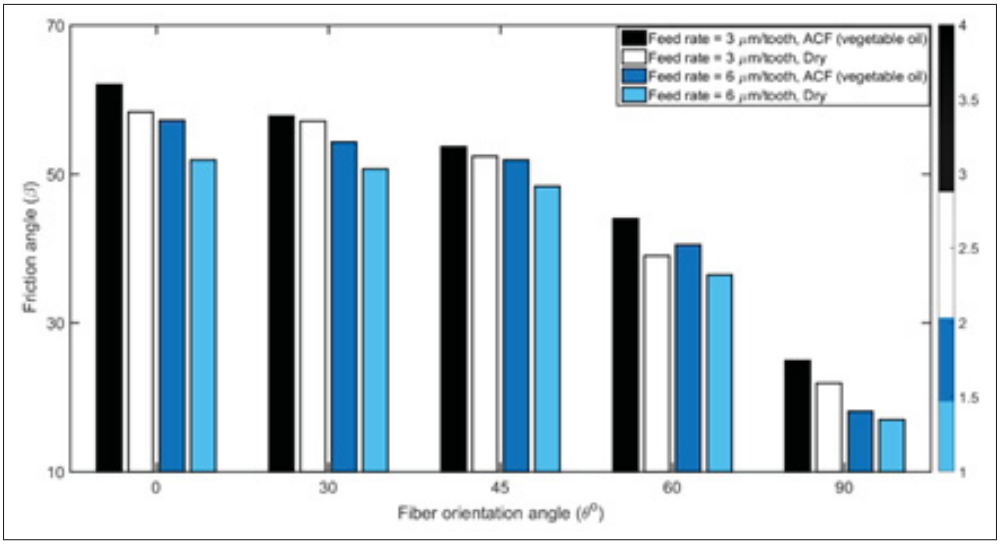

Figure 5.8 Comparison of measured friction angle as a function of fiber orientation at feed rates with 3 and 6 μm/tooth and different cutting conditions (at 20,000 rpm speed)

5.3.3 Tool wear - edge rounding

The dominant tool wear mode when machining CFRP has already been identified as the blunting of the cutting edge (Faraz, Biermann & Weinert, 2009), (Zitoune *et al.*, 2012), also known as edge rounding (Nguyen, Voznyuk, Bin Abdullah, Kim & Kwon, 2019), (Swan, Bin Abdullah, Kim, Nguyen & Kwon, 2018). Figure 5.9 shows comparative images of the tool after milling three slots (total travel distance of 66 mm) under different lubricating conditions and for tested fiber orientation angles. The higher the fiber orientation, the higher the edge rounding observed after milling. Figure 5.10 presents a comparison of edge rounding in terms of fiber orientation, milling condition and feed rate. It appears from the trends of Figure 5.9 that, irrespective of fiber orientation angles and feed rate values, the cutting edges develop a large edge radius caused by the abrasion of the tool flank and rake faces by the broken carbon fibers. Figure 5.10 displays how the measured tool edge rounding radius varies with the feed per tooth and the use (or not)

of cutting fluid. From this figure, it is noted that tool wear is much greater when no lubricant was used, due to the increase in friction.

In general, the increase in edge rounding radius was high for cutting fibers at 90° (i.e., perpendicular to the cutting direction) and least for fibers cut at 0°. This may be attributed to shear fracture that occurs during CFRP chip formation when cutting with 90° as re-ported by (Maegawa, Morikawa, Hayakawa, Itoigawa & Nakamura, 2015). This result also explains the highest cutting force observed at 90° fiber orientation (Section 5.3.1) During machining at 45°, the cutting force was not as high as for 90° (Figures 5.6 and 5.7). These results are in keeping with those reported by (Wang & Zhang, 2003).

The low edge rounding radius observed at 45° and 0° may be accounted for in terms of the chip formation. When milling at 45°, the abrasive action of the broken fibers is high. These fibers are broken because of the compression-induced shear perpendicular to the fiber direction (Kumar & Gururaja, 2020). When machining at 90°, fiber delamination occurs because of micro-buckling and only limited fibers can fracture (Rawat & Attia, 2009).

It is also observed in Figure 5.10 that the tool deterioration (edge rounding) was reduced during milling for all cutting directions using atomized vegetable oil conditions. It can be observed too, for all lubrication conditions tested, that the tool wear increases when the feed rate and thus the load on the tool is increased.

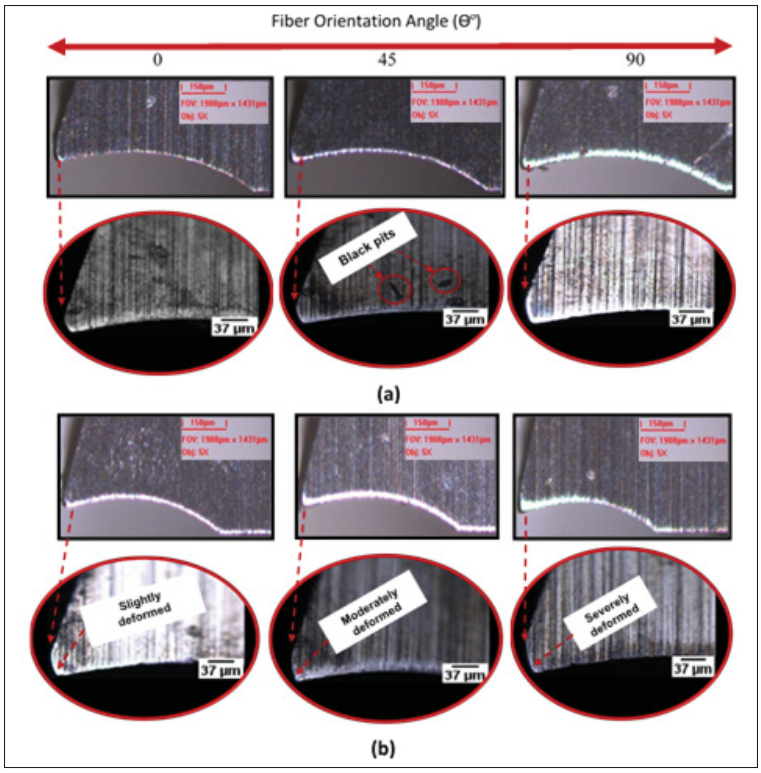

Figure 5.9 Progression of wear after milling 66 mm at 0°, 45°, and 90° fiber oriented at feed rate 3 µm/tooth, and 20,000 rpm using (a) atomization-based spray and (b) dry milling

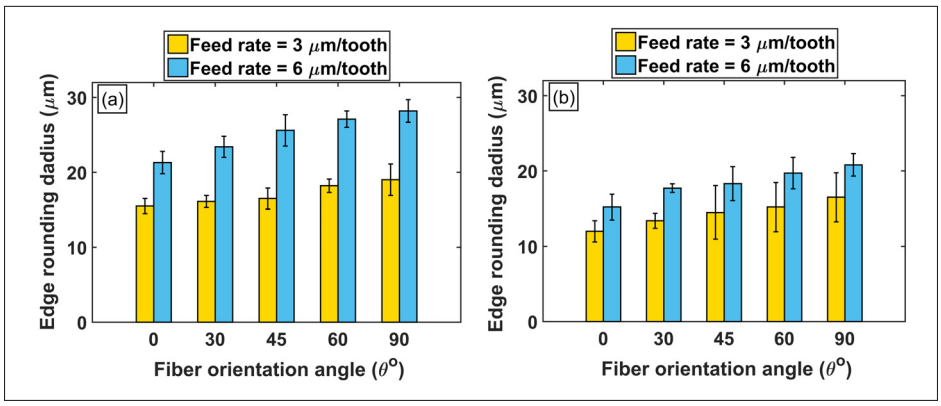

Figure 5.10 Comparison of measured edge rounding radius progress for all fiber orientations at feed rates 3 and 6 µm/tooth and speed of 20,000 rpm for (a) dry and (b) ACF vegetable oil conditions

5.3.4 Delamination

Figure 5.11 displays the percentage of delamination measured (Equation (5.6)) as a function of TFOA and feed rate on samples machined under dry and wet conditions. It can be seen that, when milling using the atomized coolant, the percentage of damage on the workpiece is greatly reduced for all the tested conditions. The resulting reduction of temperature in the cutting zone can explain this behavior since it would reduce the thermal degradation of the polymer matrix. This result is in good agreement with the observations of (Kumar & Gururaja, 2020) who found that low temperatures tend to maintain or increase the properties of the CFRP (tensile strength, shear modulus and stiffness) which, in consequence, would produce greater resistance to delamination. The maximum damage occurred when cutting dry at 45° fiber orientation using a high feed rate (Figure 5.11). The dominant chip formation mechanisms, i.e., fiber bending and shearing, for this configuration can explain this maximum delamination. Also, the more the feed rate is high, the higher the delamination that takes place, which can be attributed to the increase in cutting forces and thus on shear stress when the feed rate is increased.

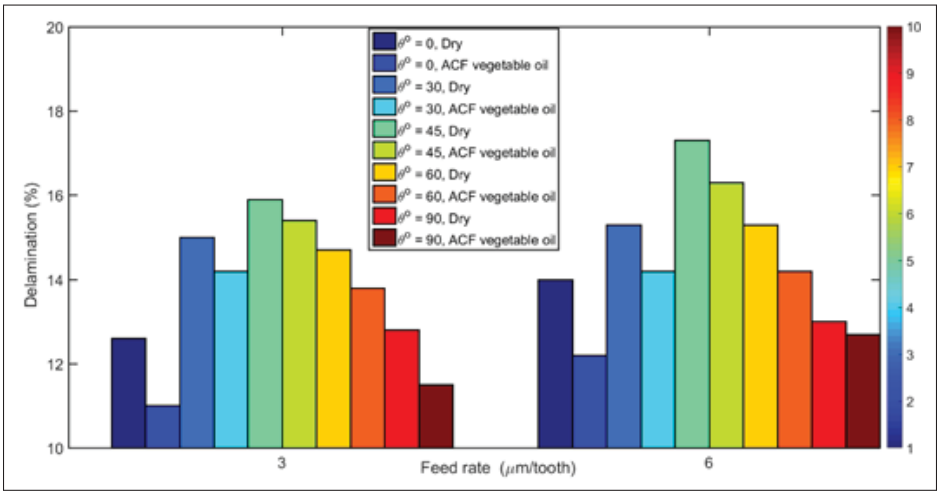

Figure 5.11 Variation in delamination percentage with fiber orientation angle at feed rates 3 and 6 µm/tooth and different cutting fluid conditions (at 20,000 rpm speed)

5.3.5 Chip formation

In general, the chip formation observed during milling of CRPFs is dominated by de-lamination and breakage. The reinforcing fibers break into dust particles of different shapes and this tendency varies depending on the direction of cutting relative to the fiber orientation. Figure 5.12 shows SEM images of fibers and chips obtained, in relation to the feed rate and TFOA. Measurements of broken fibers were taken from these images to as-certain their lengths in order to correlate them with the machining conditions (see Figure 5.12).

It is clearly noted in Figure 5.12 that the chips are broken into fiber segments of irregular lengths. Longer broken fibers were obtained at 0° TFOA while much shorter ones were generated at 45° and 90° TFOAs. The chip formation modes at 0° TFOA (i.e., delamination (Wang *et al.*, 1995), (Nguyen *et al.*, 2020)) and at 45° and 90° TFOAs (i.e., compression-induced shear fracture perpendicular to fibers and inter-laminar shear fracture along the fiber/matrix interface (Wang *et al.*, 1995), (Ramulu, Kim & Choi, 2003)) can explain the difference found in the broken fiber lengths. These broken fibers abrade the tool, which explains the high edge radius roundness observed when milling at 0° orientation (see Figure 5.10). It was also observed from Figure 5.13 that fiber length increases proportionally to the feed rate (i.e., chip thickness) for all fiber orientations. For instance, the average fiber length in-creased, from 75.1 μm at a feed rate of 3 μm/tooth with 0° orientation to 103.5 μm at feed rate 6 μm/tooth with 0° orientation.

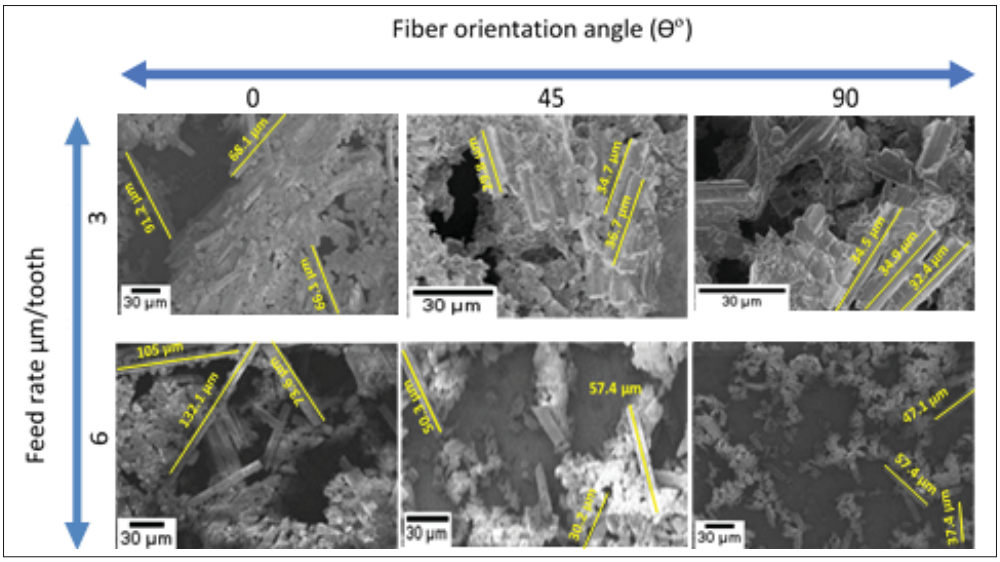

Figure 5.12 SEM images used for fiber length measurements for fiber orientations θ° = 0, 45, and 90 at feed rates 3 and 6 µm/tooth and dry milling condition (at 20,000 rpm speed)

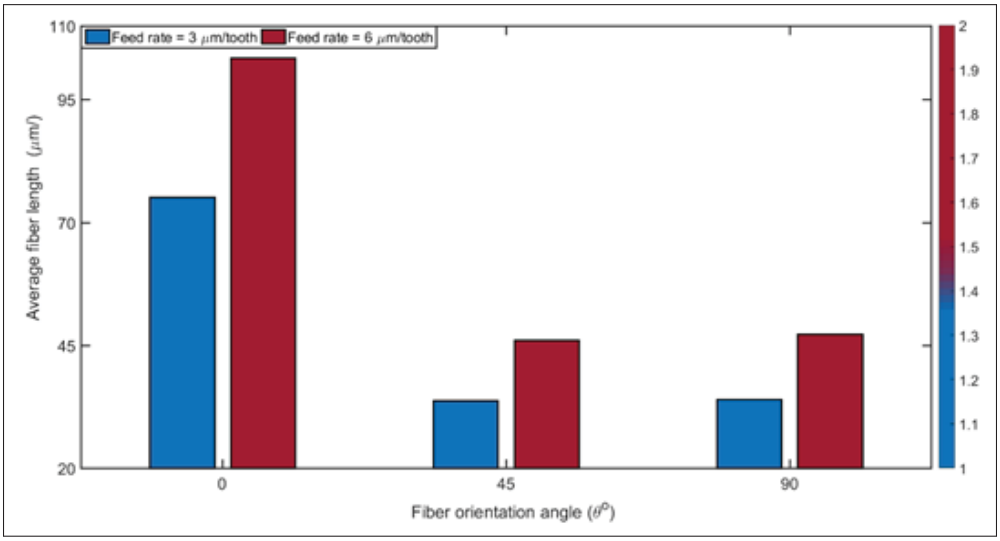

Figure 5.13 Average fiber length measurements of 0°, 45°, and 90° fiber orientations at feed rates 3 and 6 µm/tooth and dry milling condition (at 20,000 rpm speed)

5.3.6 Impact of fiber orientation on CFRP surface finish

When CFRPs are subjected to milling, the formed surface is irregular because of the pulling and separation of the fibers from the matrix (Davim & Mata, 2005). The irregular surface is also the result of variation in cutting forces when the tool cuts the fibers and then the matrix. It has been reported previously that surface damage when milling CFRP occurs in the transition zone (Liu, Chen, Huang, Gao & Chen, 2017a), (Hintze & Hartmann, 2013), (Hintze, Cordes & Koerkel, 2015).

Figure 4.14 illustrates the surface damage of unidirectional CFRP laminate at 0°, 45°, and 90° TFOAs. The TFOA appears to be the dominant factor for the surface generated (Figure 4.14) as the surfaces for the 45° and 90° orientations are more severely damaged than that for 0° orientation. In fact, at 0° TFOA, the cutting orientation is parallel to the fibers' orientation and the major chip formation mechanism is delamination, so there is minimum interaction between fibers and cutting edge. For the 90° TFOA, the cutting orientation is orthogonal to the fibers, causing the greater interaction between fibers and the cutting edge. For 45°, the fibers are both dragged and sheared. This behavior is well known in the literature (Chang, 2006), (Pecat, Rentsch & Brinksmeier, 2012).

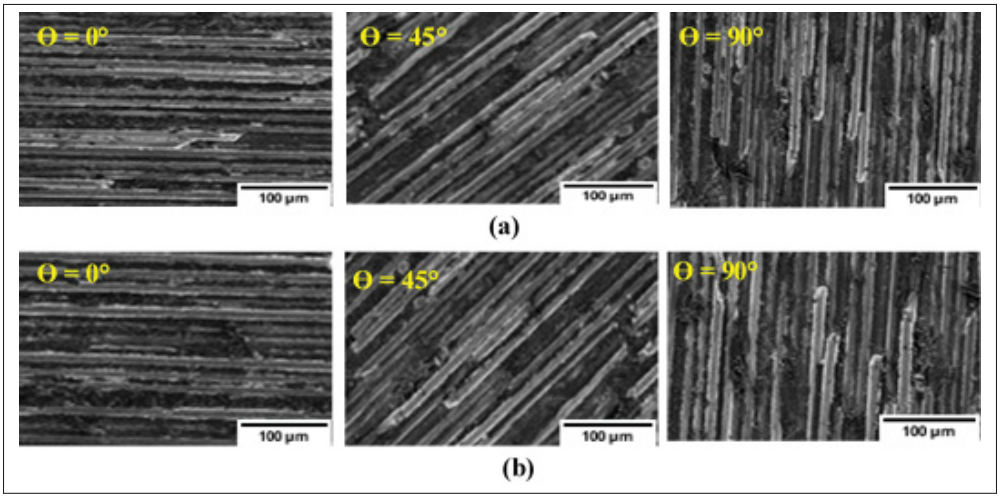

Figure 5.14 SEM images of a machined surface obtained after milling 0°, 45°, and 90° TFOA (feed rate µm/tooth and speed of 20,000 rpm): (a) ACF vegetable oil conditions and (b) dry

In the case of fibers oriented at 45° and 90°, the fibers were not completely removed because of the large bending deformation taking place. It can be thus concluded that during machining of CFRP, surface damage is related to the chip formation mechanism where bending and shearing of fibers dominate the mechanism (Xiao *et al.*, 2018).

Moreover, the TFOA seriously affects the tool cutting-edge wear, as a result of surface damage occurring within the workpiece during machining. The analysis of tool edge radius was described in Section 4.3.3. The results confirm the high effect of fiber orientations on tool wear. At 0° fiber orientation, the surface integrity is much better than at 45° or 90° TFOA. In fact, at 0°, crushing and then fracture of fibers is dominant and therefore fibers crack or fracture at the cut surface. Instead, for other TFOAs (between 45° and 90°), fracture occurs ahead of the tool, leading to further damage of the surface as a result of the uncontrolled action of the broken fibers.

Nevertheless, it should be noted that employing ACF vegetable oil did not show a pronounced effect on the machined surface when compared to dry milling. The use of ACF vegetable oil, however, as a spray in the cutting zone, is a viable lubricating method for CFRP since the spray will evaporate and will not be absorbed by the workpiece. Thus, the structural integrity of the CFRP will not be damaged because of moisture from the lub-ricant. This is in agreement with our earlier findings (Elgnemi *et al.*, 2017), (Jun *et al.*, 2008)

5.4 Conclusions

The milling performance of CFRPs when using atomized vegetable oil as a lubricant was investigated in this research work as a function of fiber orientations and cutting feed rate. The process performance indicators studied were the cutting force, the tool wear, delamination, and surface texture. The results obtained from this study led to the following conclusions:

1) When machining CFRPs, the cutting direction, in relation to the fiber orientation, strongly influences chip formation, on which depends resistance to cutting, cutting force, fiber breakage, tool wear, the quality of the machined surface and the delamination. These indicators depend on the machining parameters used and on the cut-ting conditions.

2) The delamination percentage when cutting at TFOAs of 0°, 30° 45°, 60°, and 90° were improved by 65%, 91%, 54%, 66%, and 75%, respectively, under ACF (vegetable oil) conditions at 3μm/tooth. Machining with 45° TFOA produces maximum damage at high feed rate.
3) As expected, increase in feed rate increased the cutting force because of high chip load, especially in cutting directions where the fiber strength is high and with dry machining. Using a lubricant decreased the friction between the chip and the rake face of the tool, reduced the abrasive effect of broken fibers, and thus lowered cutting force and tool wear.
4) The magnitude of resultant cutting force was found to be greater in the dry condition relative to the ACF condition by about 23%, 31%, 26%, 25%, and 23%, respectively, for the samples in the 0°, 30, 45°, 60°, and 90° TFOA at 6 μm/tooth of feed rate. However, the use of atomized vegetable oil mixed with water improved the process performance compared to dry machining in that it reduced the cutting force, the delamination percentage and the tool edge rounding.
5) The tool damage was examined and measured using a 3D optical microscope (Olympus BXFM). 90° TFOA produced a large amount of tool edge rounding. Contrastingly, 0° TFOA has the least amount of edge rounding. However, the lowest values of edge radius evolution as a measure of the tool wear were 12 μm and 16.5 μm with TFOA from 0° to 90° at feed rate 3 μm/tooth under ACF (vegetable oil) conditions.
6) The findings of this study further support the use of the vegetable oil-in-water emulsion obtained through ultrasonic atomization as an effective and environmentally friendly lubricant for improving the machining of CFRPs.

CHAPTER 6

EXPERIMENTAL INVESTIGATION ON DRY ROUTING OF CFRP COMPOSITE: TEMPERATURE, FORCES, TOOL WEAR AND FINE DUST EMISSION

T. Elgnemi[1] , V. Songmene[1,*] , J. Kouam[1] , Martin B.G. Jun[2] , and A. M. Samuel[1]

[1] Department of Mechanical Engineering, École de Technologie Supérieure (ÉTS), 1100 Notre-Dame West, Montreal, Quebec, Canada H3C 1K3
[2] Department of Mechanical Engineering, 610 Purdue Mall, West Lafayette, IN 47907, USA

Published in journal of Materials 2021, 14, 5697

Abstract

This article presents the influence of machining conditions on typical process performance indicators, namely cutting force, specific cutting energy, cutting temperature, tool wear, and fine dust emission during dry milling of CFRPs. The main goal is to determine the machining process window for obtaining quality parts with acceptable tool performance and limited dust emission. For achieving this, the cutting temperature was examined using analytical and empirical models, and systematic cutting experiments were conducted to assess the reliability of the theoretical predictions. A full factorial design was used for the experimental design. The experiments were conducted on a CNC milling machine with cutting speeds of 10000, 15000, and 20000 rpm and feed rates of 2, 4, and 6 µm/tooth. Based on the results, it was ascertained that spindle speed significantly affects the cutting temperature and fine particle emission while cutting force, specific cutting energy, and tool wear are influenced by the feed rate. The optimal conditions for cutting force and tool wear were observed at a cutting speed of 10000 rpm. Cutting temperature did not exceed the glass transition temperature for the cutting speeds tested and feed rates used. Fine particles emitted ranged from 0.5 to 10 µm aerodynamic diameters with maximum concentration of 2776.6 particles for those of 0.5 µm diameters. Finally, results of the experimental optimization are presented, and the model is validated. The results obtained may be used to better understand specific phenomena associated with milling of CFRPs and provide

the means to select effective milling parameters to improve the technology and economics of the process.

Keywords: CFRP; machining; temperature; cutting forces; dust emission; tool wear

6.1 Introduction

The use of carbon fiber reinforced polymer (CFRP) has considerably increased in the last few years. The aerospace and automotive industries especially are concerned about these materials, due to the fact that (i) CFRPs are relatively easy to manufacture using several automated lamination techniques; (ii) they feature excellent unique mechanical properties as well as good chemical and dimensional stability; and (iii) their corrosion and heat resistance are also outstanding (Wang & Zhang, 2003), (Teti, 2002), (Morkavuk, Köklü, Bağcı & Gemi, 2018). The main attraction of these materials is the low density compared to the traditional engineering materials such as steel or aluminum (Alonso & Solis, 2021). These characteristics allow for a reduction in costs (Dhari, Patel, Wang & Hazell, 2021), (Ehsani & Rezaeepazhand, 2016), which is an important requirement in any kind of industry. However, due to the multiphase and inhomogeneous nature of the material, various types of damage, e.g., fiber breakage and pullout, fuzzing, delamination, resin degradation, etc., are easily induced (He, Sheikh-Ahmad, Zhu & Zhao, 2020), (Chen *et al.*, 2019) In addition, the highly abrasive nature of the carbon fibers and the low thermal conductivity of the resin matrix lead to rapid tool wear; the laminated structure of the CFRP facilitates delamination as plies are subject to separation by cutting forces during machining (Karpat *et al.*, 2012), (Shen *et al.*, 2015).

Despite the fact that CFRPs are mostly produced near net shape, machining is often required in order to bring the component into dimensional requirements and prepare it for assembly. Milling operation remains essential and necessary to achieve the required geometry, tolerance level, and edge quality in CFRPs, which are important for assembly (Su, Yuan, Sun, Wang & Deng, 2018), (Davim & Reis, 2005). Significant progress has been made to understand the effects of fiber materials and matrix types (), (Koenig *et al.*, 1985), fiber volume fraction and orientations,

(Xu & Zhang, 2015), tool materials and geometries (Xu & Zhang, 2018), and machining parameters (Hussain, Gao, Hayat & Qijian, 2007), (Jain, Jain & Deb, 2007). (Sheikh-Ahmad, 2009), for instance, demonstrated numerous studies on the machining of a CFRP. It was shown that the machining quality or machinability of CFRP materials relies on factors such as the fiber volume fraction, fiber orientation, cutting parameters, and tool geometry. (Davim & Reis, 2005) found that both cutting speed and feed rate have a statistical and physical significance in the milling of a CFRP. In a further study of the milling of a CFRP, (Azmi, Lin & Bhattacharyya, 2012) observed that the feed rate has the most dominant effect on surface and machining force. Therefore, machining has to be conducted with great care to obtain high quality.

CFRPs are normally machined under dry conditions, i.e., without using a coolant (Ghafarizadeh *et al.*, 2016). This is due to the fact that the moisture can degrade the mechanical properties of composites, as seen by microcracking of the polymer matrix and chemical reaction of the polymer (Turner *et al.*, 2015). On the other hand, dry machining generates overheating. As a result, thermal damage to composites and tool life occur (Li, Wang & Chu, 2013).

In addition to the above-mentioned cutting mechanics, the cutting temperature has long been recognized as an important factor influencing the surface quality of milled materials and the tool life. If the cutting temperature is higher than the thermosetting matrix resin's glass transition temperature, the resin will degrade within the machined surface or surface layer. This critical temperature is around 180 °C for a typical epoxy-based CFRP material. Degradation of the resin generates delamination and weakens the material, resulting in significant flaws (Chen, 1997). However, it is reported that cutting temperature is significantly affected by the cutting speed, depth of cut, tool/workpiece material, feed rate, and fiber orientations (Ghafarizadeh *et al.*, 2016).

In order to investigate the CFRP cutting temperature, various techniques have been used to measure temperature while milling CFRP, such as a thermal camera (Khairusshima *et al.*, 2013), a K-type thermocouple, and a tool-work thermocouple (Yashiro *et al.*, 2013). (Chen, 1997) installed a thermocouple in the flank surface of a drill and performed the temperature

measurement of the flank surface using the thermocouple technique. The results showed that when the cutting speed was increased from 40 to 200 m/min at a fixed feed rate of 0.05 mm/rev, the average flank surface temperature increased from 120 to 300 °C. When the feed rate was increased from 0.05 to 0.4 mm/rev at a fixed cutting speed of 21.5 m/min, the average flank surface temperature decreased from 120 to 70 °C. To detect the temperature of the milling operation, (Kerrigan, Thil, Hewison & O'Donnell, 2012) inserted a thermocouple in the cutting tool and created a wireless telemetric system within the rotary cutting tool. They concluded that in high-speed milling, responsiveness is insufficient to quantify dynamic change. (Ghafarizadeh *et al.*, 2016) reported that the cutting temperature reaches its maximum when there is friction between the tool tip and the workpiece. They added that in this case, fibers are not cut but pressed out by the tool that generates its wear. In another study, (Yashiro *et al.*, 2013)] measured the cutting temperature during machining of a CFRP composite laminate and the temperature distribution through the laminate thickness during machining. They used the following three measurement methods: one with an infrared camera, a second one with a tool–workpiece thermocouple, and a third with thermocouples embedded between the layers of the composite. Their analysis indicated that the temperature at the tool–workpiece contact point reached 180 °C (Tg) at a cutting speed of 25 m/min and subsequently climbed to 300 °C at a cutting speed of 50 m/min. When the cutting speed was increased further, the cutting temperature tended to stabilize and remain consistent. Even at high cutting rates (300 m/min), the cutting temperature in the workpiece material was comparatively low (104 °C) compared to the tool–workpiece contact point. In recent research, (Liu *et al.*, 2014) investigated the workpiece temperature variation in helical milling of CFRP. They concluded that the workpiece temperature increases with an increasing spindle speed and axial cutting depth. They also reported that the axial cutting depth has more influence on the temperature variation of the workpiece than the spindle speed, while the influence of feed per tooth is less than the other factors.

To date, measuring cutting tool temperature is a significant challenge in milling operations due to tool rotation and complicated set-up. Therefore, numerical and analytical models have been proposed, widely considered, and used until now. (Lin, Peng, Wen, Liu & Yan, 2013) developed

a model to predict the cutting temperature of the workpiece during the end milling process while considering the flank face wear. The model's accuracy exceeds that of an analytical model, and its prediction efficiency exceeds that of the finite element approach, which can be used to optimize cutting parameters. (Wang *et al.*, 2016), (Sheng, Chiu & Lin, 2018) suggested a modelling coupling equation of cutting parameters based on the ideal cutting temperature to optimize tool life.

In addition to all the exposed issues of composite machining, dry machining of CFRP composites leads to the generation of significant amounts of airborne dust particles. These particles can be inhaled and can even penetrate the skin or the eye, which is a direct cause of a health hazard. Moreover, the dust generated from machining CFRP is harmful to the machine tool as well (Klein *et al.*, 1998). Carbon fibers are electrically conductive, and due to the small size of the dust particles and the fibers, and their ability to become airborne, these particles will likely penetrate tight spaces between machine components and into the machine control box (Konig & Rummenholler, 1993). Numerous works have been conducted to identify the main factors responsible for the generation of dust particles in order to minimize the emission of these dangerous particles during the machining of CFRP (Teitsworth, 1999), (Iyer, 2015), (Nguyen-Dinh, Hejjaji, Zitoune, Bouvet & Salem, 2020). (Boatman, Covert, Kalman, Luchtel & Omenn, 1988) conducted a study to identify the influence of the nature of composite materials on the size and the number of harmful particles during the trimming process. CFRP and GFRP materials were machined in this work. They found that harmful particles resulting from GFRP composites have a higher number and longer lengths than those resulting from CFRP composites.

On top of that, the number of harmful particles is almost equally distributed along with particle size (0.5 to 8 µm). However, when machining a CFRP composite, the majority of the harmful particles lie below 2 µm (almost 85%). It may be noticed that these studies dealing with dust particles generated throughout machining composite materials do not provide all the pertinent information on the influence of machining parameters on the emission of harmful particles. Additionally, no information has been provided on the tool geometry used. In another study, (Haddad *et al.*, 2014) investigated the influence of tool geometry and cutting conditions on

surface defects and the dust generated during CFRP milling. It was observed that an increase in the number of particles occurred with an increasing cutting speed. The feed rate appeared to have less of an effect at a constant cutting speed on the number of particles generated. On the other hand, a low cutting speed and high feed rate supported the apparition of mechanical damages that are responsible for the poor surface quality Sheikh-Ahmad (2009).

(Miller, 2014) carried out a variety of tests on the machining of composite materials and the different particulate sizes of the machined dust. The tests were conducted using uni-directional and multi-directional laminates. He observed that the aerodynamic diameter of particles obtained by machining the uni-directional composites was about 0.15 m. He also questioned the credibility of the measurement of the percentage of particles that are harmful to alveoli by (Haddad *et al.*, 2014).]. Regarding the influence of the tool geometry, however, it has been observed that the amount or number of harmful particles measured, when using four flutes end mills, is 150 and 120% superior to those generated when trimming is conducted with coated and uncoated burr tools (Nguyen-Dinh *et al.*, 2020). These results have been attributed to the fact that, once the burr tools are used, the temperature of machining is superior to the one generated when machining is conducted with four flutes end mills, and this increases the adherence of the carbon and matrix dust in between the tool grooves of the burr tools (Haddad *et al.*, 2014). It should be mentioned that these burr tools have been initially designed by the manufacturer of tools to minimize the cutting forces and also the delamination when trimming or milling CFRP, and not for the decrease in the amount or number of harmful particles. Thus, in our point of view, we can say that an optimal design of the cutting tool groove may reduce the cutting forces and also the number of harmful particles.

Summarizing the previous work available on the machining of composites, numerous studies have been conducted on the relationship between machining quality and cutting force and tool wear. However, few investigations have focused on the interaction effect of cutting force, cutting temperature, and dust emission in CFRP milling simultaneously.

The present work is primarily motivated by the need to focus on the interaction effect of cutting parameters (cutting speed and feed rate) on the following machining process performance indicators: cutting force, specific cutting energy, cutting temperature, tool wear, and fine dust emission (in terms of number of particles) during dry milling of CFRP. A complete experimental design has been developed with two factors (feed speed and cutting speed), each with three levels in order to obtain nine combinations, for milling of a multidirectional CFRP laminate. A chip breaker router type of end mill was considered to investigate the effect of machining parameters on cutting force, tool wear, cutting temperatures, and the dust generated. Down milling was deliberately chosen, being the preferred method for finishing operations, while machining temperatures were acquired using K-type thermocouples. Additionally, an analytical model was proposed to predict the temperature and then, experimental tests were used to verify the results obtained using the model. In this study, the relationships among milling temperature, milling force, fine dust emission, and cutting parameters are analyzed using response surface methodology (RSM), and the corresponding mathematical models are established to optimize the cutting parameters. Finally, the effect of cutting parameters on the dust generated while machining composite parts has also been investigated.

Section 6.2 proposes an analytical temperature field modeling method. Section 6.3 describes the material and outlines the experimental techniques for the testing of milling. Section 6.4 covers the analysis and experimental validation of the proposed model, and results. Conclusions are presented in Section 6.5.

6.2 Analytical modeling of the temperature and specific energy

The machining process performance is influenced by a large number of factors including the temperature in the cutting zone, the chip formation, the cutting forces and the tool wear. All these factors are affected by the machining parameters, the cutting tool geometry and material and the machining conditions. For the machining of the CRFP, the temperature is of great importance as high temperature could lead to matrix softening, delamination and consequently deteriorate the CFRP. The cutting temperature, the cutting energy, the cutting and shearing

forces also influence the dust emission during machining. Some of this information can be determined experimentally, while other information must be estimated indirectly.

An estimation of such critical factors could help selecting machining parameters that guarantee production of quality parts, good productivity and an acceptable level of dust emission. Some analytical approaches were developed for the prediction of cutting temperature (Groover, 2020). For example, the input parameters of the temperature model can be calculated according to the Nathan Cook model using experimental data to predict the cutting temperature. In this model, we assumed that the ambient temperature is Ta = 22°. The cutting temperature (T) can be calculated as:

$$T = 0.4\frac{U}{\rho.C}\left(\frac{V.f_z}{K}\right)^{0.333} \tag{6.1}$$

$$T_{total} = Ta - T \tag{6.2}$$

where U is the specific energy of the material; ρ is the density the material, C is the volumetric specific heat of the material (j/(mm3 C°)), V is the cutting speed, f_z is the feed per tooth and K is the material diffusivity.

The diffusivity K may be determined from the specific heat $C\rho$, the density ρ, and the thermal conductivity α as follows (Bard, Schönl, Demleitner & Altstädt, 2019)(Wróbel, Rdzawski, Muzia & Pawlak, 2009):

$$K = \frac{\alpha}{\rho.C\rho} \tag{6.3}$$

It is known that the specific cutting energy is the amount of energy used in removing a unit volume of the workpiece material per unit time during machining.

For conventional alloys such as aluminum alloys and steels, the specific cutting energy is well documented; but it is not the case for composites or for CFRP. Meanwhile, the other input parameters of the cutting temperature model can be calculated based on the specific energy U which can be calculated from the cutting force (Fc), the cutting speed (V) and the metal removal rate (MRR) (Groover, 2020).

$$U = \frac{Fc.V}{MRR} = \frac{Fc.V}{Ac.V} = \frac{Fc}{Ac} \tag{6.4}$$

where Ac is the undeformed chip area which is given by (Xiao *et al.*, 2018):

$$Ac = a_c + a_t \tag{6.5}$$

where: at is the thickness of the unidirectional laminate; and ac is the chip thickness, which varies continuously with the engagement angle ϕ of the tool, and is expressed as (Maegawa *et al.*, 2016):

$$a_c = f_z \sin \varnothing \tag{6.6}$$

where f_z is the feed per tooth.

The cutting forces Fc can be measured or estimated from the shear angle (ϕ) as follows (Elgnemi, Jun, Songmene, Samuel *et al.*, 2021):

$$Fc = -Fx \sin \varnothing + Fy \cos \varnothing \tag{6.7}$$

where Fx and Fy are forces to be measured using a table dynamometer.

Since the undeformed thickness of the chip is almost the same as the depth of cut used, (given the brittle nature of the CFRP (Sheikh-Ahmad, 2009), the shear angle ϕ can be estimated through the tool rake angle α by (Zhang *et al.*, 2001):

$$\varnothing \approx \tan^{-1}\left(\frac{cos\alpha}{1 - sin\alpha}\right) \tag{6.8}$$

For this study, the cutting forces were measured, and the temperature was estimated then validated using experimental machining data. The fine dust emission was sampled during machining and the tool wear was estimated after a given number of machining passes.

6.3 Experimental setup

Down milling experiments were carried out using a HURON-K2X10 3-axis CNC machine tool with maximum spindle speed (N) 28000 rpm, power (P) 50 kW and torque (T) 50 Nm. A dynamometer (type Kistler 9255B) was clamped on the machine table and connected to

the charge amplifiers (Kistler 5010) (Kistler Materials 2020, 13, 1181 5 of 22 Instrument Corporation, New York, NY, USA) that generated output signals, which were transmitted to a data translation card (type DT 9836, Data Translation Inc., Marlborough, MA, USA), linked to a personal computer. All signals, monitored independently, were digitized and recorded using LabView software program in order to analyze force measurements. An Aerodynamic Particle Sizer (APS, model 3321, TSI Inc., Shoreview, MN, USA) capable of measuring the aerodynamic size of particles from 0.5 to 20 microns. The dust samples were sucked by a pump (1.5 L/min) through a 10 mm suction tube, with the end of a tube placed near the machining area. The suction tube was connected to the dust measurement system, which consisted of aerodynamic particle sizer (APS) spectrometer. The collected data was then analyzed using the TSI's Aerosol Instrument Manager soft-ware. The experimental scheme is illustrated in Figure 6.1. The dust sampling was done during the machining process (doors closed). The APS record signal was initiated 3 seconds before the cutting process started and was completed, after the end of the testing, when the dust measurement was near to zero.

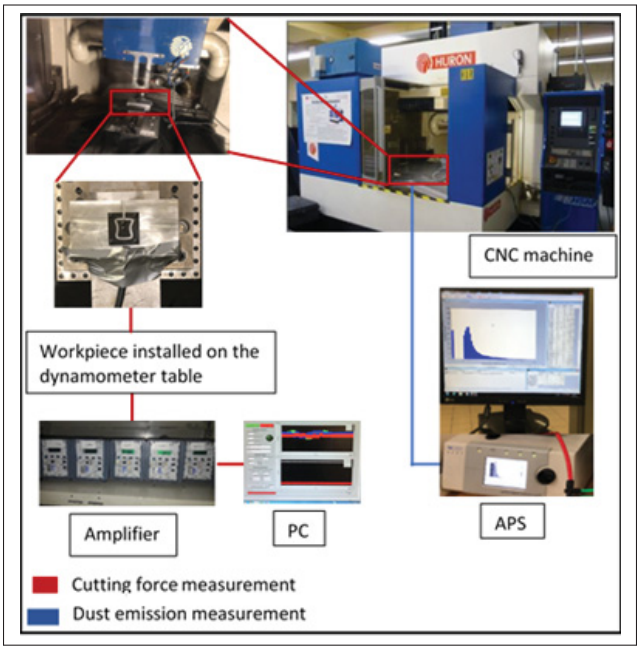

Figure 6.1 Photographs showing setup for machining CFRP and measurement system, and shape and geometrical dimensions of workpiece used in this study

6.3.1 Workpiece material and tool details

Multi-layer CFRP sheets of 1.56 mm (1/16 in) thickness were milled in each experi-ment. Each CFRP sheet consists of four unidirectional tapes of equal thickness that are laid up in (0F/90/0F/90/0F/90/0F/90) configuration. Figure 6.2 (a) demonstrates the fabric prepreg orientation scheme. The workpiece materials were cut into small sheets of 38 mm length x 38 mm width. The total cutting length tested during experiments was Lc = 105 mm routing. Normally, the use of cutting fluid is not allowed in the secondary process of aircraft CFRP part machining; therefore, dry cutting was employed in this part of the study. Table 6.1 shows the mechanical and physical properties of the workpiece as obtained from the CFRP supplier (McMaster-Carr, Illinois, United States).

Table 6.1 Mechanical and physical properties of CFRP used

Property	Value
Volume of fibers in each tape	54%
Young's modulus of the fibers	225 Gpa
Young' modulus of the sheets	65 Gpa
Density (ρ)	1.81 g/cm^3
Heat capacity (c)	0.06 J/g.C°
Thermal conductivity (α)	0.5 J/s-mm C°

A 3.175 mm diameter router end mill (ET-6-1250-F manufactured by Performance Micro Tool, Janesville, WI 53547, USA) with chip breaker and with reverse V-shaped ends was used for milling operations, see Figure 6.2 (b). The edges are serrated to break up the chips into smaller pieces and fast removal of material during roughing. This router is designed specially to produce profiling in composite materials. Fishtail ends with V-shaped ends are suited to produce a flat surface at the bottom and improve chip removal from the workpiece. The dimensions and the specifications of the end mill are shown in Figure 6.2 and Table 6.2.

Table 6.2 Specifications of the tool used in the experiments

Cutting dia	Flute length	No of flutes	Overall length	Rake angle
3.175 mm	6.477 mm	6	38.1 mm	6°

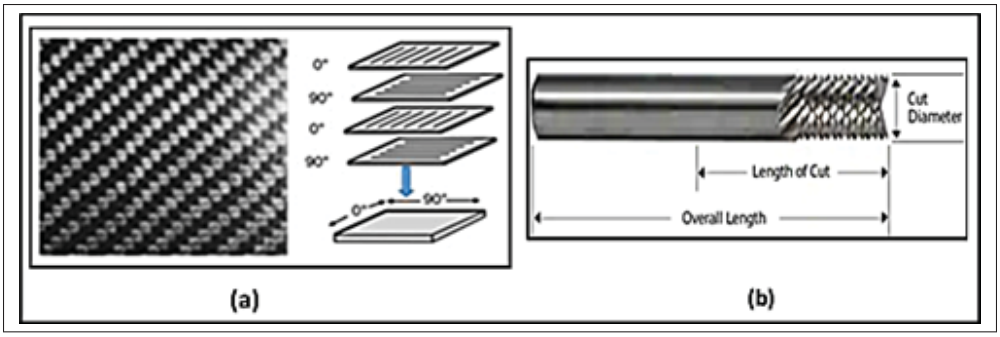

Figure 6.2 (a) Composite lay-up, (b) chip breaker routed geometry

6.3.2 Temperature measurement

Two K-type thermocouples (made from nickel–chromium wires each of 0.076 mm diameter (0.003 in.) were used for measuring the temperature during machining. The characteristics of the thermocouples are presented in Table 6.3 Figure 5.6 shows a schematic representation of the cutting temperature/forces measurement system used. The thermocouples were installed on the tool, at 2.2 mm from the tool tip to ensure the performance of temperature measurement. The thermocouple was held first by adhesive, then glued to the tooth by cement (OMEGABOND® 400 # OB-400) which is an excellent thermal conductor. The tool was then left for 24 hours in the open air. Once baked, the cement was covered with epoxy resin to protect it and ensure adhesion. The epoxy resin forms a sort of bridge between two teeth and protects the cement, which is very brittle, from the flow of chips. In all cases, the axial depth of cut was kept constant at 2 mm, such that the thermocouples were located at a distance of 0.2 mm from the cutting area. The tool was then mounted in a special holder (Type M-320, manufactured by Michigan Scientific Corporation). It is equipped with connections for thermocouples and data was subsequently relayed to and recorded (simultaneously with cutting force traces).

Table 6.3 Characteristics of thermocouples

Brand	**OMEGA®**	
Type	K	Reference
Red - Positive	Chrome - Nickel	CHROMEGA® TFAL-0.003 (∅ 0.076 mm)
Yellow - Negative	Aluminum - Nickel	ALOMEGA® TFCY-0.003 (∅ 0.076 mm)

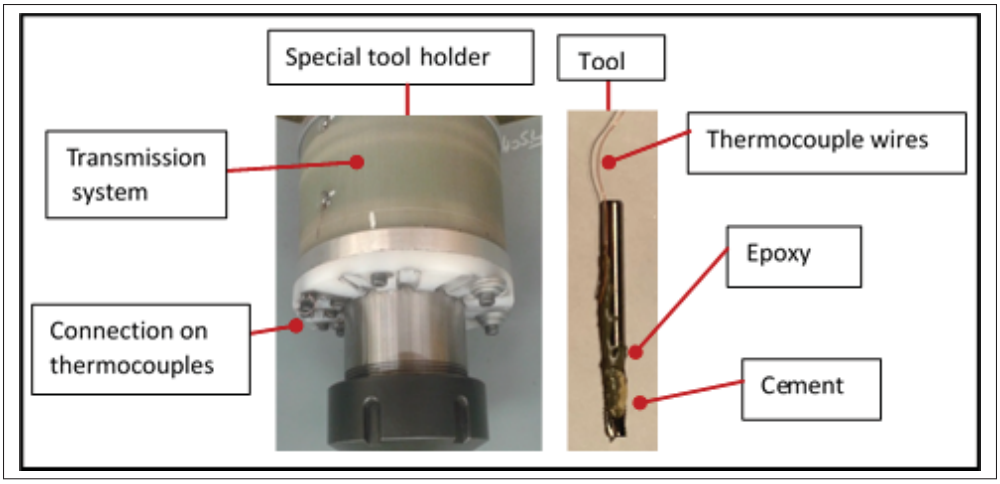

Figure 6.3 Schematic of cutting temperature measurement system (Tool holder and tool with thermocouples)

6.3.3 Dust emission measurement

Measurement of fine particles (diameter range 0.5 - 20 μm) was carried out using an Aerodynamic Particle Sizer (APS, model 3321, TSI Inc., Shoreview, MN, USA). Dust samples were sucked by a pump (1.5 L/min) through a suction tube, with the end of the tube placed near the machining area. The suction tube was connected to the dust measurement system, which consisted of the APS. The experimental scheme is illustrated in Figure 6.1.

6.3.4 Machining parameters and design of experiments

Machining parameters such as cutting speed, axial depth of cut, and feed per tooth affect the cutting temperature. However, the cutting speed and feed per tooth are the more crucial and dominating factors. Therefore, the milling experiments emphasized on these two parameters, while the remaining parameters were set to be constants, e.g., the axial depth of cut was set as 2 mm. The two machining parameters that are studied are (a) feed per tooth (fz), (b) cutting speed (vc). Three feed per tooth levels (2, 4, 6 micrometer/tooth), and three speed levels (10000, 15000, and 20000 rpm) were examined in the experiments. To increase reliability and accuracy of the results, each test was repeated two times. A full factorial design of experiments across the

two factors of feed, speed, and their corresponding levels requires a total of $3^2 = 9$ experiments. The cutting parameters and their levels are listed in Table 6.4.

Table 6.4 Machining parameters and selected levels

Factors	Level 1	Level 2	Level 3
s: spindle speed (rpm)	10000	15000	20000
f_z: feed per tooth (μm)	2	4	6
Lc: cutting length (mm)	105		
∂p: axial depth of cut (mm) (ρ)	2		

6.4 Results and discussions

6.4.1 Cutting force

The bar diagram in Figure 6.4 shows the average of the measured cutting forces Fc obtained from cutting tests with the error bars indicating standard deviation. Each bar diagram shows the magnitude of the average cutting forces during milling of the CFRP using a specific feed rate and spindle speed. From Figure 6.4, it can be seen that the cutting forces increase proportionally as the feed rate (i.e., chip thickness) increases. This phenomenon can be attributed to an increase in chip loads and volume of material removal at a higher feed rate, leading to an increase in the magnitude of Fc.

Our observation from Figure 6.4 is that under identical cutting conditions, cutting forces increase as spindle speed increases from 10000 to 20000 rpm. The rate of increase of cutting forces with cutting speed is believed to be associated with the cutting temperatures. Our observation of the tool cutting temperature is described in *Section 6.4.2* and confirms the correlation between the increase in the cutting temperature and the cutting forces. This result may be explained based on the article of (Wang *et al.*, 1995), which states that cutting speed has two opposing effects on the mechanics of chip formation. A higher cutting speed raises the chip's strain rate, potentially resulting in in-creasing the cutting forces. At the same time, high-speed cutting generates more heat, which would soften the material and minimize the forces. In a previous

study (Elgnemi *et al.*, 2017) on CFRP composite using atomization-based cutting fluid sprays it was reported that cutting forces decrease with an increase in cutting speed when machining CFRP. In the experiments conducted in this work, however, we consistently observed higher forces at higher (20000 rpm) speed than at lower (10000 rpm) speed. Therefore, it may be concluded here that depending on the workpiece material, tool geometry, and cutting condition, either of these effects may dominate the process and increase or decrease the cutting forces.

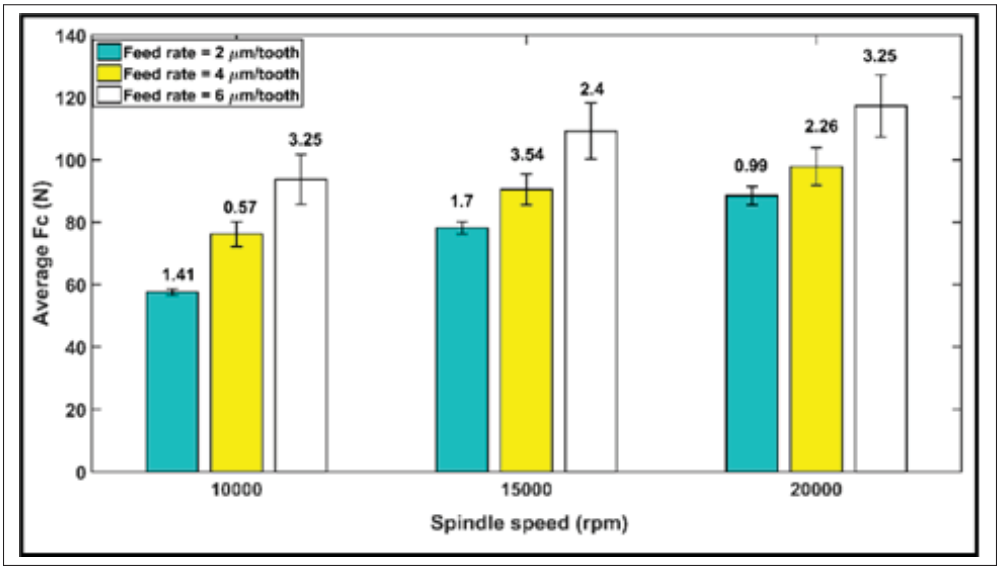

Figure 6.4 Variation of the average cutting forces with standard deviation at cutting speeds of 10000, 15000, and 20000 rpm, and feed rates of 2, 4, and 6 μm/tooth

6.4.2 Cutting temperature

Figure 6.5 shows the evolution of the temperature registered during milling with respect to spindle speeds of 10000, 15000, and 20000 rpm (i.e., vc = 100, 150, and 200 m/min) at the feed rates of 2, 4, and 6 µm/tooth, respectively, after machined distances Lc = 105 mm. The machining temperatures range from 69 to 170 °C. It can be also seen from Figure 5 that the overall machining temperature increases with an increase in spindle speed from 10000 to 20000 rpm. This is could be due to the increase in the friction between the cutting tool and the machined surface (Yashiro *et al.*, 2013). (Gara, M'hamed & Tsoumarev, 2018) measured the

cutting temperature during machining of a multidirectional CFRP laminate. The experiments were conducted on a computer numerical control (CNC) machine with the cutting speed ranging from 80 to 200 m/min and the feed rate from 0.008 to 0.060 mm/tooth. The data were analyzed in order to establish empirical models showing the dependence of cutting temperature on tool geometry and cutting conditions. Based on the results, it was concluded that cutting speed is the factor influencing cutting temperature the most.

Considering the impact of feed rate, the cutting temperature decreased with an increase in the feed rate. This is in agreement with the common knowledge that, at high material removal rates (high feed per tooth), the largest share of heat is absorbed by the chip (Sheikh-Ahmad, 2009). In the case of low material removal rates (low feed per tooth), the heat is absorbed equally by the chip and the tool. Further, with increasing material removal rates, the chip transports much more heat from the active area, whereas at low material removal rates, the portion of the heat conducted into the tool plays a more significant role (Yashiro *et al.*, 2013). This behavior is clearly observed in Section 6.4.4 upon analysis of the specific cutting energy.

As Figure 6.5 reveals, the machining temperatures recorded are still far from the glass transition temperature of the tested CFRP (Tg = 187 °C). In this case, it can be assumed that there is no thermal damage. The present study found that the CFRP machined using a spindle speed of 10,000 rpm (i.e., vc = 100 m/min) and 6 μm/tooth feed rate exhibited a reduced cutting temperature during milling under dry conditions. Based on the above analysis, it may be concluded that reduced chip thickness (lower feed rate/higher spindle speed) generates the highest temperatures, resulting in increased thermal damage. In contrast, increased chip thickness (higher feed rate/lower spindle speed) generates the lowest temperatures.

6.4.3 Validation of modeling temperature results

For validation purposes, a comparison between the cutting temperature measured by the K-type thermocouple from the experimental tests and the predicted cutting temperature calculated based on the proposed model, Equation (6.1), under the same cutting conditions, is performed.

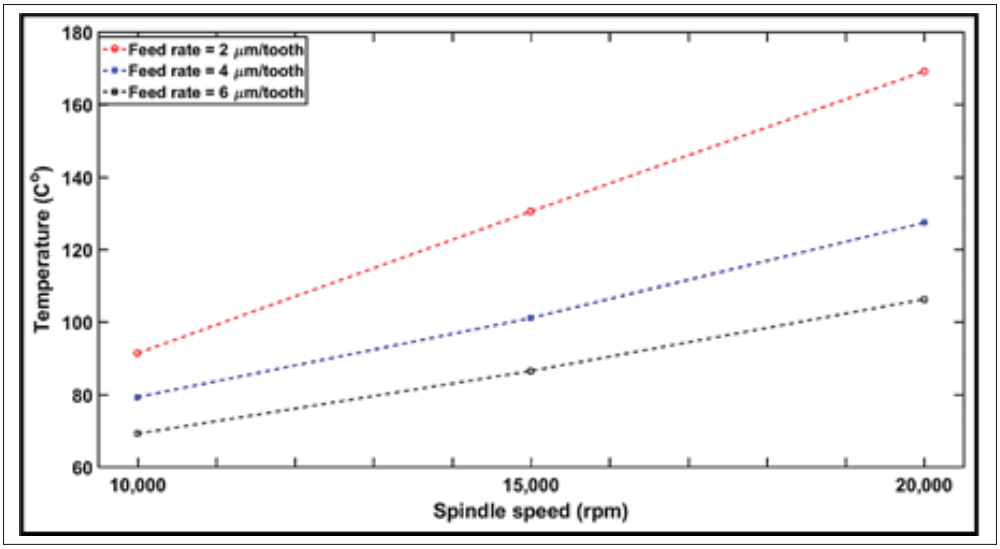

Figure 6.5 Variation in cutting temperature as a function of spindle speed and feed rate

The results are displayed in Figure 6.6. It should be noted that the cutting conditions for the milling experiments were presented in Section 6.3.4, while the model was performed for material parameters of the CFRP cited from (Groover, 2020) and given in Table 6.1. Figure 6.6 also illustrates the maximum temperature generated during milling with respect to feed rate at spindle speeds of 10000, 15000, and 20000 rpm (i.e., 100, 150, and 200 m/min). The simulated value of the temperature with respect to speed is found to rise with an increase in spindle speed and is predicted to be minimum for the 10000-rpm speed (i.e., vc = 100 m/min). This agrees with the experimental results. A good agreement was also observed between the experimental and predicted values of the temperature for the feed rate, similar to Figure 6.6. The relative errors between the predicted and experimental values of temperature are found to be about 7%. Nevertheless, because the temperatures were measured at 0.2 mm from the axial depth of cut, ap, it could be argued that the temperature is higher for the model than for the experiments. Consequently, it may be summarized that the model can predict the temperature with a good degree of accuracy.

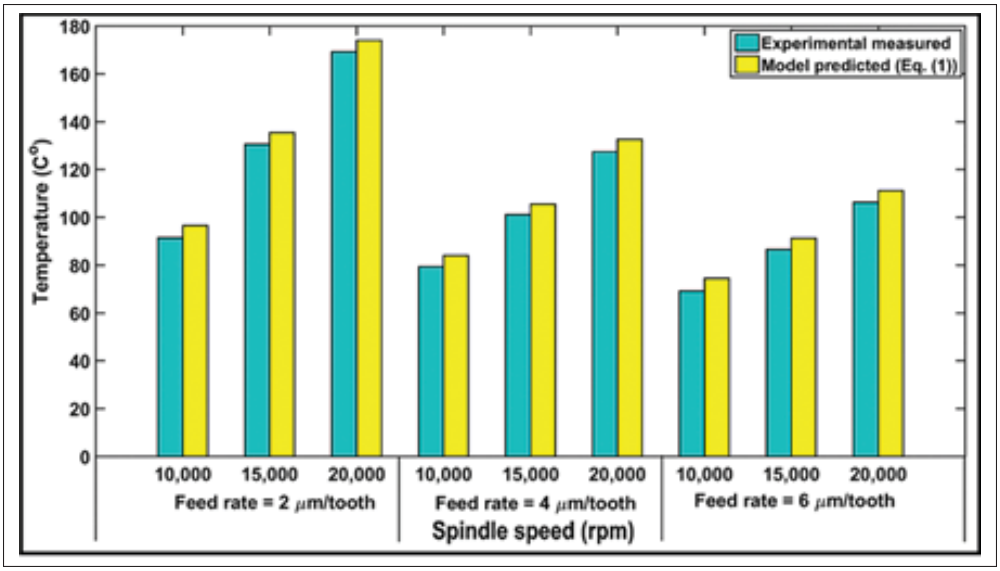

Figure 6.6 Comparison of measured and predicted temperatures as a function of spindle speeds and feed rates

6.4.4 Specific cutting energy

The experimental cutting forces data were used to estimate the energy involved in the milling process (see Equation (6.4)). Specific cutting energy (or specific cutting pressure), defined as the cutting force per unit area of the uncut chip, was calculated based on Equation (6.4), as shown in Figure 6.7. The chip thicknesses ac of each laminate ranged from 0.0023 to 0.0044 mm, corresponding to the feed per tooth values of 2, 4, and 6 μm/tooth. It can be seen in Figure 6.7 that the average specific cutting energy for the cutting force Fc decreased with an increase in feed rate but increased when the spindle speed increased. This is due to the fact that specific cutting energy is critically dependent on the feed rate (i.e., chip thickness), which is a function of the cutting engagement angle, ϕ. Our observation of the specific cutting energy is described in Section 6.2, Equation (6.6), which confirms the correlation between the increase in the specific cutting energy and the feed rate (i.e., chip thickness). It also indicates that the highest specific cutting energy recorded is 40.7 N/mm^2 at 20,000 rpm (vc = 200 m/min) and a feed rate of 2 μm/tooth (0.002 mm/rev) and the lowest specific cutting energy is 12.7 N/mm^2 at 10,000 rpm (vc = 100 m/min) and a feed rate of 6 μm/tooth (0.006 mm/rev). However, the specific cutting

energy for CFRP composites is well below that of metals. The comportment of specific cutting energy regarding cutting speed is similar to that of the cutting force (Section 6.4.1), whereas it varies considerably with feed rate. A significantly higher specific cutting energy is required for removing small chips (small feed rate). For a high cutting speed and large chip size, the specific cutting energy for the tested composite tends to become constant. Therefore, from a material removal rate point of view, better machinability of CFRPs can be achieved with high feed rates and cutting speeds.

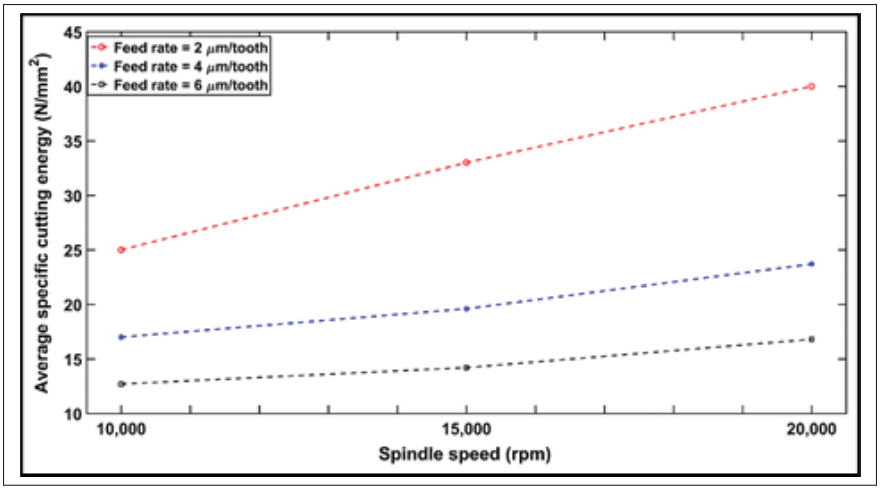

Figure 6.7 Variation of average specific cutting energy (Equation (4)) as a function of spindle speeds and feed rates

6.4.5 Study of tool wear

Dry machining of CFRP has an adverse impact on the operator as well as the environment in general. Therefore, a detailed study was undertaken to investigate tool wear under dry conditions using a router end mill. Tool wear was measured quantitatively based on the tool wear weight method, which is defined as the difference in tool weight before the machining and tool weight after the machining and is usually expressed as a percentage. Figure 6.8 illustrates the progression of tool wear (%) vs. the cutting conditions for a cutting distance of Lc = 105 mm. It can be observed that the tool wear increases when the feed rate (i.e., chip thickness) is increased. This can be directly related to the increase in the forces required to remove the larger

chip thickness. This result also explains the high cutting force observed at 6µm/tooth feed rate in Section 6.4.1. Moreover, an increasing spindle speed offers a wider contact surface between the tool and the workpiece, thus resulting in superior surface contact and greater time consumption. As a result, an increase in tool wear is observed (Haddad *et al.*, 2014). One can also conclude from Figure 6.8 that a significant improvement in the machinability of a CFRP in terms of tool wear can be achieved by decreasing the feed rate and spindle speed.

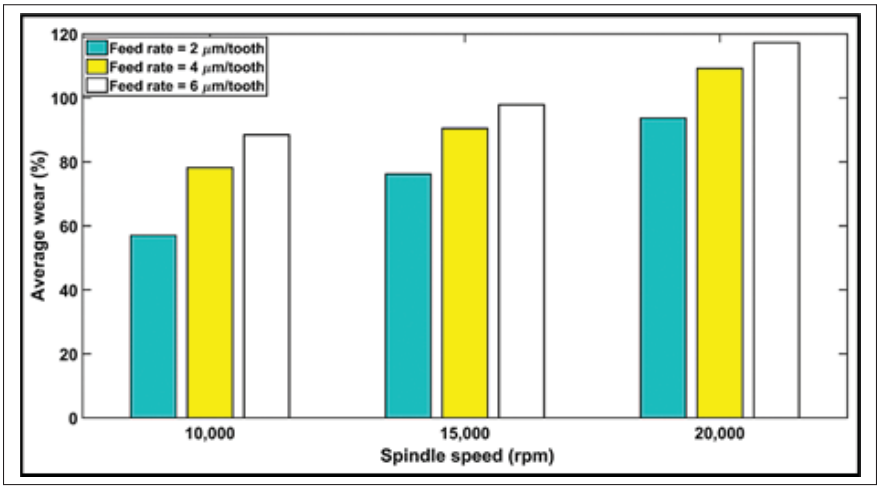

Figure 6.8 Variation in tool wear (%) with respect to spindle speed and feed rate after cutting distance Lc of 105 mm

6.4.6 Particle emission during milling

The maximum number of dust particles corresponding to different sizes as obtained in the experiments performed are plotted in Figure 6.9, depicting the peak-to-peak magnitudes for all cutting conditions. According to the collected data, the highest numbers of particles were registered for particles in the range 0.5 – 1 μm, followed by those with sizes between 2 and 7.5 μm, indicating a decrease in the number of particles with an increase in the feed rate, but an opposite effect with an increase in the spindle speed. Overall, the highest numbers of particles are obtained at 20000 rpm spindle speed with 2 μm/tooth feed rate for 0.5 – 1 μm sized particles, as is also the case for the 1 – 7.5 μm sized particles. In contrast, at a 10000-rpm spindle speed with a 6 μm/tooth feed rate, minimum numbers of particles are obtained. The following two

important points were consistently noted in all the experiments: firstly, regardless of the feed rate used or the highest number of particles, the size of particles increased with speed, ranging from 0.5 to 2.5 μm at 10000 rpm, and 0.5 to 7.5 μm at 20000 rpm. This is explained by the higher cutting temperatures, as elaborated in Section 6.4.2 where an increase in the temperature was correlated with an increase in the number of particles. The second observation was that regardless of the spindle speed or the peak emission, the 2 and 4 μm/tooth feed rates displayed similar highest number of particles at a 15000-rpm speed. However, when using a feed rate of 2 μm/tooth, a second peak of particle emission appears for particle size ranging from 2.0 to 2.5 μm. Likewise, the 4 and 6 µm/tooth feed rates offered the same highest number of particles at a 20,000-rpm speed. This observation is evident from the total particle number concentration (see Figure 6.10). However, the feed rate seems to have a limited influence as compared to that of speed. This is also observable in the analysis of variance (ANOVA) presented in Table 6.5. The influences of spindle speed and feed rate can be explained by the chip formation process during the machining of composites (Boatman *et al.*, 1988), (Ngoc, Hue, Van Hung & Duc, 2020). The shearing process, the chip separation and deformation, and the frictions in the shearing zone and at the chip–tool and tool–workpiece interfaces produce a lot of dust (Khettabi, Songmene, Zaghbani & Masounave, 2010). At low speeds, the chip crack is controlled by its brittleness. Therefore, there is limited contact and friction between its lips due to the crack opening (Dabade & Joshi, 2009). A burr tool would generate a minimum number of particles when compared to a flat (traditional) tool, as reported by (Haddad *et al.*, 2014). Thus, it can be concluded that tool geometry is an important factor in dust emission. One can also conclude from Figures 6.9 and 6.10 that in order to reduce the dust emission at low spindle speed, chip thickness should be increased by either decreasing the spindle speed or increasing the feed rate.

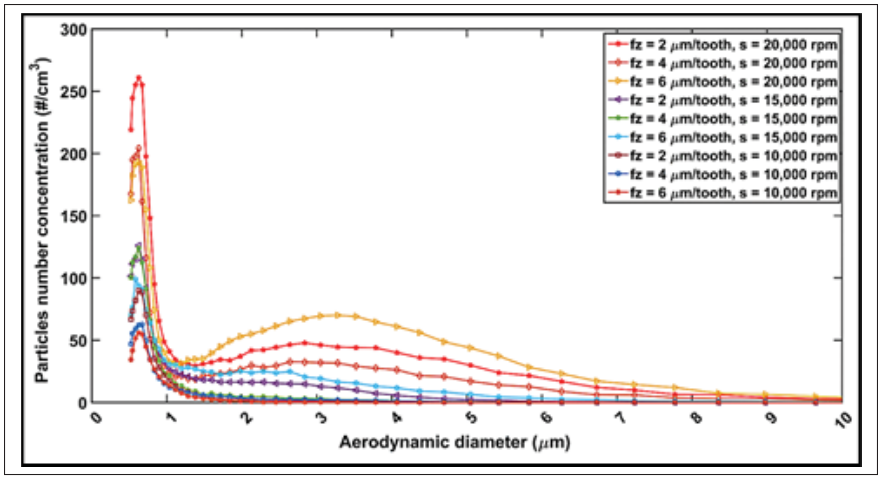

Figure 6.9 Number of fine particles vs. particle size during milling of CFRP for different cutting conditions

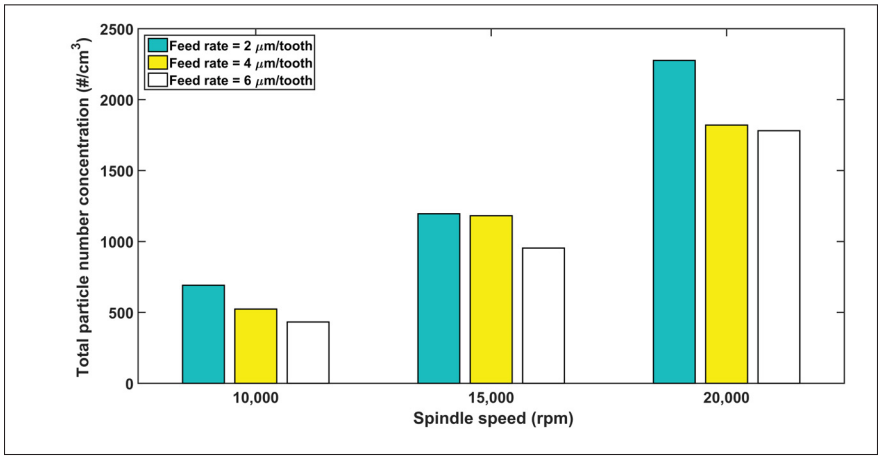

Figure 6.10 Total particles number concentration related to particle size and cutting parameters

6.4.7 Analysis of variance (ANOVA)

The main purpose of ANOVA is to use a statistical method to appreciate the effects of individual controlling parameters on the results obtained. The analysis was carried out at a 5% significance level (i.e., 95% confidence level). The significance of control factors in ANOVA is determined by comparing the F values of each control factor, as described in Table 6.5. The factors that produced statistically significant effects were selected to develop the experimental prediction

model. According to Table 6.5 (a), in the analysis of variance for the cutting force, for example, two factors, namely feed rate and spindle speed, have p-values below 0.05, which makes them statistically significant at the 95% confidence interval. The speed has the greatest effect on the cutting force, followed by the feed. These factors were used to develop the empirical model. It is also seen that the interactions f * f, s * s, and f * s are not statistically significant for the cutting force, which was, therefore, not selected to develop the empirical model. Similarly, calculations were applied for other factors in evaluating their significance, as shown in Table 6.5 (b–e). Table 6.5 (b) presents the analysis of variance for specific cutting energy, with two of the factors displaying p-values less than 0.05, indicating their statistical significance at the 95% confidence level. The feed rate had the highest effect on the specific cutting energy. With respect to temperature, Table 6.5 (c) indicates that the speed was statistically significant followed by the feed rate and interaction f * s, while the interactions f * f and s * s had no influence. It can be seen from Table 6 (d) that the feed rate had the greatest effect on tool wear, with the spindle speed as the next most influent factor. The fine particle emission was also analyzed. In this work, the fine particles studied have diameters ranging from 0.5 to 10 mm. According to Table 6.5 (e), the spindle speed (F-Ratio = 428.28) with a p-value of 0.000 is most significant, while the feed rate and interaction s * s are less significant at the 95% confidence level. The observations of the fine particle emission as described in Section 6.4.6 confirm the relationship between the increase in the total number of particles emitted and spindle speed. The Pareto diagrams in Figure 6.11 illustrate the effect of the input parameters (feed and speed) on the output parameters (cutting force, temperature, specific cutting energy, tool wear, and dust emission). It can be seen from Figure 6.11 that the feed rate has a significant influence on specific cutting energy and tool wear, while spindle speed was shown to be the most effective factor with respect to the cutting force, temperature, and total particles number.

6.4.8 Response surface methodology

The response surface methodology (RSM) establishes a mathematical relationship between two sets of data (Mia & Dhar, 2016) with one set being the independent variables, i.e., cutting

Table 6.5 Analysis of variance (ANOVA) for output factors

(a) ANOVA for cutting force Fc					
source	**DF**	**SS**	**MS**	**F-Ratio**	**p-Value**
f	1	967.74	967.74	254.87	0.001 *
s	1	1532.80	1532.80	403.69	0.00 **
f * f	1	33.62	33.62	8.85	0.06
s * s	1	13.00	13.00	3.43	0.16
f * s	1	13.32	13.32	3.51	0.15
Error	3	11.39	3.80		
Total	8	2571.88			
(b) ANOVA for specific cutting energy U					
f	1	509.68	509.68	385.69	0.00 **
s	1	117.04	117.04	88.57	0.003 *
f * f	1	27.13	27.13	20.53	0.020
s * s	1	0.16	0.16	0.12	0.75
f * s	1	33.64	33.64	25.46	0.015
Error	3	3.96	1.32		
Total	8	691.62			
(c) ANOVA for Temperature T					
f	1	2777.80	2777.80	267.40	0.00 **
s	1	4428.17	4428.17	426.27	0.00 **
f * f	1	78.13	78.13	7.52	0.07
s * s	1	2.42	2.42	0.23	0.66
f * s	1	414.12	414.12	39.87	0.008*
Error	3	31.16	10.39		
Total	8	7731.80			
(d) ANOVA for Tool Wear					
f	1	52.81	82.81	153.80	0.001 **
s	1	9.46	9.46	27.55	0.013 *
f * f	1	2.70	2.70	7.87	0.068
s * s	1	0.43	0.43	1.27	0.34
f * s	1	4.16	4.16	12.31	0.040
Error	3	1.03	0.34		
Total	8	70.61			
(e) ANOVA for Fine Particle Emission					
f	1	219.98	219.98	21.68	0.019 *
s	1	4.345,61	4.345,61	428.28	0.000 **
f * f	1	857	857	0.85	0.426
s * s	1	222.81	222.81	21.96	0.018 *
f * s	1	31.13	35.13	3.46	0.16
Error	3	30.44	10.147		
Total	8	4.862,56			

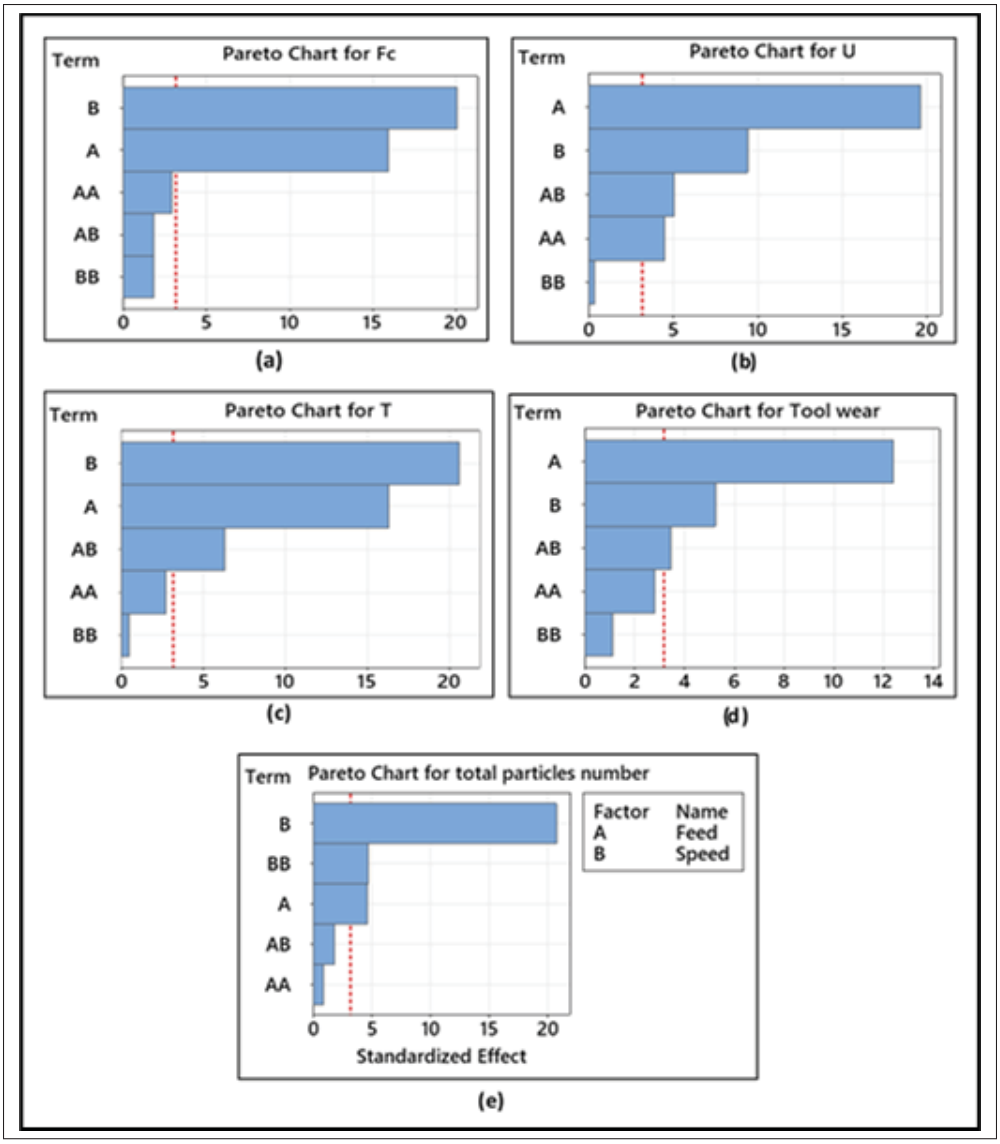

Figure 6.11 Pareto charts of the standardized effects of (a) cutting force Fc, (b) specific cutting energy U, (c) temperature T, (d) tool wear, and (e) total particle numbers concentration. A (feed rate), B (speed) AB interaction between feed rate (A) and speed (B)

speed and feed rate, whereas the other set is the dependent variables or quality characteristics, i.e., cutting force, specific cutting energy, temperature, tool wear, and dust emission. This mathematical relation can be either first order (linear) or second order (quadratic). In the present work, the second order (quadratic) RSM models were applied using a statistical software Minitab ® 20.3 to establish relationships between the input parameters (independent variables) and the

output responses (dependent variables). It should be mentioned that we applied the first order model but, the result shown that the model is not fit. The correlation coefficients R^2 and R^2 adjusted for output parameters (cutting force, specific cutting energy, temperature, and total particle numbers) are given in Table 6.6. The results obtained for the coefficients indicate that the model used is quite adequate for prediction purposes as shown in APPENDIX I. The predictive fit model equations for cutting force, specific cutting energy, temperature, tool wear, and total particle numbers were obtained as follows:

$$F_c(N) = 16.55 + 6.35f + (3.2 \times 10^{-3}s) \tag{6.9}$$

$$U\left(\frac{N}{mm^2}\right) = 22.62 - 7.63f + 2.04 \times 10^{-3}s + 0.92f^2 - (3 \times 10^{-4}f.s) \tag{6.10}$$

$$T(^{o}C) = 7.3 - 4.5f + (9.5 \times 10^{-3}s) - (1.02 \times 10^{-3}f.s) \tag{6.11}$$

$$Toolwear(\%) = 8.3 - 2.375f - (1.57 \times 10^{-4}s) + 0.3f^2 + 10^{-4}f.s \tag{6.12}$$

$$Tpn\left(\frac{\#}{cm^3}\right) = 1900 - 957f - 0.23s + (1.36 \times 10^{-4}s^2) \tag{6.13}$$

Table 6.6 Correlation coefficients R^2 and R^2 adjusted for Equations (9-13)

Equation No.	**Output parameters**	R^2	R^2 **Adjusted**
1	cutting force	97.2%	96.3%
2	Specific cutting energy	99.4%	98.8%
3	Temperature	98.5%	97.7%
4	Tool wear	97.9%	95.8%
5	Total particle numbers (Tpn)	98.4%	97.5%

6.4.9 Response surfaces and contour plots for output parameters

Three-dimensional (3D) response surfaces and the corresponding two-dimensional (2D) contour plots were determined for the modeled parameters as a function of the independent factors, feed per tooth, and spindle speed. The response surfaces due to the effects of these two factors on the cutting force, specific cutting energy, temperature, tool wear, and dust emission are illustrated

in Figure 6.12. The corresponding contour plots are shown in Figure 6.13. As presented by Figure 6.12 (a,d), the cutting force and tool wear increase for all three feed rates as the spindle speed increases from 10000 to 20000 rpm. The obtained maximum cutting force (Fc) and tool wear are 110 N and 12%, respectively, at a feed rate of 6 μm/tooth and a spindle speed of 20000 rpm. On the other hand, from Figure 6.12 (b,c), the specific cutting energy and the temperature decrease significantly for all three feed rates and increase as the spindle speed increases from 10,000 to 20000 rpm. The obtained maximum specific cutting energy (U) and temperature (°C) are 35 N/mm^2 and 140 °C, respectively, at a feed rate of 2 μm/tooth and a spindle speed of 10000. Figure 5.12 (e) shows that the total particles number increases significantly with the increase in spindle speed from 10000 to 20000 rpm and decreases as the feed rate increases. The obtained maximum total particles number is 20000 cm^3 at 20000 rpm and a feed rate of 2 μm/tooth. In addition, the elliptical nature of the contour lines in Figure 6.13 (d,e) implies that there is a significant interaction between the feed rate and the spindle speed. The interactions between the independent variables in the contour plots have an important impact on the response because high interactions mean the existence of maximum, minimum, or saddle points in the response surface, which help in estimating the optimization process. On the other hand, in the contour plots in Figure 6.13 (a–c), the nearly linear contour lines imply that interaction between the feed rate and the spindle speed in the case of the corresponding output parameters is weak.

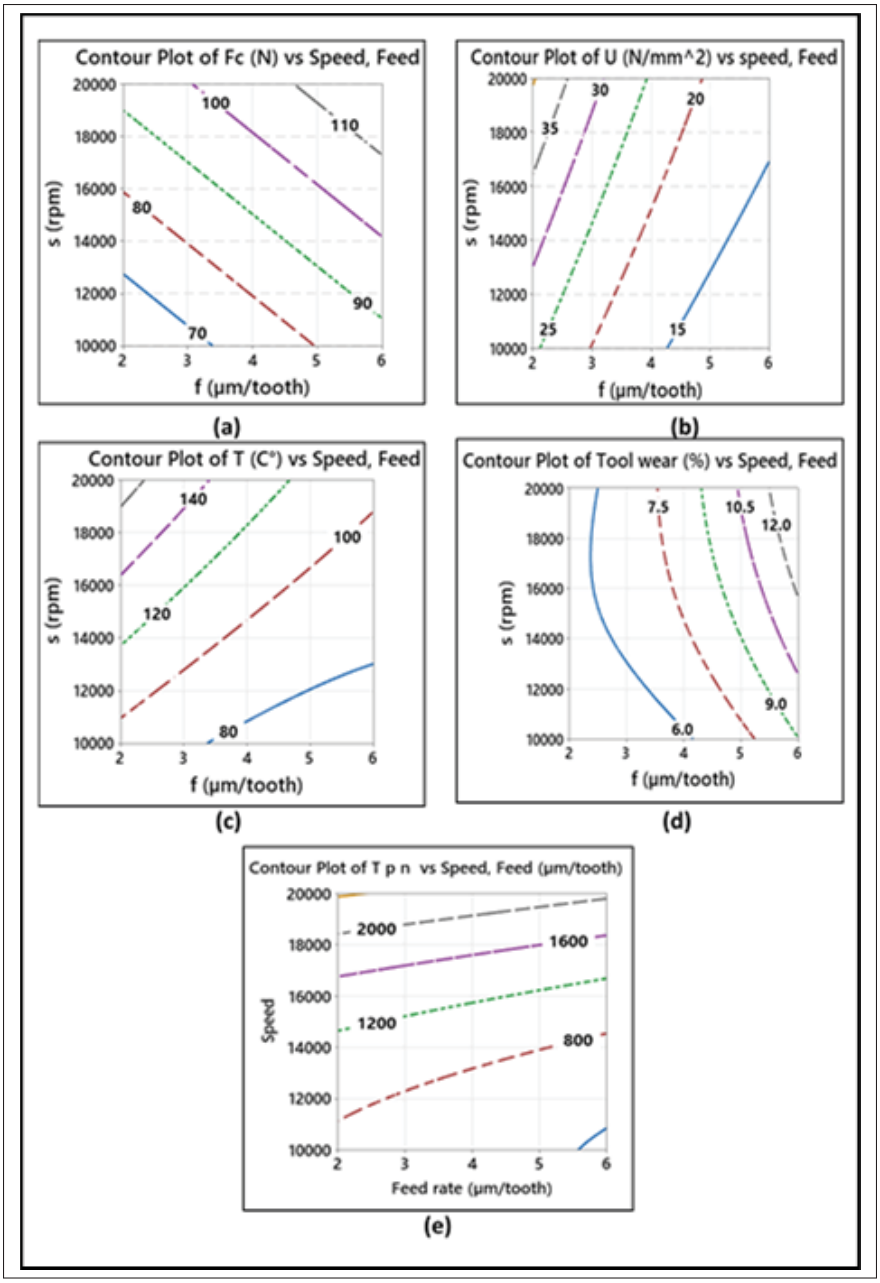

Figure 6.12 Corresponding contour plots showing effect of cutting parameters on (a) cutting force, (b) specific cutting energy, (c) temperature, (d) tool wear, (d) total particles number Tpn (#/cm^3)

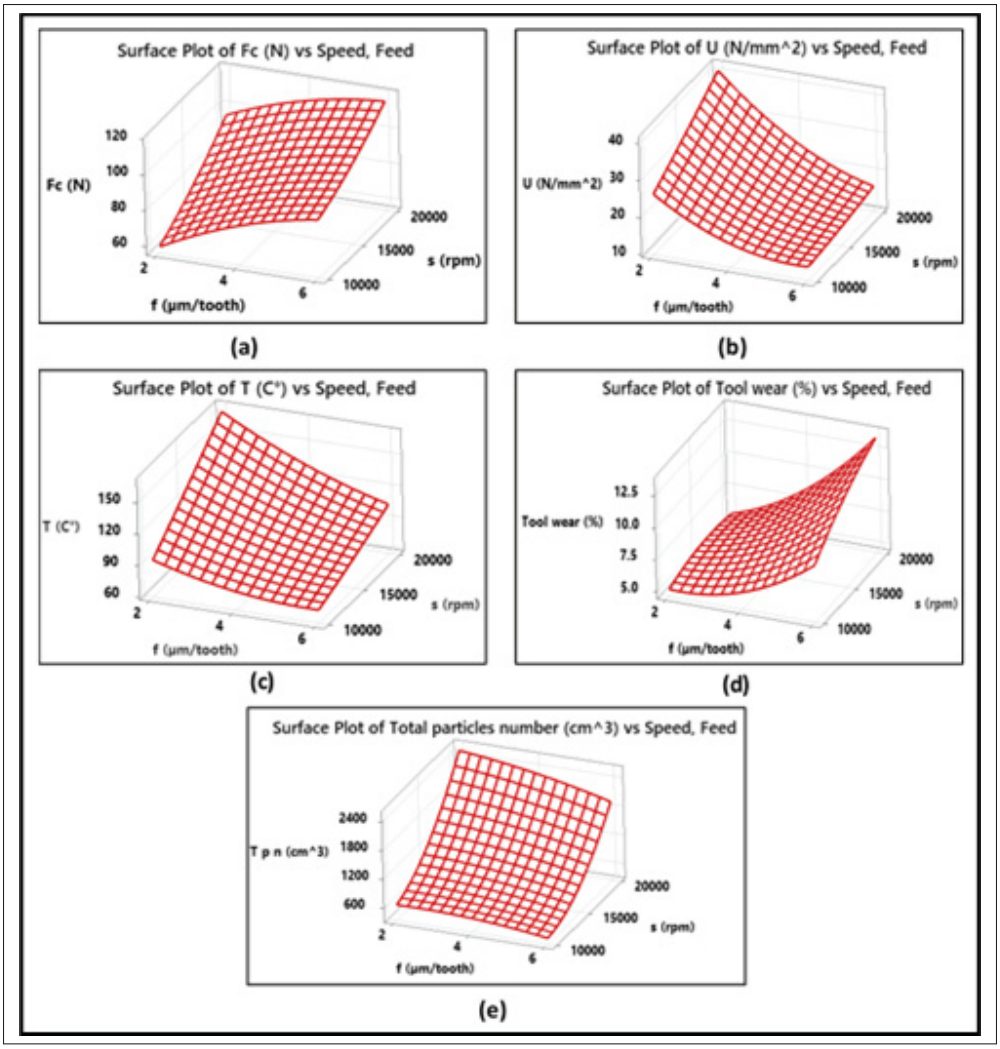

Figure 6.13 3D surface plots showing effect of cutting parameters on (a) cutting force, (b) specific cutting energy, (c) temperature, (d) tool wear, and (e) total particles number

6.4.10 Analysis of responses

The values from the experiment and the predicted values obtained from the empirical models (Equations (6.9) – (6.13)) are shown in Figure 6.14. Table 6.7 compares the values of the optimum cutting parameters for output parameters and their predicted values (the optimal spindle speed was 10000 rpm). It is concluded that a low cutting speed and a low feed rate are preferred to minimize the cutting force and the tool wear. In addition, in order to maintain a low

temperature, specific cutting energy, and dust emission levels, a low cutting speed and a high feed rate are preferred. Such a combination would help in maintaining an acceptable removal rate and thus render good productivity.

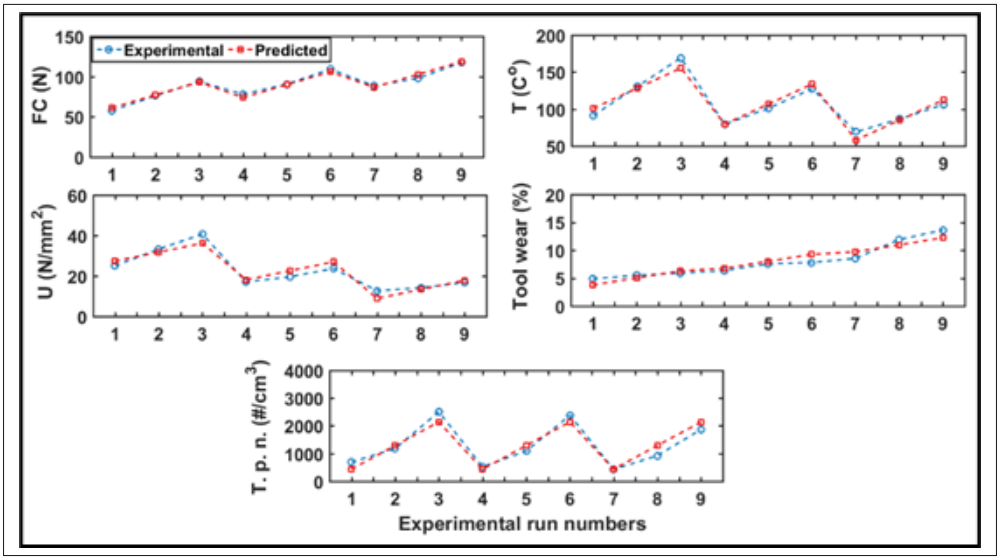

Figure 6.14 Comparison between experimental data and predicted data

Table 6.7 Comparison between experimental data and predicted data for the recommended spindle speed

No.	s (rpm)	f (µm/tooth)	Responses		
			Variables	**Exp.**	**Predicted**
1	10000	2	Force (N)	57.6	61.2
2	10000	6	U (N/mm^2)	12.7	8.92
3	10000	6	T (^oC)	69.20	58.08
4	10000	2	Tool wear	4.89	3.78
5	10000	6	Total number of particles ($\#/cm^3$)	432.3	438.03

6.5 Conclusions

The present study attempted to investigate routing milling of CFRPs under dry machining conditions. The effect of cutting parameters (feed rate, spindle speed) on the cutting force, cutting temperature, tool wear, and dust emission was assessed. From the experimental results and statistical analysis of the data, the following may be concluded.

1) Feed rate has a greater effect on cutting force and tool wear than the spindle speed in the milling of CFRP composite materials but has no influence on dust emission.
2) Cutting speed is the main parameter that controls the cutting temperature in milling of CFRP composite materials, followed by feed rate.
3) The predicted temperatures from the analytical model agreed well with the experimental observations within a range of ±10%.
4) The cutting temperature does not exceed the glass transition temperature for the cutting speeds (10000, 15000, 20000 rpm) and feed rates (2, 4, 6 μm/tooth) used.
5) The specific cutting energy for the cutting forces considered was investigated as a material property. It was found to increase with an increase in the spindle speed but decrease with an increase in the feed rate.
6) During the machining, fine particles were emitted (aerodynamic diameters ranging from 0.5–10 μm). The maximum concentration of fine particles reached 2776.6 $\#/cm^3$, while the minimum number reached 432.3 $\#/cm^3$. The spindle speed significantly affects fine dust generation, whereas the feed rate is not statistically significant. The total number concentration of fine particles decreased with an increase in the feed rate.
7) The optimum levels of the control factors for minimizing the cutting force, tool wear, cutting temperature, specific cutting energy, and fine particles emission were derived using the ANOVA approach. The optimal conditions for cutting force and tool wear were observed at cutting speed = 10000 rpm and feed rate = 2 μm/tooth, while those for a specific cutting energy, cutting temperature, and total number of particles were observed at cutting speed = 10000 and feed rate = 6 μm/tooth.

CONCLUSIONS

The work presented in this thesis primarily focused on an investigation of the machining performance of CFRP. The milling environment included dry conditions, and the application of atomization-based cutting fluids. The cutting conditions consist of high cutting speed, feed rate, and different fiber orientation angles FOA. In addition, the present study attempted to investigate routing milling of CFRPs under dry machining conditions. The effects of cutting parameters (feed rate, moderate cutting speed) on the cutting force, cutting temperature, tool wear, and dust emission were assessed. The results obtained are covered in the form of three published articles presented in chapters 4, 5 and 6 of the thesis.

In the first article, the effectiveness of atomization based cutting fluid application in improving the machinability of CFRP was studied experimentally. In the study, two types of cutting fluids, general purpose semisynthetic coolant and vegetable oil were applied by atomization, and their performances in reducing cutting forces, tool wear, surface roughness, and delamination werestudied over a range of high cutting speeds and feed rate values.

In the second article, performance of a vegetable oil-in-water emulsion, obtained using ultrasonic atomization but no surfactant, was examined during high speed milling of CFRP in terms of fiber orientation. The performance of wet milling is compared with that of a dry milling process. The fiber orientation angles tested were 0°, 30° 45°, 60° and 90°.

In the third article, the interaction effect of cutting parameters (moderate cutting speed and feed rate) on the following machining process performance indicators: cutting force, specific cutting energy, cutting temperature, tool wear, and fine dust emission (in terms of a number of particles) were studied during dry milling of CFRP. Analytical modeling and empirical modeling were also employed to the prediction cutting temperature distribution on the cutting tool.

In the light of the results obtained, the major conclusions are summarized as follows:

1) Compared to milling in dry conditions, after the application of atomized cutting fluid (ACF) to the cutting zone, cutting forces and tool wear improved significantly. Also, significant improvement in surface roughness was observed under ACF (vegetable oil) condition, for instance, at a spindle speed of 40000 rpm with ACF (vegetable oil), we met the best surface roughness at feed rates 2, 4, and 6 μm/tooth which is impossible to meet with dry conditions. It should be mentioned that Ra less than 3.2 μm is recommended by aerospace industries. In addition, the application of cutting fluid reduced the level of dust and airborne contamination that are generated in machining.

2) Analysis of variance (ANOVA) results show that the process parameters significantly affect the performance characteristics. Spindle speed mainly affects the Ra and the feed rate largely affects the cutting force.

3) Atomized general purpose semisynthetic coolant and vegetable oil were examined in this study. The application of vegetable oil was more effective in reducing cutting forces and improving the tool wear. In addition, vegetable oil is an friendly lubricant for improving the machining of CFRPs.

4) The magnitude of resultant cutting force was found to be greater in the dry condition relative to the ACF condition by about 23%, 31%, 26%, 25%, and 23%, respectively, for the samples in the 0°, 30° 45°, 60° and 90° FOA at 6 μm/tooth of feed rate.

5) Tool wear was examined and measured using a 3D optical microscope (Olympus BXFM). 90° produced a large amount of tool edge rounding. In contrast, 0° fiber orientation resulted in the least amount of edge rounding. However, the lowest values of edge radius evolution as a measure of the tool wear were 12 μm and 16.5 μm with FOA from 0° to 90° at feed rate 3 μm under ACF (vegetable oil) conditions.

6) The delamination percentage when cutting at 0°, 30° 45°, 60° and 90° were improved by 65%, 91%, 54%, 66%, and 75%, respectively, under ACF (vegetable oil) conditions at 3μm/tooth feed rate. Machining with 45° FOA produces maximum damage at high feed rate.

7) Feed rate has a greater effect on cutting force and tool wear than cutting speed, whereas cutting speed is the main parameter that controls the cutting temperature and dust emission in milling of CFRP composite materials.

8) The predicted temperatures from the analytical model agreed well with the experimental observations within a range of ±10%.

9) During the machining, fine particles were emitted (aerodynamic diameters ranging from 0.5–10 μm). The maximum concentration of fine particles reached 2776.6 $\#/cm^3$, while the minimum number reached 432.3 $\#/cm^3$.

SCIENTIFIC CONTRIBUTIONS

My scientific contributions presented in this thesis were initiated by the economical requirements to develop new methods of reducing the manufacturing impact in the machining of aerospace components and of the need to develop comparative evaluation methods from both machinability and environmental perspectives. These contributions are summarized as mentioned below:

1) The feasibility of shifting from conventional dry techniques to the atomization-based method, where the atomized cutting fluid is sprayed directly into the cutting zone to lubricate the chip and tool interface, and to dissipate the heat generated by fast evaporation. Because of the significantly higher evaporation rate of the atomized cutting fluid, the applied coolant does not get absorbed into the workpiece material. Therefore, atomization of the cutting fluid may provide a viable method for applying cutting fluid in CFRP cutting.
2) The milling performance of CFRPs when using atomized vegetable oil as a lubricant was investigated in this research work as a function of fiber orientations and cutting feed rate. The process performance indicators studied were the cutting force, the tool wear, delamination, and surface texture.
3) The present study attempted to investigate routing milling of CFRPs under dry machining conditions. Effect of cutting parameters (feed rate, spindle speed) on cutting force, cutting temperature, tool wear, and dust emission were assessed.
4) The amount of fine dust generated could be reduced by selecting suitable cutting parameters during the milling of CFRPs according to data, models, and machining strategies established in this research work.

RECOMMENDATIONS FOR FUTURE RESEARCH WORK

During the current research effort, many avenues were opened which can be explored for future research. They are as follows:

1) **Cutting fluid application**

   In this research, the effectiveness of atomization based cutting fluid application in improving the machinability of CFRP is studied experimentally. In this method, the atomized cutting fluid is sprayed directly into the cutting zone to lubricate the chip and tool interface, and also to dissipate the generate heat by fast evaporation. However, there is opportunity for performing additional analysis in order to ensure that the structural integrity of CFRP was not damaged by moisture caused by the use of atomization based cutting fluid application.

2) **Cutting temperature**

   In this research, the thermocouples were installed on the tool to measure the cutting zone area. It may be possible to install the thermocouples on the workpiece to measure the cutting temperature at the top surface near the cutting zone. This would allow the temperature difference between the machined surface and the cutting edge to be measured, which would validate the hypothesis that the majority of the heat produced during cutting is carried away by the chip and the tool and does not occur.

3) **Particle analysis**

   It is the prospect that the techniques, tools, and processes developed as part of this research can be used to contribute to further the understanding of machinability of composite materials and make their way into production use. We recommend to investigate the Evolution of ultrafine particles emissions size and harmful dust masses concentration generated from the source should be considered when dry machining composite to ensure a safe operation.

APPENDIX

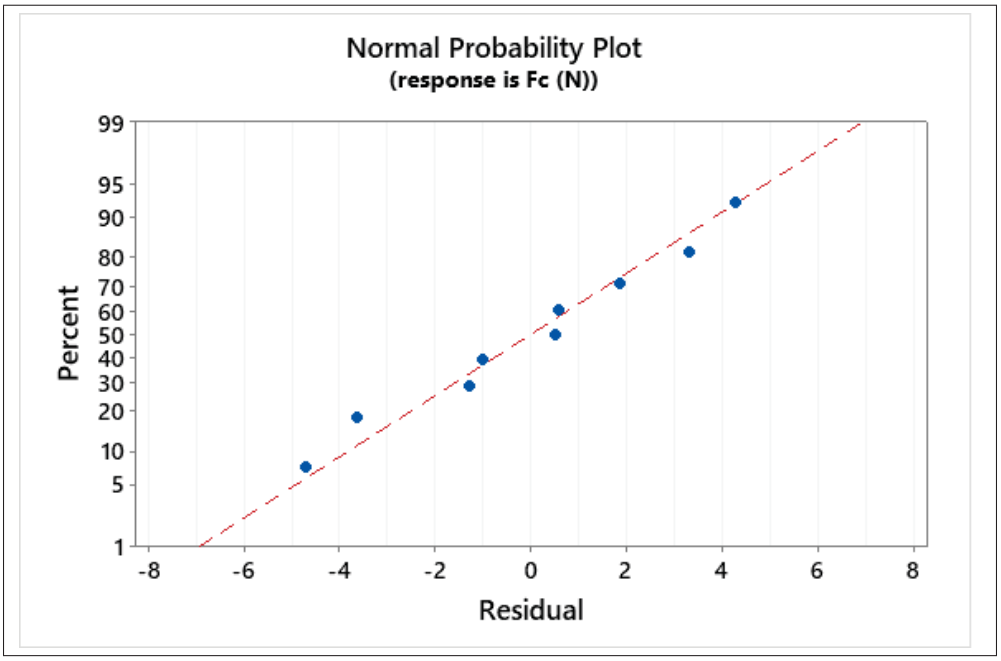

Figure-A -1 Normal probability plot for cutting force (Fc)

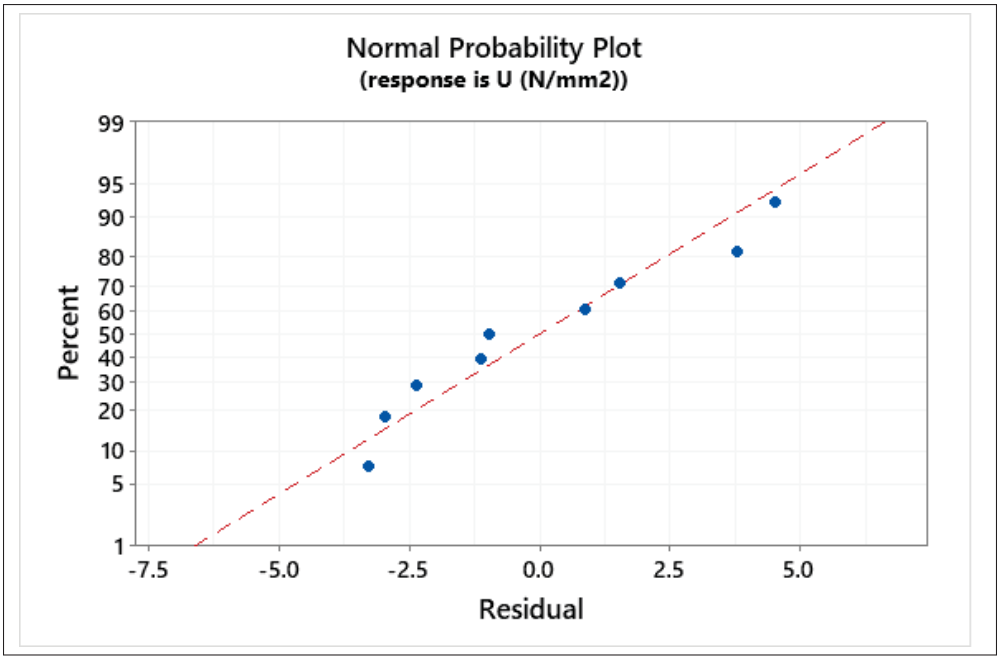

Figure-A -2 Normal Probability Plot for specific cutting energy (U)

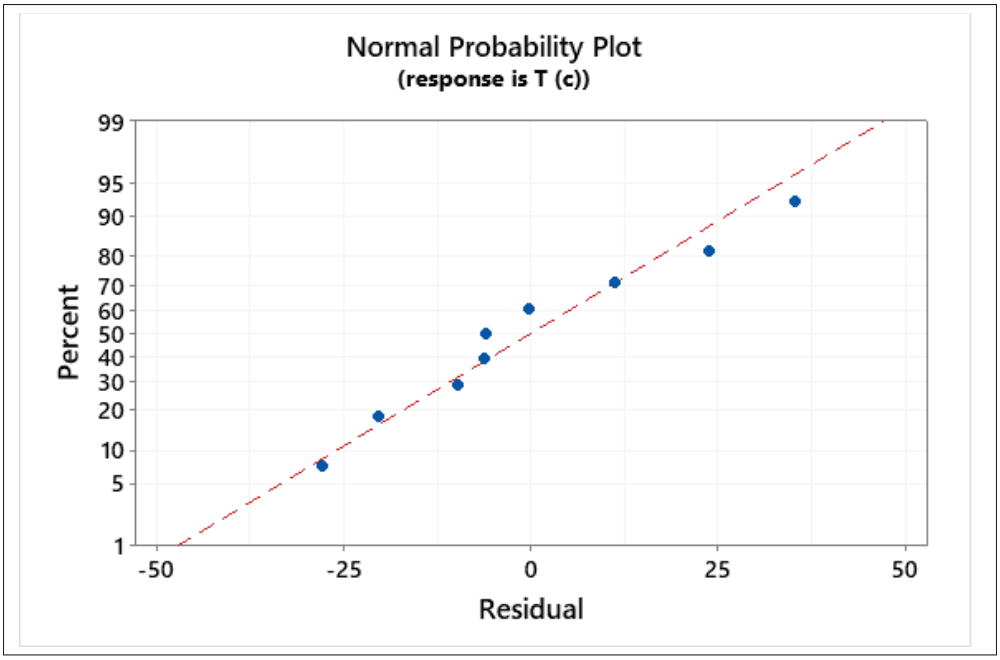

Figure-A -3 Normal probability plot for Temperature (T)

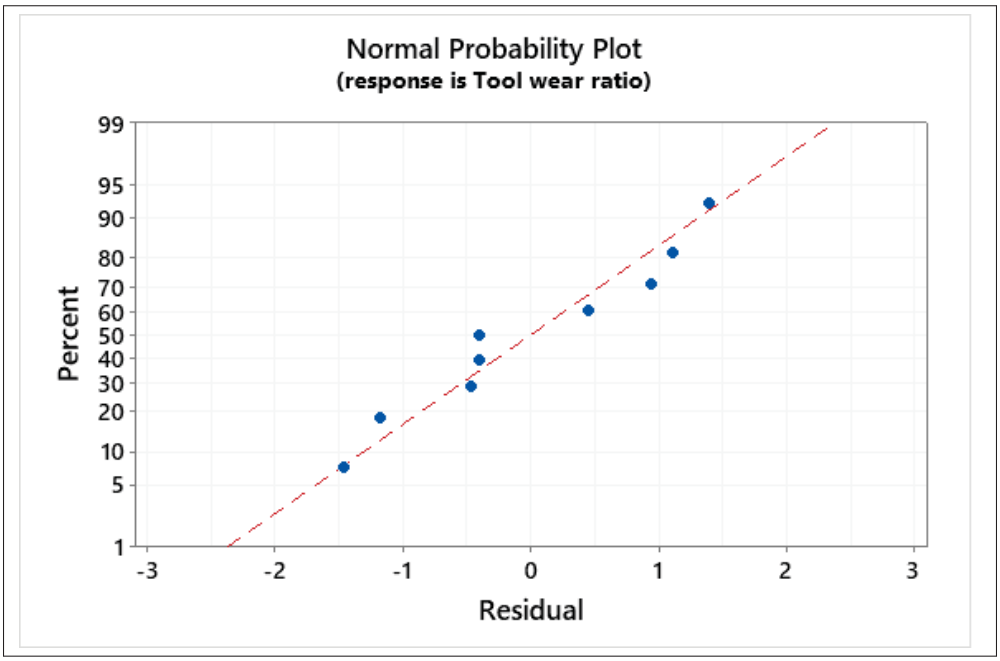

Figure-A -4 Normal probability plot for Temperature (T)

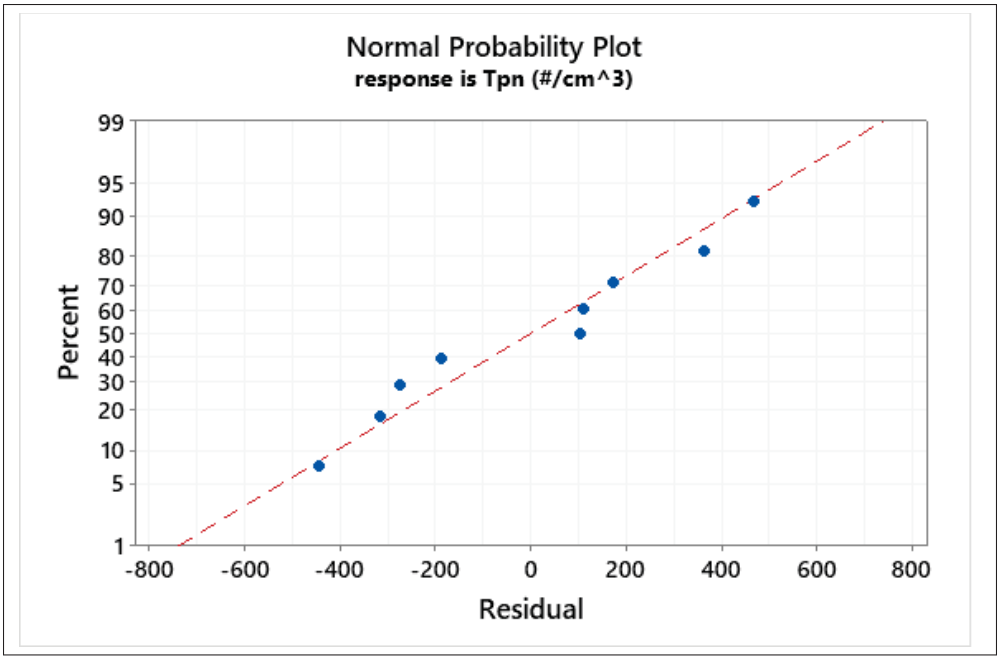

Figure-A -5 Normal probability plot for Temperature (T)

BIBLIOGRAPHY

Abdalla, H., Baines, W., McIntyre, G. & Slade, C. (2007). Development of novel sustainable neat-oil metal working fluids for stainless steel and titanium alloy machining. Part 1. Formulation development. *The International Journal of Advanced Manufacturing Technology*, 34(1-2), 21–33.

Alonso, L. & Solis, A. (2021). High-velocity impact on composite sandwich structures: A theoretical model. *International Journal of Mechanical Sciences*, 201, 106459.

Altintas, Y. & Ber, A. (2001). Manufacturing automation: metal cutting mechanics, machine tool vibrations, and CNC design. *Appl. Mech. Rev.*, 54(5), B84–B84.

Alves, S. M. & de Oliveira, J. F. G. (2006). Development of new cutting fluid for grinding process adjusting mechanical performance and environmental impact. *Journal of materials processing technology*, 179(1-3), 185–189.

Azmi, A., Lin, R. & Bhattacharyya, D. (2012). Machinability study of glass fibre reinforced composite during end milling. *Int J Adv Manuf Technol In Press: doi*, 10.

Bard, S., Schönl, F., Demleitner, M. & Altstädt, V. (2019). Influence of fiber volume content on thermal conductivity in transverse and fiber direction of carbon fiber-reinforced epoxy laminates. *Materials*, 12(7), 1084.

Basmaci, G., Yoruk, A. S., Koklu, U. & Morkavuk, S. (2017). Impact of cryogenic condition and drill diameter on drilling performance of CFRP. *Applied Sciences*, 7(7), 667.

Bhatnagar, N., Ramakrishnan, N., Naik, N. & Komanduri, R. (1995). On the machining of fiber reinforced plastic (FRP) composite laminates. *International journal of machine tools and manufacture*, 35(5), 701–716.

Boatman, E., Covert, D., Kalman, D., Luchtel, D. & Omenn, G. (1988). Physical, morphological, and chemical studies of dusts derived from the machining of composite-epoxy materials. *Environmental research*, 45(2), 242–255.

Brinksmeier, E., Walter, A., Janssen, R. & Diersen, P. (1999). Aspects of cooling lubrication reduction in machining advanced materials. *Proceedings of the Institution of Mechanical Engineers, Part B: Journal of Engineering Manufacture*, 213(8), 769–778.

Burton, G., Goo, C.-S., Zhang, Y. & Jun, M. B. (2014). Use of vegetable oil in water emulsion achieved through ultrasonic atomization as cutting fluids in micro-milling. *Journal of Manufacturing Processes*, 16(3), 405–413.

Caggiano, A., Improta, I. & Nele, L. (2018). Characterization of a new dry drill-milling process of Carbon Fibre Reinforced Polymer laminates. *Materials*, 11(8), 1470.

Calzada, K. A., Kapoor, S. G., DeVor, R. E., Samuel, J. & Srivastava, A. K. (2012). Modeling and interpretation of fiber orientation-based failure mechanisms in machining of carbon fiber-reinforced polymer composites. *Journal of Manufacturing Processes*, 14(2), 141–149.

Campbell, F. C. (2010). *Structural composite materials*. ASM international.

Chang, C.-S. (2006). Turning of glass–fiber reinforced plastics materials with chamfered main cutting edge carbide tools. *Journal of materials processing technology*, 180(1-3), 117–129.

Chao, P. & Hwang, Y. (1997). An improved Taguchi's method in design of experiments for milling CFRP composite. *International journal of production research*, 35(1), 51–66.

Chatterjee, A. (2009). Thermal degradation analysis of thermoset resins. *Journal of applied polymer science*, 114(3), 1417–1425.

Che, D., Saxena, I., Han, P., Guo, P. & Ehmann, K. F. (2014). Machining of carbon fiber reinforced plastics/polymers: a literature review. *Journal of Manufacturing Science and Engineering*, 136(3).

Chen, W.-C. (1997). Some experimental investigations in the drilling of carbon fiber-reinforced plastic (CFRP) composite laminates. *International Journal of Machine Tools and Manufacture*, 37(8), 1097–1108.

Chen, Y., Guo, X., Zhang, K., Guo, D., Zhou, C. & Gai, L. (2019). Study on the surface quality of CFRP machined by micro-textured milling tools. *Journal of Manufacturing Processes*, 37, 114–123.

Colligan, K., Ramulu, M. et al. (1992). The effect of edge trimming on composite surface plies. *Manufacturing Review(USA)*, 5(4), 274–283.

Dabade, U. A. & Joshi, S. S. (2009). Analysis of chip formation mechanism in machining of Al/SiCp metal matrix composites. *Journal of Materials Processing Technology*, 209(10), 4704–4710.

Dandekar, C. R. & Shin, Y. C. (2012). Modeling of machining of composite materials: a review. *International Journal of Machine tools and manufacture*, 57, 102–121.

Das, T. K., Ghosh, P. & Das, N. C. (2019). Preparation, development, outcomes, and application versatility of carbon fiber-based polymer composites: a review. *Advanced Composites and Hybrid Materials*, 1–20.

Davim, J. P. & Mata, F. (2005). Optimisation of surface roughness on turning fibre-reinforced plastics (FRPs) with diamond cutting tools. *The International Journal of Advanced Manufacturing Technology*, 26(4), 319–323.

Davim, J. P. & Reis, P. (2005). Damage and dimensional precision on milling carbon fiber-reinforced plastics using design experiments. *Journal of materials processing technology*, 160(2), 160–167.

Dhari, R. S., Patel, N. P., Wang, H. & Hazell, P. J. (2021). Progressive damage modeling and optimization of fibrous composites under ballistic impact loading. *Mechanics of Advanced Materials and Structures*, 28(12), 1227–1244.

Ehsani, A. & Rezaeepazhand, J. (2016). Stacking sequence optimization of laminated composite grid plates for maximum buckling load using genetic algorithm. *International Journal of Mechanical Sciences*, 119, 97–106.

Elgnemi, T., Ahmadi, K., Songmene, V., Nam, J. & Jun, M. B. (2017). Effects of atomization-based cutting fluid sprays in milling of carbon fiber reinforced polymer composite. *Journal of Manufacturing Processes*, 30, 133–140.

Elgnemi, T.-S.-M., Jun, M. B.-G., Songmene, V., Samuel, A. M. et al. (2021). Milling performance of CFRP composite and atomised vegetable oil as a function of fiber orientation. *Materials*, 14(8), 2062.

Eneyew, E. D. & Ramulu, M. (2012, 11). Hole Surface Quality and Damage When Drilling Unidirectional CFRP Composites. Retrieved from: https://doi.org/10.1115/IMECE2012-88426.

Faraz, A., Biermann, D. & Weinert, K. (2009). Cutting edge rounding: An innovative tool wear criterion in drilling CFRP composite laminates. *International Journal of Machine Tools and Manufacture*, 49(15), 1185–1196.

Filipovic, A. & Stephenson, D. A. (2006). Minimum quantity lubrication (MQL) applications in automotive power-train machining. *Machining Science and Technology*, 10(1), 3–22.

Freyer, B. H., Heyns, P. S. & Theron, N. J. (2014). Comparing orthogonal force and unidirectional strain component processing for tool condition monitoring. *Journal of Intelligent Manufacturing*, 25(3), 473–487.

Gaitonde, V., Karnik, S., Rubio, J. C., Correia, A. E., Abrao, A. & Davim, J. P. (2008). Analysis of parametric influence on delamination in high-speed drilling of carbon fiber reinforced plastic composites. *Journal of materials processing technology*, 203(1-3), 431–438.

Gara, S., M'hamed, S. & Tsoumarev, O. (2018). Temperature measurement and machining damage in slotting of multidirectional CFRP laminate. *Machining Science and Technology*, 22(2), 320–337.

Geng, D., Liu, Y., Shao, Z., Lu, Z., Cai, J., Li, X., Jiang, X. & Zhang, D. (2019). Delamination formation, evaluation and suppression during drilling of composite laminates: a review. *Composite Structures*, 216, 168–186.

Ghafarizadeh, S., Lebrun, G. & Chatelain, J.-F. (2016). Experimental investigation of the cutting temperature and surface quality during milling of unidirectional carbon fiber reinforced plastic. *Journal of composite materials*, 50(8), 1059–1071.

Giasin, K., Ayvar-Soberanis, S. & Hodzic, A. (2016). Evaluation of cryogenic cooling and minimum quantity lubrication effects on machining GLARE laminates using design of experiments. *Journal of Cleaner Production*, 135, 533–548.

Giurgiutiu, V. (2015). Structural health monitoring of aerospace composites.

Gnanadurai, R. R. & Varadarajan, A. (2016). Investigation on the effect of cooling of the tool using heat pipe during hard turning with minimal fluid application. *Engineering science and technology, an international journal*, 19(3), 1190–1198.

Groover, M. P. (2020). *Fundamentals of modern manufacturing: materials, processes, and systems*. John Wiley & Sons.

Gryglewicz, S., Piechocki, W. & Gryglewicz, G. (2003). Preparation of polyol esters based on vegetable and animal fats. *Bioresource Technology*, 87(1), 35–39.

Haddad, M., Zitoune, R., Eyma, F., Castanié, B. & Bougherara, H. (2012). Surface quality and dust analysis in high speed trimming of CFRP. *Applied Mechanics and Materials*, 232, 57–62.

Haddad, M., Zitoune, R., Eyma, F. & Castanie, B. (2014). Study of the surface defects and dust generated during trimming of CFRP: Influence of tool geometry, machining parameters and cutting speed range. *Composites Part A: Applied Science and Manufacturing*, 66, 142–154.

Han, R., Liu, J. & Sun, Y. (2005). Research on experimentation of green cutting with water vapor as coolant and lubricant. *Industrial Lubrication and Tribology*.

He, Y., Sheikh-Ahmad, J., Zhu, S. & Zhao, C. (2020). Cutting force analysis considering edge effects in the milling of carbon fiber reinforced polymer composite. *Journal of Materials Processing Technology*, 279, 116541.

Hintze, W. & Hartmann, D. (2013). Modeling of delamination during milling of unidirectional CFRP. *Procedia Cirp*, 8, 444–449.

Hintze, W., Hartmann, D. & Schütte, C. (2011). Occurrence and propagation of delamination during the machining of carbon fibre reinforced plastics (CFRPs)–An experimental study. *Composites Science and Technology*, 71(15), 1719–1726.

Hintze, W., Cordes, M. & Koerkel, G. (2015). Influence of weave structure on delamination when milling CFRP. *Journal of Materials Processing Technology*, 216, 199–205.

Ho-Cheng, H. & Dharan, C. (1990). Delamination during drilling in composite laminates.

Hocheng, H., Puw, H. & Huang, Y. (1993). Preliminary study on milling of unidirectional carbon fibre-reinforced plastics. *Composites Manufacturing*, 4(2), 103–108.

Hu, N. & Zhang, L. (2004). Some observations in grinding unidirectional carbon fibre-reinforced plastics. *Journal of materials processing technology*, 152(3), 333–338.

Hussain, G., Gao, L., Hayat, N. & Qijian, L. (2007). The effect of variation in the curvature of part on the formability in incremental forming: An experimental investigation. *International Journal of Machine Tools and Manufacture*, 47(14), 2177–2181.

Impero, F., Dix, M., Squillace, A., Prisco, U., Palumbo, B. & Tagliaferri, F. (2018). A comparison between wet and cryogenic drilling of CFRP/Ti stacks. *Materials and Manufacturing Processes*, 33(12), 1354–1360.

Iqbal, A., Zhao, G., Zaini, J., Gupta, M. K., Jamil, M., He, N., Nauman, M. M., Mikolajczyk, T. & Pimenov, D. Y. (2021). Between-the-holes cryogenic cooling of the tool in hole-making of Ti-6Al-4V and CFRP. *Materials*, 14(4), 795.

Ismail, S. O., Sarfraz, S., Niamat, M., Mia, M., Gupta, M. K., Pimenov, D. Y. & Shehab, E. (2021). Comprehensive study on tool wear during machining of fiber-reinforced polymeric composites. In *Machining and Machinability of Fiber Reinforced Polymer Composites* (pp. 129–147). Springer.

Iyer, A. K. (2015). *Characterization of Composite Dust generated during Milling of Uni-Directional and Random fiber composites*. (Ph.D. thesis).

Jain, N. K., Jain, V. & Deb, K. (2007). Optimization of process parameters of mechanical type advanced machining processes using genetic algorithms. *International Journal of Machine Tools and Manufacture*, 47(6), 900–919.

Joshi, S., Rawat, K. & Balan, A. (2018). A novel approach to predict the delamination factor for dry and cryogenic drilling of CFRP. *Journal of Materials Processing Technology*, 262, 521–531.

Jun, M. B., Joshi, S. S., DeVor, R. E. & Kapoor, S. G. (2008). An experimental evaluation of an atomization-based cutting fluid application system for micromachining. *Journal of manufacturing science and engineering*, 130(3).

Kamogawa, K., Matsumoto, M., Kobayashi, T., Sakai, T., Sakai, H. & Abe, M. (1999). Dispersion and stabilizing effects of n-hexadecane on tetralin and benzene metastable droplets in surfactant-free conditions. *Langmuir*, 15(6), 1913–1917.

Kamogawa, K., Akatsuka, H., Matsumoto, M., Yokoyama, S., Sakai, T., Sakai, H. & Abe, M. (2001). Surfactant-free O/W emulsion formation of oleic acid and its esters with ultrasonic dispersion. *Colloids and Surfaces A: Physicochemical and Engineering Aspects*, 180(1-2), 41–53.

Kamogawa, K., Okudaira, G., Matsumoto, M., Sakai, T., Sakai, H. & Abe, M. (2004). Preparation of oleic acid/water emulsions in surfactant-free condition by sequential processing using midsonic- megasonic waves. *Langmuir*, 20(6), 2043–2047.

Karaguzel, U., Bakkal, M. & Budak, E. (2016). Modeling and measurement of cutting temperatures in milling. *Procedia CIRP*, 46, 173–176.

Karpat, Y. & Polat, N. (2013). Mechanistic force modeling for milling of carbon fiber reinforced polymers with double helix tools. *CIRP Annals*, 62(1), 95–98.

Karpat, Y., Bahtiyar, O. & Değer, B. (2012). Mechanistic force modeling for milling of unidirectional carbon fiber reinforced polymer laminates. *International Journal of Machine Tools and Manufacture*, 56, 79–93.

Kerrigan, K., Thil, J., Hewison, R. & O'Donnell, G. (2012). An integrated telemetric thermocouple sensor for process monitoring of CFRP milling operations. *Procedia CIRP*, 1, 449–454.

Khairussaleh, N. K. M., Haron, C. H. C. & Ghani, J. A. (2016). Study on wear mechanism of solid carbide cutting tool in milling CFRP. *Journal of materials research*, 31(13), 1893.

Khairusshima, M. N. & Sharifah, I. (2017). Study on tool wear during milling CFRP under dry and chilled air machining. *Procedia engineering*, 184, 506–517.

Khairusshima, M. N., Hassan, C. C., Jaharah, A., Amin, A. & Idriss, A. M. (2013). Effect of chilled air on tool wear and workpiece quality during milling of carbon fibre-reinforced plastic. *Wear*, 302(1-2), 1113–1123.

Khettabi, R., Songmene, V., Zaghbani, I. & Masounave, J. (2010). Modeling of particle emission during dry orthogonal cutting. *Journal of materials engineering and performance*, 19(6), 776–789.

Klein, R., Dahmen, M., Pütz, H., Möhlmann, C., Schloms, R. & Zschiesche, W. (1998). Workplace exposure during laser machining. *Journal of Laser Applications*, 10(3), 99–105.

Koenig, W., Wulf, C., Grass, P. & Willerscheid, H. (1985). Machining of fibre reinforced plastics. *CIRP Annals*, 34(2), 537–548.

König, W. & Grass, P. (1989). Quality definition and assessment in drilling of fibre reinforced thermosets. *CIRP Annals*, 38(1), 119–124.

Konig, W. & Rummenholler, S. (1993). Technological and industrial safety aspects in milling FRP. *ASME Mach Adv Comp*, 45(66), 1–14.

KOPLEV, A. et al. (1980). Cutting of CFRP with single edge tools.

Kremer, A. & El Mansori, M. (2009). Influence of nanostructured CVD diamond coatings on dust emission and machinability of SiC particle-reinforced metal matrix composite. *Surface and Coatings Technology*, 204(6-7), 1051–1055.

Kremer, A. & El Mansori, M. (2011). Tool wear as-modified by particle generation in dry machining. *Wear*, 271(9-10), 2448–2453.

Kumar, D. & Gururaja, S. (2020). Machining damage and surface integrity evaluation during milling of UD-CFRP laminates: Dry vs. cryogenic. *Composite Structures*, 247, 112504.

Li, H., Qin, X., He, G., Jin, Y., Sun, D. & Price, M. (2016). Investigation of chip formation and fracture toughness in orthogonal cutting of UD-CFRP. *The International Journal of Advanced Manufacturing Technology*, 82(5-8), 1079–1088.

Li, K.-M., Wang, C. & Chu, W.-Y. (2013). An improved remote sensing technique for estimating tool–chip interface temperatures in turning. *Journal of Materials Processing Technology*, 213(10), 1772–1781.

Lin, S., Peng, F., Wen, J., Liu, Y. & Yan, R. (2013). An investigation of workpiece temperature variation in end milling considering flank rubbing effect. *International Journal of Machine Tools and Manufacture*, 73, 71–86.

Liu, G., Chen, H., Huang, Z., Gao, F. & Chen, T. (2017a). Surface quality of staggered PCD end mill in milling of carbon fiber reinforced plastics. *Applied Sciences*, 7(2), 199.

Liu, J., Chen, G., Ji, C., Qin, X., Li, H. & Ren, C. (2014). An investigation of workpiece temperature variation of helical milling for carbon fiber reinforced plastics (CFRP). *International Journal of Machine Tools and Manufacture*, 86, 89–103.

Liu, Y., Deng, J., Wu, F., Duan, R., Zhang, X. & Hou, Y. (2017b). Wear resistance of carbide tools with textured flank-face in dry cutting of green alumina ceramics. *Wear*, 372, 91–103.

López de Lacalle, L. N. & Lamikiz, A. (2010). Milling of carbon fiber reinforced plastics. *Advanced Materials Research*, 83, 49–55.

Lopez de Lacalle, N., Lamikiz, A., Campa, F., Valdivielso, A. F. & Etxeberria, I. (2009). Design and test of a multitooth tool for CFRP milling. *Journal of composite materials*, 43(26), 3275–3290.

Maegawa, S., Morikawa, Y., Hayakawa, S., Itoigawa, F. & Nakamura, T. (2015). Effects of fiber orientation direction on tool-wear processes in down-milling of carbon fiber-reinforced plastic laminates. *International journal of automation technology*, 9(4), 356–364.

Maegawa, S., Morikawa, Y., Hayakawa, S., Itoigawa, F. & Nakamura, T. (2016). Mechanism for changes in cutting forces for down-milling of unidirectional carbon fiber reinforced polymer laminates: modeling and experimentation. *International Journal of Machine Tools and Manufacture*, 100, 7–13.

Marani, M., Songmene, V., Kouam, J. & Zedan, Y. (2018). Experimental investigation on microstructure, mechanical properties and dust emission when milling Al-20 Mg 2 Si-2Cu metal matrix composite with modifier elements. *The International Journal of Advanced Manufacturing Technology*, 99(1), 789–802.

Mathews, W., Lee, C.-F. & Peters, J. E. (2003). Experimental investigations of spray/wall impingement. *Atomization and Sprays*, 13(2&3).

Mazumdar, S. (2001). *Composites manufacturing: materials, product, and process engineering*. CrC press.

Mia, M. & Dhar, N. R. (2016). Manuscript title: Response Surface and Neural Network based Predictive Models of Cutting Temperature in Hard Turning.

Miller, J. L. (2014). *Investigation of machinability and dust emissions in edge trimming of laminated carbon fiber composites*. (Ph.D. thesis).

Miracle, D. B., Donaldson, S. L. et al. (2001). Introduction to composites. *ASM handbook*, 21, 3–17.

Montgomery, D. C. (2017). *Design and analysis of experiments*. John wiley & sons.

Morkavuk, S., Köklü, U., Bağcı, M. & Gemi, L. (2018). Cryogenic machining of carbon fiber reinforced plastic (CFRP) composites and the effects of cryogenic treatment on tensile properties: a comparative study. *Composites Part B: Engineering*, 147, 1–11.

Ngoc, D. N., Hue, T. N., Van Hung, B. & Duc, V. D. (2020). Dust emission during machining of CFRP composite: a calculation of the number and mass of the thoracic particles. *International conference on engineering research and applications*, pp. 341–349.

Nguyen, D., Voznyuk, V., Bin Abdullah, M. S., Kim, D. & Kwon, P. Y. (2019). Tool wear of superhard ceramic coated tools in drilling of CFRP/Ti stacks. *International Manufacturing Science and Engineering Conference*, 58752, V002T03A089.

Nguyen, D., Abdullah, M. S. B., Khawarizmi, R., Kim, D. & Kwon, P. (2020). The effect of fiber orientation on tool wear in edge-trimming of carbon fiber reinforced plastics (CFRP) laminates. *Wear*, 450, 203213.

Nguyen-Dinh, N., Hejjaji, A., Zitoune, R., Bouvet, C. & Salem, M. (2020). New tool for reduction of harmful particulate dispersion and to improve machining quality when trimming carbon/epoxy composites. *Composites Part A: Applied Science and Manufacturing*, 131, 105806.

Niknam, S. A. & Songmene, V. (2014). Analysis of friction and burr formation in slot milling. *Procedia CIRP*, 17, 755–759.

Pecat, O., Rentsch, R. & Brinksmeier, E. (2012). Influence of milling process parameters on the surface integrity of CFRP. *Procedia Cirp*, 1, 466–470.

Puw, H. & Hocheng, H. (1993). Machinability test of carbon fiber-reinforced plastics in milling. *Material and manufacturing process*, 8(6), 717–729.

Pwu, H. & Hocheng, H. (1998). Chip formation model of cutting fiber-reinforced plastics perpendicular to fiber axis.

Rahman, M., Ramakrishna, S. & Thoo, H. (1999). Machinability study of carbon/PEEK composites. *Machining science and technology*, 3(1), 49–59.

Ramulu, M., Faridnia, M., Garbini, J. & Jorgensen, J. (1991). Machining of graphite/epoxy composite materials with polycrystalline diamond (PCD) tools.

Ramulu, M., Young, P. & Kao, H. (1999). Drilling of graphite/bismaleimide composite material. *Journal of Materials engineering and performance*, 8(3), 330–338.

Ramulu, M., Kim, D. & Choi, G. (2003). Frequency analysis and characterization in orthogonal cutting of glass fiber reinforced composites. *Composites Part A: Applied Science and Manufacturing*, 34(10), 949–962.

Rawat, S. & Attia, H. (2009). Wear mechanisms and tool life management of WC–Co drills during dry high speed drilling of woven carbon fibre composites. *Wear*, 267(5-8), 1022–1030.

Raynor, P. C., Kim, S. W. & Bhattacharya, M. (2005). Mist generation from metalworking fluids formulated using vegetable oils. *Annals of Occupational Hygiene*, 49(4), 283–293.

Rukosuyev, M., Goo, C. S. & Jun, M. B. (2010). Understanding the effects of the system parameters of an ultrasonic cutting fluid application system for micro-machining. *Journal of Manufacturing Processes*, 12(2), 92–98.

Sakai, T. (2008). Surfactant-free emulsions. *Current Opinion in Colloid & Interface Science*, 13(4), 228–235.

Sakuma, K. & Seto, M. (1983). Tool wear in cutting glass-fiber-reinforced plastics: the relation between fiber orientation and tool wear. *Bulletin of JSME*, 26(218), 1420–1427.

Santhanakrishnan, G., Krishnamurthy, R. & Malhotra, S. (1988). Machinability characteristics of fibre reinforced plastics composites. *Journal of Mechanical Working Technology*, 17, 195–204.

Sato, M., Tamura, N. & Tanaka, H. (2011). Temperature variation in the cutting tool in end milling. *Journal of Manufacturing Science and Engineering*, 133(2).

Shahrajabian, H., Hadi, M. & Farahnakian, M. (2012). Experimental investigation of machining parameters on machinability of carbon fiber/epoxy composites. *International Journal of Engineering and Innovative Technology*, 3(3), 30–36.

Shashidhara, Y. & Jayaram, S. (2010). Vegetable oils as a potential cutting fluid—an evolution. *Tribology international*, 43(5-6), 1073–1081.

Shaw, M., Pigott, J. & Richardson, L. (1951). Effect of cutting fluid upon chip–tool interface temperature. *Trans. ASME*, 71(2), 45–56.

Shaw, M. C. & Cookson, J. (2005). *Metal cutting principles*. Oxford university press New York.

Sheikh-Ahmad, J. & Yadav, R. (2008). Model for predicting cutting forces in machining CFRP. *International Journal of Materials and Product Technology*, 32(2-3), 152–167.

Sheikh-Ahmad, J. Y. (2009). *Machining of polymer composites*. Springer.

Shen, Z., Lu, L., Sun, J., Yang, F., Tang, Y. & Xie, Y. (2015). Wear patterns and wear mechanisms of cutting tools used during the manufacturing of chopped carbon fiber. *International Journal of Machine Tools and Manufacture*, 97, 1–10.

Sheng, J., Chiu, Y.-J. & Lin, B.-J. (2018). Determination of a coupling equation for milling parameters based on optimal cutting temperature. *The International Journal of Advanced Manufacturing Technology*, 98(1), 129–141.

Shirazinia, M., Moya, R. & Muñoz, F. (2011). Properties of laminated curves manufactured with steamed veneers from fast-growth tropical wood in Costa Rica. *Madera y Bosques*, 17(2), 85–101.

Shyha, I., Soo, S. L., Aspinwall, D. & Bradley, S. (2010). Effect of laminate configuration and feed rate on cutting performance when drilling holes in carbon fibre reinforced plastic composites. *Journal of materials processing technology*, 210(8), 1023–1034.

Siniawski, M. T., Saniei, N., Adhikari, B. & Doezema, L. A. (2007). Influence of fatty acid composition on the tribological performance of two vegetable-based lubricants. *Journal of Synthetic Lubrication*, 24(2), 101–110.

Songmene, V., Kouam, J. & Balhoul, A. (2018). Effect of minimum quantity lubrication (MQL) on fine and ultrafine particle emission and distribution during polishing of granite. *Measurement*, 114, 398–408.

Su, F., Yuan, J., Sun, F., Wang, Z. & Deng, Z. (2018). Modeling and simulation of milling forces in milling plain woven carbon fiber-reinforced plastics. *The International Journal of Advanced Manufacturing Technology*, 95(9-12), 4141–4152.

Swan, S., Bin Abdullah, M. S., Kim, D., Nguyen, D. & Kwon, P. (2018). Tool wear of advanced coated tools in drilling of CFRP. *Journal of Manufacturing Science and Engineering*, 140(11), 111018.

Takeyama, H. & Iijima, N. (1988). Machinability of glassfiber reinforced plastics and application of ultrasonic machining. *CIRP Annals*, 37(1), 93–96.

Teitsworth, J. (1999). The effectiveness of local exhaust-ventilated (shrouded)-hand power tools used for grinding/sanding composite materials. *Occupational Health and Industrial Medicine*, 1(40), 5.

Teti, R. (2002). Machining of composite materials. *CIRP Annals*, 51(2), 611–634.

Tian, H., Lu, C., Yang, J., Banger, K., Huntzinger, D. N., Schwalm, C. R., Michalak, A. M., Cook, R., Ciais, P., Hayes, D. et al. (2015). Global patterns and controls of soil organic carbon dynamics as simulated by multiple terrestrial biosphere models: Current status and future directions. *Global Biogeochemical Cycles*, 29(6), 775–792.

Turner, J., Scaife, R. J. & El-Dessouky, H. (2015). Effect of machining coolant on integrity of CFRP composites. *Advanced Manufacturing: Polymer & Composites Science*, 1(1), 54–60.

Ucar, M. & Wang, Y. (2005). End-milling machinability of a carbon fiber reinforced laminated composite.

Wang, C., Liu, G., An, Q. & Chen, M. (2017). Occurrence and formation mechanism of surface cavity defects during orthogonal milling of CFRP laminates. *Composites Part B: Engineering*, 109, 10–22.

Wang, D., Ramulu, M. & Arola, D. (1995). Orthogonal cutting mechanisms of graphite/epoxy composite. Part I: unidirectional laminate. *International Journal of Machine Tools and Manufacture*, 35(12), 1623–1638.

Wang, H., Sun, J., Li, J., Lu, L. & Li, N. (2016). Evaluation of cutting force and cutting temperature in milling carbon fiber-reinforced polymer composites. *The International Journal of Advanced Manufacturing Technology*, 82(9-12), 1517–1525.

Wang, X. M. & Zhang, L. (2003). An experimental investigation into the orthogonal cutting of unidirectional fibre reinforced plastics. *International journal of machine tools and manufacture*, 43(10), 1015–1022.

WANG, X. & ZHANG, L. (1999). Machining damage in unidirectional fibre-reinforced plastics. In *Abrasive Technology: Current Development and Applications I* (pp. 429–436). World Scientific.

Wang, Y. G., Yan, X. P., Chen, X., Sun, C. Y. & Liu, G. (2011). Cutting performance of carbon fiber reinforced plastics using PCD tool. *Advanced Materials Research*, 215, 14–18.

Wróbel, G., Rdzawski, Z., Muzia, G. & Pawlak, S. (2009). Determination of thermal diffusivity of carbon/epoxy composites with different fiber content using transient thermography. *Journal of achievements in materials and manufacturing engineering*, 37(2), 518–525.

Xia, T., Kaynak, Y., Arvin, C. & Jawahir, I. (2016). Cryogenic cooling-induced process performance and surface integrity in drilling CFRP composite material. *The International Journal of Advanced Manufacturing Technology*, 82(1), 605–616.

Xiao, J., Gao, C. & Ke, Y. (2018). An analytical approach to cutting force prediction in milling of carbon fiber reinforced polymer laminates. *Machining Science and Technology*, 22(6), 1012–1028.

Xu, W.-X. & Zhang, L.-C. (2015). Ultrasonic vibration-assisted machining: principle, design and application. *Advances in Manufacturing*, 3(3), 173–192.

Xu, W. & Zhang, L. (2018). Tool wear and its effect on the surface integrity in the machining of fibre-reinforced polymer composites. *Composite Structures*, 188, 257–265.

Yashiro, T., Ogawa, T. & Sasahara, H. (2011). 3329 Cutting Temperature Measurement on Milling Process of CFRP. *Proceedings of International Conference on Leading Edge Manufacturing in 21st century: LEM21 2011.6*, pp. _3329–1_.

Yashiro, T., Ogawa, T. & Sasahara, H. (2013). Temperature measurement of cutting tool and machined surface layer in milling of CFRP. *International Journal of Machine Tools and Manufacture*, 70, 63–69.

Zhang, L., Zhang, H. & Wang, X. (2001). A force prediction model for cutting unidirectional fibre-reinforced plastics.

Zhang, S., Li, J. & Wang, Y. (2012). Tool life and cutting forces in end milling Inconel 718 under dry and minimum quantity cooling lubrication cutting conditions. *Journal of Cleaner Production*, 32, 81–87.

Zhao, X. & Li, Y. (2010). Tool wear pattern and mechanics in high speed cutting microwave printed circuit board. *Key Engineering Materials*, 426, 515–519.

Zimmerman, J. B., Clarens, A. F., Hayes, K. F. & Skerlos, S. J. (2003). Design of hard water stable emulsifier systems for petroleum-and bio-based semi-synthetic metalworking fluids. *Environmental science & technology*, 37(23), 5278–5288.

Zitoune, R., Krishnaraj, V., Almabouacif, B. S., Collombet, F., Sima, M. & Jolin, A. (2012). Influence of machining parameters and new nano-coated tool on drilling performance of CFRP/Aluminium sandwich. *Composites Part B: Engineering*, 43(3), 1480–1488.